ABSTRACT

IASMIN, MAHBUBA. Quantifying Fat, Oil, and Grease (FOG) Deposits Formation Kinetics. (Under the direction of Dr. Joel Ducoste).

Fat, oil, and grease (FOG) deposits are calcium based saponified solids that may clog sewer lines and eventually cause sanitary sewer overflows (SSOs). SSOs can pose a significant threat to public health due to the exposure of pathogens and other harmful contaminants. Since 2007, USEPA has set a requirement to public water treatment facilities to spend 15 billion dollars on new pipes and wastewater infrastructure to control overflows. While recent research has provided insight into the chemical characteristics of these insoluble FOG deposits, detailed research is yet to be performed that provides the fundamental understanding of the formation of FOG deposits and their kinetics based on the source and environmental conditions in sewer collection systems. Therefore, the objective of this study was to identify and investigate potential source and environmental factors that may affect formation mechanism of FOG deposits and their kinetics. In addition, the current study evaluated potential empirical models from literature and developed a mathematical model based on mass action principles that can capture the kinetics of FOG deposit formation process. Lab-scale experiments were performed that produced calcium based saponified solids under alkali driven hydrolysis conditions. Tests were performed under the following factors: 1) types of fats used in restaurants, i.e., unsaturated (canola) vs. saturated (beef tallow), 2) types of calcium sources in sewer system, background wastewater (calcium chloride) vs. biogenic concrete corrosion (calcium sulfate), 3) pH (neutral, 10, and ≈14), 4) temperature (room temperature, 22 °C vs. warm temperature, 45 °C), 5) presence of initial free fatty acids (palmitic vs. linoleic), 6) use of detergents (non-ionic vs. anionic) in food service establishments (FSEs), 7) mixing intensities (230 rpm vs. 460 rpm), and 8) lipase (*Candida rugosa*) driven hydrolysis in sewers. Kinetic samples were collected and analyzed using a fingerprinting technique, known as Fourier transform infrared (FTIR) analysis. The final solids were analyzed for the fraction and types of fatty acids, mineral and metal analysis, and rheological properties. Experimental kinetic data was compared with two

empirical models (Cotte saponification model and Foubert crystallization model) and a mass-action-based saponification model.

The results of this study showed that the saponified solids displayed the same fatty acid profiles as their chemical precursors, and therefore, suggest that the large fraction of palmitic in FOG deposits is likely due to alternative fate and transport of unsaturated free fatty acids (FFA) within the sewer collection system. The presence of FFAs in FSE effluents, produced due to high temperature cooking and/or other fat hydrolysis processes, will lead to increased quantity and higher rates of FOG deposit formation. The results suggest that the high temperature operations in FSEs in cooking and/or sanitizing applications can have significant influence in conversion of the unsaturated fats to predominantly palmitic. The pure detergent sources (i.e., non-anionic and anionic) increased the production of saponified solids, but did not display a significant change in the fatty acid profiles. However, the commercially available detergent used in household applications not only increased the production of saponified solids but also displayed significantly high fractions of palmitic in these solids. Therefore, the external agents added to the surfactants to make-up the commercial detergents in households and/or FSEs dishwashing applications may need to be carefully investigated and/or modified to reduce FOG deposit formations in sewer systems. Lipase driven hydrolysis was also shown to enhance the production of FOG deposits. While selective removal of palmitic may be a strategy to reduce the FOG deposit formation, FSEs can play a significant role in the reduction in these formations by focusing on some key issues without compromising restaurant quality, public health, and sanitation: a) optimum usage of detergents; and b) use of a heat-exchange chamber prior to kitchen wastewater discharge into GI to significantly reduce the water temperature below 45 °C.

The mass-action-based saponification model displayed better ability to predict the FOG deposit formation kinetics compared to the empirical models due to its additional mass balance equations that track the saponified solids precursor chemical constituents (i.e., Ca, FOG, and FFA). Therefore, the use of the mass-action-based saponification model is recommended for use in large scale sewer system network models to determine the most susceptible FOG accumulation zones or “hotspots” where maintenance is needed to prevent potential SSOs.

Quantifying Fat, Oil, and Grease (FOG) Deposits Formation Kinetics

by
Most. Mahbuba Iasmin

A dissertation submitted to the Graduate Faculty of
North Carolina State University
in partial fulfillment of the
requirements for the degree of
Doctor of Philosophy

Civil Engineering

Raleigh, North Carolina

2014

APPROVED BY:

_____	_____
Dr. Joel Ducoste Committee Chair	Dr. Francis de los Reyes
_____	_____
Dr. Michael Leming	Dr. Lisa Dean

DEDICATION

I dedicate my dissertation work to my loving family.

BIOGRAPHY

Mahbuba Iasmin earned her Bachelor of Civil Engineering degree from Bangladesh University of Engineering and Technology in June, 2007. She earned her Master in Environmental Engineering degree from the same university in August, 2009. Later in the same month of 2009, she joined the doctoral program in civil engineering at North Carolina State University.

While pursuing for the doctoral degree, Mahbuba worked as Graduate Research and Teaching Assistant for the department of Civil, Construction, and Environmental Engineering. She was also a Preparing for the Professoriate (PTP) fellow in the calendar year 2012-2013, mentored by Dr. Ducoste, as part of Preparing Future Leaders (PFL) program at NC State.

During the course of her graduate study at NC State, Mahbuba presented her research in local and regional conferences. Her research was accepted in Water Research Journal and she also co-authored in papers published in Environmental Science and Technology. Mahbuba wishes to continue her career in research and teaching in the field of environmental engineering.

Mahbuba's dissertation topic, Quantifying Fat, Oil, and Grease (FOG) Deposits Formation Kinetics, was supervised by Dr. Joel Ducoste.

ACKNOWLEDGMENTS

It is a pleasure to thank the many people who made this dissertation possible.

It is difficult to overstate my gratitude to my PhD advisor, Dr. Joel Ducoste. With his motivation, enthusiasm, and great efforts to explain things clearly and simply, I really enjoyed this work. I am immensely grateful for his continuous guidance and support throughout my doctoral study and research. I could not have imagined a better advisor and mentor.

Besides my advisor, I would like to thank the rest of my dissertation committee: Dr. Francis de los Reyes, Dr. Michael Leming, and Dr. Lisa Dean, for their encouragement, time, and help throughout the course of the study.

My sincere gratitude also goes to Dr. Simon Lappi, David Black, Jake Rhodes, Punith Naik, and Dr. Walter Weare for their help and support during the course of this study.

I thank my fellow lab-mates for the wonderful times we spent together: Erin Gallimore, Yi Wang, Chris Dominic, Colleen Bowker, Roya Yousefelahiyeh, Tony, David, Nandita, Siddharth, and Jun Meng.

I feel fortunate to have family, in-laws, and friends who were there for me at the good and difficult times, had faith in me, and encouraged me in all my endeavors.

This section would be incomplete without the two persons in my life: my husband Raashed and my father, who were my constant guidance and consolation during this journey – one in real life and the other as a shadow.

TABLE OF CONTENTS

LIST OF TABLES

CHAPTER 3 Materials and Methods

CHAPTER 4 Factors that influence properties of FOG deposits and their formation in sewer collection systems

CHAPTER 5 Quantifying Fat, Oil, and Grease deposit formation kinetics in Sewer Collection Systems

CHAPTER 6 Effects of initial free fatty acids, detergents, and lipase on kinetics of fat, oil, and grease deposit formations in sewer collection systems

LIST OF FIGURES

CHAPTER 2 Literature Review

CHAPTER 3 Materials and Methods

CHAPTER 4 Factors that influence properties of FOG deposits and their formation in sewer collection systems

Appendix S

CHAPTER 6 Effects of initial free fatty acids, detergents, and lipase on kinetics of fat, oil, and grease deposit formations in sewer collection systems

Appendix S

CHAPTER 1 Introduction

Fat, oil, and grease (FOG) deposits are calcium based saponified solids that can clog sewer systems and eventually cause sanitary sewer overflows (SSOs). SSOs can pose significant threat to public health due to the exposure of pathogens and other harmful contaminants. Since 2007, USEPA has set a requirement to public water treatment facilities to spend 15 billion dollars on new pipes and wastewater infrastructure to control overflows. The investments on new pipes are necessary to cope with the wastewater produced due to the increasing population size. However, the fundamental understanding of the formation of FOG deposits and their kinetics based on the source and environmental conditions in sewer systems is still unclear. Therefore, the objective of this study was to identify and investigate potential source and environmental factors that may affect the FOG deposit formations and their kinetics. In addition, the current study also evaluated potential empirical models from literature and developed a mathematical model based on mass action principles that can capture the kinetics of FOG deposit formation process.

The thesis is divided in the following chapters. Chapter 2 provides a literature review and background information about the fundamentals of FOG deposit formation. It explains the fat saponification process and discusses the source and environmental factors in sewer systems that may potentially affect fat saponification, and therefore, the FOG deposit formation process. Chapter 2 also provides background information about Fourier transform infrared (FTIR) spectral analysis that was used to quantify the formation of calcium-based saponified solids. Later, this chapter discusses the available empirical models that may potentially explain the fat saponification process.

Chapter 3 presents the materials and methods used in this research study. It discusses the sources of the materials, the experimental setup, and details of the methods adopted, i.e., FTIR spectral analysis, minerals and metal analysis, fatty acid profiling, and methods to determine the rheological properties of calcium-based saponified solids.

The results of the current study are presented in journal format in Chapters 4 - 6. To date, the results have been partially published in Environmental Science and Technology by He et al. (2011). The results presented in Chapter 4 have also been accepted in Water Research Journal and proofs have been reviewed for final publication. Chapter 4 discusses the factors that influence the properties of FOG deposits and their formation in sewer collection systems. Factors that are discussed include types of fats used in food service establishments (FSEs), types of calcium sources (i.e., calcium chloride and calcium sulfate), and the environmental factors, i.e., pH and temperature in sewer systems that may affect the FOG deposit formation. The physical, chemical, and rheological properties of the saponified solids are discussed.

Chapter 5 describes the quantification of FOG deposit formation kinetics in sewer systems. The kinetics of saponified solids quantified under different source and environmental conditions are compared. Two empirical models, Cotte et al. (2006) saponification model and Foubert et al. (2002) crystallization model along with a mass-action based saponification model were investigated to predict the kinetics. The quantification of the model parameters was performed using a hybrid scheme which combined a heuristic optimization known as particle swarm optimization (PSO) with a gradient-based search algorithm (fmincon). The trends in the model parameters are discussed and the relationships between the model parameters and experimental conditions have been determined using JMP Pro, a statistical software.

Chapter 6 focuses on the effects of initial free fatty acids (FFAs), detergents, and lipase on the formation of calcium based saponified solids. The chapter also describes the effects of mixing intensity under well-mixed a environment to investigate its effect on the kinetics of FOG deposits. The results related to the fatty acid profiles and FTIR spectra of the saponified solids are primarily discussed. The chapter concludes with the possible modifications in the FSE operations that can help reduce the FOG deposit formation process without compromising food quality, public health, and sanitation.

Chapter 7, conclusions and recommendations, summarizes and highlights the important results presented in Chapters 4-6. The recommendations for the future work are also discussed to further enhance the scope of the study.

References

Cotte, M., Checroun, E., Susini, J., Dumas, P., Tchoreloff, P., Besnard, M. (2006). Kinetics of oil saponification by lead salts in ancient preparations of pharmaceutical lead plasters and painting lead mediums. *Talanta, 70*(5), 1136-1142

Foubert, I., Vanrolleghem, P. A., Vanhoutte, B., & Dewettinck, K. (2002). Dynamic mathematical model of the crystallization kinetics of fats. *Food Research International, 35*(10), 945-956

He, X., Iasmin, M., Dean, L. O., Lappi, S. E., Ducoste, J. J., & de los Reyes III, F. L. (2011). Evidence for fat, oil, and grease (FOG) deposit formation mechanisms in sewer lines. *Environmental Science & Technology*, *45*(10), 4385-4391

CHAPTER 2 Literature Review

1 Introduction

Fat, oil, and grease (FOG), generated daily from commercial food service establishments (FSEs) can accumulate in sewer systems as hardened grease deposits and is responsible for approximately 25 to 35% of annual sanitary sewer overflows (SSOs) in United States (Southerland, 2002; Ducoste et al., 2008). SSOs are mainly untreated discharges that contain harmful contaminants, which can significantly impact both environmental and public health (EPA, 2004). Researchers have found that FOG deposits contain mostly saturated fats, with palmitic being the primary fatty acid, and calcium being the primary metal in the majority of FOG deposit samples in sewer systems (Ducoste et al., 2008; Keener et al., 2008). Consequently, researchers have hypothesized that the formation of FOG deposits may be a result of a well known soap-making chemical reaction process called saponification (Keener et al., 2008). However, Keener et al. lacked experimental evidence showing that FOG from FSEs react with calcium ions typically found in the sewer systems to form calcium-based fatty acid salts or FOG deposits. Recently, He et al. (2011) demonstrated a strong similarity between laboratory-based calcium salts of fatty acids and laboratory-based FOG deposits, using Fourier Transform Infrared Analysis-Attenuated Total Reflection (FTIR-ATR) method. Later, He et al. (2013) also hypothesized that the un-reacted oil in the sewer systems acts more as a carrier than as a source of free fatty acid for the saponification reaction. He et al. suggested that FOG deposit formation process could be a result of a two-step process: a) aggregation of excess calcium (more than needed for the stoichiometric saponification reaction) and the free fatty acid micelles following double layer compression and b) saponification reaction between aggregated calcium and free fatty acid. Keener et al. (2008) also found that the calcium concentrations in the FOG deposits are significantly higher than the water hardness level in sewer systems. The excess calcium in the concrete sewer system may be a result of a process known as Microbiologically Induced Concrete Corrosion (MICC) that can lead to the formation of solid FOG deposits (Parker, 1945a & b; Biczok,

1967; Gutiérrez-Padilla, 2010; Bielefeldt et al., 2010). Research studies performed to date have proven that the formation of solid FOG deposits can be the result of a saponification process. However, the effects of sewer environmental conditions (such as, pH and temperature), possible sources of calcium and fat types that can affect the FOG deposit formation process as well as its kinetics are still unknown. Therefore, the goal of this study is to investigate the roles of potential sources of calcium, pH, temperature, and fat types on the FOG deposit formation process and its kinetics.

2 Fat Saponification and its Kinetics

2.1 Fat Saponification

Fat saponification has been well characterized in the literature and is described simply as the reaction between fats, oils, free fatty acids (FFAs), or methyl esters and an alkali solution. These products (i.e., soaps) are monovalent salts of carboxylic acids that have a general structure RCO_2M, where R is straight chain aliphatic group of carbon chain lengths between C12 and C18, and M represents a cation produced from the reaction with the alkali group (Hui, 1996). The application of the alkali solution directly to fats and oils is considered direct saponification while adding alkali to FFAs is considered FFA neutralization. The third approach of soap formation involves first reacting fats and oils with alcohol (i.e. a process called esterification) to form methyl esters, which is then reacted with alkali solution. Home-made soaps are prepared under room temperature conditions and high alkali content environment, which is known as cold saponification. Cold soaps are usually of water-in-oil type and presumably produced by neutralization of the fatty acid present in oil (Smith, L., 1932). The strong similarities in the chemical constituents of hand-made soaps and FOG deposits (i.e. fat/fatty acids, metal, and alkali/base) observed by Ducoste et al. (2008) suggest the need to perform direct saponification or FFA neutralization experiments. A possible strategy for understanding FOG deposit formation kinetics is to first understand soap formation kinetics.

Smith (1932) provided the first comprehensive experimental assessment of the kinetics of direct fat saponification or FFA neutralization for soap formation. Smith found that the kinetics of soap formation from direct saponification or FFA neutralization generally took the form of an "S" shape curve, which suggests that there is an induction period, a rapid reaction period, and finally a retardation period (Figure 2). Smith concluded that the process of fat saponification to produce soaps is a homogeneous process that occurred in the soap phase, which is in contact with both the aqueous alkali and oil. The process begins with the oil and lye solution being vigorously mixed to produce an emulsion that Smith believes is stabilized by particles of soap initially formed by saponification. Once 25-30% of the stoichiometric of soap has been formed, the process becomes autocatalytic (i.e., as more product soap is formed, more of the oil and alkali can be absorbed by the soap and allow the saponification process to continue). The process slows down once the available oil has been completely absorbed in the soap phase.

Poulenat et al. (2003) performed a FTIR spectroscopic analysis of sunflower oil saponification kinetics. Poulenat et al. confirmed the "S" shaped saponification kinetics found in Smith (1932) and described the induction period where intense mixing is required to facilitate an oil-alkali emulsion that is stabilized by soap particles. The oil-alkali interface was suggested as the limiting factor that controlled saponification.

Cotte et al. (2006) investigated the kinetics of lead soap formation from saponification that included the impact of lead salt type (PbO, $PbCO_3$, Pb_3O_4, PbS, PbOHCl, and $Pb_2CO_3Cl_2$), temperature (100-180 °C), and the presence of water on the saponification kinetics. They found that the presence of water when PbO was used at 100°C increased the amount of soap formed from below 10 to 95 percent of the stoichiometric amount within two hours of reaction. The PbO soap kinetics also displayed an "S" shaped curve as seen by Smith (1932) and Poulenat et al. (2003). While investigating alternate lead salts, Cotte et al. found that only PbO and Pb_3O_4 were able to produce measurable soap formation (95% for PbO within two hours and 63% for Pb_3O_4 within three hours). All other lead salts produced less than 3% of the stoichiometric amount. The lack of soap formation for these other lead salts and a

lower formation for Pb_3O_4 has been attributed to the lower pH of the aqueous solution at the start of the saponification. High temperature and high pH conditions are favorable to complete fat hydrolysis and faster soap formation. Soaps are generally initiated in higher pH environments to produce near stoichiometric amounts in a short time frame (Mohr, 1979).

The analysis performed by Smith (1932), Poulenat et al. (2003), and Cotte et al. (2006) have demonstrated the complexity of the soap formation process and have provided some insight into parameters that need to be explored in the possible saponification process for FOG deposit formation.

2.2 Source and Environmental Parameters

Evaluating the kinetics of FOG deposit formation is necessary to understand their rate of formation under the environmental conditions available in the sewer systems. Literature reviews suggest that the possible environmental parameters affecting kinetics of FOG deposit formation are mixing conditions, temperature, pH, and the type of fat (Ducoste et al., 2008). Studies performed to date have indicated that the rate of saponification may be influenced by the rate of stirring and the subsequent consistency of the emulsion (Norris and McBain, 1922). Industrially manufactured soaps are usually prepared under boiling conditions, such as 100 °C (Smith, 1932). However, temperatures that are typically observed in sewer systems range from 5-25 °C (Ducoste et al., 2008). While temperatures in GI may reach 45 °C, they still do not rise to the level of traditional saponification practices. FSEs also use alkaline detergents (pH >10), degreasers, and sanitizers, which may perform as an oxidizer to promote saponification (Ducoste et al., 2008). Therefore, experiments need to be performed that investigate how these non-traditional saponification conditions influence the rate of FOG deposit formation.

There are a variety of cooking oils in use by FSEs with a wide range of fatty acid compositions (saturated, mono-unsaturated, and poly-unsaturated). However, the saturated

fat content of FOG deposits has been observed to be well above the values found in many common cooking oils and animal fats (i.e., values for oils ranged from 7-20%; animal fats ranged from 33-48%; and FOG deposits have a range of 20-90%) (Ducoste et al., 2008). These results suggest that there may be either a selective incorporation of these saturated fatty acids or an alternative fate of unsaturated fatty acids that does not allow for their inclusion in FOG deposits. Therefore, it may be important to determine the influence of type of fat in the formation of fatty acid salts.

Matsui et al. (2005), while examining biological treatment of wastewater from restaurant kitchens using an immobilized bioreactor, noted that unsaturated fatty acids following initial triglyceride hydrolysis by lipase may be preferentially broken down through beta-oxidation by microorganisms. The preferential consumption of these unsaturated fatty acids consequently leaves behind saturated fatty acids in wastewater that can react with calcium to form solid tacky substances, calcium di-stearate and di-palmitate. Recently, He (2011) also demonstrated lipolytic activity in the anaerobic environment of the GIs. It's possible that these biological processes contribute to altering the fate and transport of unsaturated FFAs in the sewer collection system and can possibly explain the significant accumulation of palmitic in FOG deposits. Therefore, exploration of lipase driven hydrolysis is needed to find its contribution in the FOG deposit formation process.

FOG deposit samples display tacky and adhesive-like characteristics along with visual characteristics, such as layering effects that are attributed to the fluctuating flow profile as observed in restaurants, industrial waste discharges, and frequency of wet weather events (Keener et al., 2008). Keener et al. mentioned that the moisture content may not be a primary factor in the FOG deposit formation process due to its wide variation in FOG samples, i.e. 6 to 86%. FOG deposit samples were also found to display a sandstone-like structure, grainy and hard, suggesting a porous, rigid structure that developed with time in the presence of debris accumulated in the voids. The appearance of FOG deposits in sewer systems seems quite similar to cave stalactites as can be seen in Figure 1. To better understand how these

FOG deposits form, we need to investigate the physical properties of metallic salts of fatty acids, such as their rheological properties.

Figure 1 FOG deposits formed in sewer systems (Southern water, UK)

2.3 FTIR in kinetics of Saponified Solids Formation

Poulenat et al. (2003) used the FTIR-ATR spectroscopic technique to determine the kinetics of high-oleic sunflower oil saponification. Relative quantity of soap vs. remaining triacylglycerol (TAG) has been computed using absorbances of the metallic carboxylate group and metal-oxygen absorption bands based on a method followed by Putinier (1970) as shown in Equation 1. Sherman (1997) has suggested dividing the infrared spectrum into two parts for better identification of the spectrum. The first part (wave numbers between 4000 and 1500 cm^{-1}) aids in identifying the various functional groups. The second part (wave numbers between 1500 and 600 cm^{-1}) called the fingerprint region, represents the

characteristic vibrations of the molecule as a whole. Sherman (1997) and Lee (1997) mentioned that the fingerprint region is usually complex and displays a unique pattern for each organic compound. Poulenat et al. (2003) chose four specific regions to identify the characteristic bands of oleic soaps, three (region 1 at 4000-2800 cm^{-1}; region 2 at 1800-1350 cm^{-1}; and region 3 at 1350-1180 cm^{-1} and near 720 cm^{-1}) being in the sodium chloride region and the fourth (670-440 cm^{-1}) in the potassium bromide region. Three modes of vibration attributed to carboxylate bonds of metallic salts of fatty acids can be observed while soap is present in a FTIR sample, apart from the metal-oxygen bond at or around 670 cm^{-1}: 1) the symmetric stretching vibration, ω_1, between 1300 and 1420 cm^{-1}, 2) the asymmetric stretching vibration, ω_2, between 1550 and 1610 cm^{-1}, and 3) a bending vibration, ω_3, between 950 and 800 cm^{-1} (Poulenat et al., 2003; Sherman, 1997). However, Poulenat et al. (2003) only used the asymmetric stretching vibration, ω_2 in computation of relative soap formation since the absorbance value in this region was the strongest in their study. Literature reviews suggest that the FTIR-ATR technique is well suited for examining fat saponification and therefore will be adopted in this study to determine the relative soap formation at each time location.

$$\%\, soap = \frac{soap\ absorbance}{soap\ absorbance + TAG\ absorbance} \quad (1)$$

2.4 Modeling Fat Saponification Kinetics

As discussed earlier, literature reports have suggested that the saponification reaction has an autocatalytic nature and follow a typical "S" shape curve as shown in Figure 2. The "S" shape profile begins with an initial induction period followed by a sharp rise due to autocatalytic reaction and reaches the maximum due to limiting reaction constituents (Smith, L., 1932; Jones, 1958; Poulenat et al., 2003; Cotte et al., 2006). Smith (1932) and Poulenat et al. (2003) however did not propose a model to capture the "S" shaped kinetics. There is also a lack of kinetics models in the literature that have focused their application to calcium soap formation. Cotte et al. (2006) modeled soap formation using PbO and additionally, a few

crystallization models are available that also followed “S” shaped kinetics. It is hypothesized that calcium based fatty acid salts will likely undergo this “S” shaped kinetics. A detailed description of these two models is provided in the following sections.

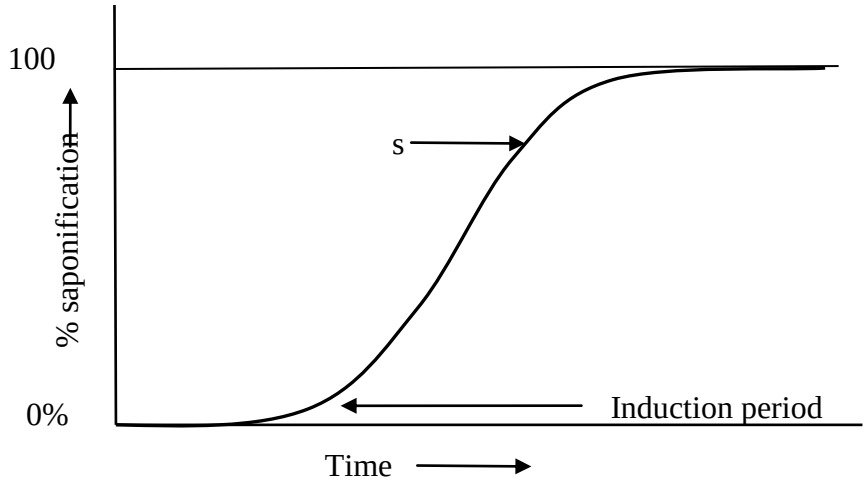

Figure 2 Typical saponification curve: Percent saponification vs time (Jones, L.D., 1958)

2.4.1 Fat Saponification Models

Cotte et al. (2006) proposed a model that characterizes the entire experimental ‘S’ shape kinetics of triolein saponification by lead salts, at temperatures ranging from 100 to 180°C. In Cotte et al.’s model, a two-step reaction process was proposed that involved: 1) a slow dissolution of metal salt in an aqueous solution and 2) the reaction between the dissolved metal species (D) and the oil (O) to form soap (S) and an alcohol (A) by-product (Equations 2 and 3).

$$L \rightarrow D \ (k_1) \tag{2}$$

$$D + O \rightarrow S + A \ (k_2) \tag{3}$$

The final differential equation for the formation of soap was described as follows (Cotte et al., 2006):

$$\frac{df}{dt} = k_2[r_0\{1 - exp(-k_1 t)\} - f](1 - f) \quad (4)$$

$$r_0 = k_3 \frac{m^0_{metal}/M_{metal}}{m^0_{oil}/M_{oil}} \quad (5)$$

where k_1, k_2, and k_3 are fitting parameters, r_0 is the initial metal salt/oil molar ratio, m^0 are the initial masses of metal salt and oil, and M are molar masses of metal salt and oil. Cotte et al. found the model to fit the aqueous PbO data well.

2.4.2 Fat Crystallization Models

Three alternative fat crystallization models have been reported in the literature: the Avrami equation (Metin and Hartel, 1998), re-parameterized Gompertz equation (Kloek et al., 2000), and Foubert model (Foubert et al., 2002). Avrami equation assumes that a dispersed phase is nucleated by small germ nuclei that already exist in the liquid phase. As the process moves forward, the number of germ nuclei decreases over time from consumption by the growing grains of the new phase (Avrami, 1939, 1940). The Avrami equation can be described as follows:

$$f(t) = c\left(1 - e^{-kt^n}\right) \quad (6)$$

where $f(t)$ is the percent solid fat content, c is the maximum percent solid fat content, k is the crystallization rate constant, and n is the Avrami factor that accounts for the nucleation time dependence and the number of dimensions that crystal growth occurs. Equation 6 can describe the rapid reaction period and the final retardation period but is unable to account for the possible initial slow induction period. A simple correction has been applied to Equation 6 by subtracting an induction time (t_{ind}) from t to describe the delay in crystallization

(Rogowski, 2005). Kloek et al. (2000) used a re-parameterized Gompertz equation (Equation 7) to predict crystallization:

$$f(t) = a_G exp\left\{-exp\left[\frac{\mu_e}{a_G}(\lambda - 1) + 1\right]\right\} \quad (7)$$

where *f(t)* is the amount of crystallization at time *t*, a_G is the maximum crystallization fractions, *e* is a constant (2.718), μ is the maximum rate in the rapid reaction period, and λ is the length of the induction period.

Foubert et al. (2002) developed a crystallization model based on Wunderlich (1990) phase transition chemical reaction and has the potential to describe fat saponification:

$$O(liquid) \leftrightarrow S(solid) \quad (8)$$

Wunderlich assumed that the reaction order will depend on the presence of impurities or phase distributions with different levels of perfection. In their model, Foubert et al. assumed that the crystallization process is first order and nth order, in the forward and reverse directions, respectively. The differential equation that described Foubert et al.'s model was written in terms of the remaining crystallizable fat content (*h*):

$$\frac{dh}{dt} = k_2 h^n - k_1 h \quad (9)$$

$$h = \frac{a-f}{a} \quad (10)$$

where, *f* represents the amount of solid fat and *a* represents the maximum solid fat content, k_1 and k_2 are the fitting parameters.

In Equation 9, Foubert et al. did not provide any theoretical justification for the reaction to proceed in reverse, but speculated that it may be related to the re-melting of some crystals due to the dissipation of latent heat of crystallization. Foubert et al.'s model was compared with the reparameterized Gompertz model and Avrami model and was found to better

capture the asymmetry in ‘S’ shaped kinetics curves, which Smith (1932) has also noted in his research.

It may be possible to use Wunderlich’s approach to describe fat saponification as it relates to FOG deposit formation where *h* describes the remaining oil content, and *f* describes the amount of FOG deposit. As with Foubert et al., it may not be clear at present what would cause the FOG deposit formation reaction to be reversible. However, research performed by Jandacek (1991) showed that calcium soaps (calcium palmitate, calcium laureate, and calcium oleate) were 16-53% soluble in the presence of liquid fatty acids, particularly oleic. Consequently, the existence of free fatty acids in the presence of FOG deposits may cause some dissolution of the deposit and therefore the possibility of a reversible FOG deposit formation reaction.

In summary, Cotte et al. (2006) provided a direct modeling framework to simulate the kinetics of fat saponification while Foubert et al. (2002) developed a model based on Wunderlich (1990) phase transition approach that may be extended to modeling metal soaps formed by fat saponification. Both models have the potential for simulating the FOG deposit formation kinetics once it has been determined experimentally. However, it is important to note that none of the abovementioned models provides a way of tracking potential reactant constituents as well as process intermediates that are typically involved in the saponification process, i.e., fat, free fatty acids, and metal concentrations. Such a model would provide more information into the process of FOG deposit formation, specifically when there would be limits placed on precursor reactants to reduce the potential for FOG deposit accumulation.

3 Effect of Concrete Corrosion in FOG deposit formation

Microbiologically induced concrete corrosion (MICC) is a well-known phenomenon where deterioration of concrete occurs with the presence of sulfur reducing bacteria (SRB) and sulfur oxidizing bacteria (SOB), respectively. This biogenic corrosion leads to leaching of

calcium as well as other ions, such as $SO_4^{2-}$and OH^- from inner concrete surface. Research studies have shown that while exposed to bacteria, the corrosion rate of concrete can be as high as 0.208 mm/yr depending upon the type and strength of the concrete (Gutierrez-Padilla et al., 2010). Research studies have also reported that the microbial acid attack can release 28 mg of calcium and 47 mg of sulfate per gm of concrete under pH 3.0 conditions (Bielefeldt et al., 2010). Keener et al. (2008) observed that the calcium levels in FOG deposits were well above the levels of water hardness and a preferential accumulation of calcium occurs. This phenomenon of preferential selection suggests the presence of another potential source of calcium, which may be significantly contributing to FOG deposit formation, apart from the wastewater itself. Therefore, research is needed to understand whether calcium leaching out of concrete due to possible biogenic corrosion as well as calcium from water hardness takes part in saponification.

4 Research questions

This research will seek to provide answers to the following research questions:

a. The liquid/solid fat can undergo alkali hydrolysis under sewer environmental conditions and form calcium-based fatty acid salts, i.e., calcium-based saponified solids. The FOG deposit formation process may vary with the type of fat or calcium source under varying environmental conditions (pH and temperature). Therefore, does the source of fat or calcium impact alkali driven hydrolysis during the formation of FOG deposits?
b. The kinetics of FOG deposits may be affected by sewer environmental conditions, such as pH and temperature. How fast do the FOG deposits form within the environmental conditions that are typically found in sewer collection systems?
c. Can a model be developed that can capture the kinetics of FOG deposits?
d. Does the change in mixing conditions affect the kinetics of FOG deposits?

e. Can the presence of initial free fatty acids produced in food service establishments (FSEs) or grease interceptors (GIs) due to their maintenance pump-out frequencies affect the FOG deposit formation process?
f. Can lipase activity in grease interceptors affect the FOG deposit formation process?

5 Objectives of the current study

To determine the solutions of the research questions above, the objectives of the present study include laboratory scale experimental tests related to characterizing the kinetics of Fat, Oil, and Grease (FOG) deposit formations based on fat/oil types, environmental conditions, such as pH and temperature, calcium source types, presence of initial free fatty acids, and presence of detergents under different mixing conditions. The variables in the research matrix are as follows:

1. Fat/oil type (Canola oil vs. Beef tallow)
2. pH (7, 10, and ≈14)
3. Temperature (22 °C and 45 °C)
4. Calcium source type (Calcium chloride vs. Calcium sulfate)
5. Mixing intensity (230 rpm and 460 rpm)
6. Presence of initial free fatty acid (0.5 %wt and 10 %wt of source fat types: palmitic and linoleic acid)
7. Presence of detergents (0.05 %wt and 5 %wt of source fat; types: anionic and non-ionic detergents)
8. Presence of lipase (*Candida rugosa*)

Final saponified solids were analyzed for calcium, fatty acid compositions, and their rheological properties. Cotte et al. (2006) saponification model and Foubert et al. (2002) crystallization model will be applied to the experimental results to determine the kinetic

parameters under the tested operating conditions. The kinetics of the saponified solids will also be compared with a proposed mathematical model that has been developed based on mass action principles of alkali hydrolysis of triglyceride and saponification of free fatty acid and free calcium ions.

References

Biczók, I., & Szilvássy, Z. (1964). Concrete corrosion and concrete protection *Akadémiai kiadó*

Bielefeldt, A., Gutierrez-Padilla, M. G. D., Ovtchinnikov, S., Silverstein, J., & Hernandez, M. (2010). Bacterial kinetics of sulfur oxidizing bacteria and their biodeterioration rates of concrete sewer pipe samples. *Journal of Environmental Engineering*, 136, 731

Cotte, M., Checroun, E., Susini, J., Dumas, P., Tchoreloff, P., Besnard, M., (2006). Kinetics of oil saponification by lead salts in ancient preparations of pharmaceutical lead plasters and painting lead mediums. Talanta,70(5), 1136-1142

Ducoste, J. J., Keener, K. M., Groninger, J. W., & Holt, L. M. (2008). Fats, roots, oils, and grease (FROG) in centralized and decentralized systems. *Water Environment Research Foundation.*IWA Publishing, London

Report to Congress: Impacts and Control of CSOs and SSOs (2004). *U.S. Environmental Protection Agency*

Foubert, I., Vanrolleghem, P. A., Vanhoutte, B., & Dewettinck, K. (2002). Dynamic mathematical model of the crystallization kinetics of fats. Food Research International, 35(10), 945-956

Gutiérrez-Padilla, M. G. D., Bielefeldt, A., Ovtchinnikov, S., Hernandez, M., & Silverstein, J. (2010). Biogenic sulfuric acid attack on different types of commercially produced concrete sewer pipes. *Cement and Concrete Research*, 40(2), 293-301

He, X., Iasmin, M., Dean, L. O., Lappi, S. E., Ducoste, J. J., and de los Reyes III, F.L. (2011). Evidence for fat, oil, and grease (FOG) deposit formation mechanisms in sewer lines. *Environmental Science and Technology*, 45(10), 4385-4391

He, X. (2011). Characterization of grease interceptors for removing fat, oil, and grease (FOG) and mechanisms of FOG deposit formations in sewer systems. PhD dissertation. North Carolina State University

He, X., de los Reyes III, F. L., Leming, M. L., Dean, L. O., Lappi, S. E., and Ducoste, J. J. (2013). Mechanisms of Fat, Oil and Grease (FOG) Deposit Formation in Sewer Lines. *Water Research*, *47*(13), 4451-4459

Hermansyah, H., Kubo, M., Shibasaki-Kitakawa, N., & Yonemoto, T. (2006). Mathematical model for stepwise hydrolysis of triolein using candida rugosa lipase in biphasic oil–water system. *Biochemical Engineering Journal*, 31(2), 125-132.

Hsu, C. P. S. (1997). Infrared spectroscopy. *Handbook of Instrumental Techniques for Analytical Chemistry*, 249

Jones, L. D. (1958). Saponification stressing the newer methods. *Journal of the American Oil Chemists' Society*, 35(11), 630-634

Keener, K.M., Ducoste, J.J., Holt, L.M. (2008). Properties influencing fat, oil, and grease deposit formation. *Water Environment Research*, 80, 2241-2246

Lee, M. (1997). TECH 710/ Identifying an unknown compound by infrared spectroscopy. Modular Laboratory Program in Chemistry. *Chemical Education Resources, Inc.* Pennsylvania, USA

Mohr, M. S. (1979). The art of soapmaking: A complete introduction to the history and craft of fine soapmaking: Complete recipes for hand soaps, herbal shampoos, natural toothpaste, vegetarian soap, laundry soap, and many rich and fragrant homemade soaps *Camden House Pub*

Norris, M. H., & McBain, J. W. (1922). CLXII.—A study of the rate of saponification of oils and fats by aqueous alkali under various conditions. J.Chem.Soc., Trans., 121, 1362-1375

Parker, C. (1945a). The corrosion of concrete I: The isolation of a species of bacterium associated with the corrosion of concrete exposed to atmospheres containing hydrogen sulfide. *Aust. J. Exp. Biol. Med. Sci.*, 23(2), 81-90

Parker, C.D. (1945b). The corrosion of concrete 2. The function of Thiobacillus-Concretivorous (Nov-Spec) in the corrosion of concrete exposed to atmospheres containing hydrogen sulfide. *Aust. J. Exp. Biol. Med. Sci.*, 23(2), 91-98

Poulenat, G., Sentenac, S., & Mouloungui, Z. (2003). Fourier-transform infrared spectra of fatty acid salts—Kinetics of high-oleic sunflower oil saponification. *Journal of Surfactants and Detergents*, 6(4), 305-310

Putinier, R. (1970). The quantitative analysis of components in lubricating greases by differential infrared spectrophotometry. *NGLI Spokes*, 34, 204

Smith, L. (1932). The kinetics of soap making. Transactions and Communications. *Journal of the Society of Chemical Industry*, pp 337-348

Southerland, R. (2002). Sewer fitness: Cutting the fat. *American City and Country*, 117(15), 27-31

Wunderlich, B. (1990). Thermal Analysis. *New York: Academic Press*

CHAPTER 3 Materials and Methods

The materials and methods presented in this chapter were used to complete the research objectives described in Chapter 2. In this chapter, the sources of the materials used, the experimental setup, and the details of the methods adopted in determining the physical, chemical, and rheological properties of the calcium-based saponified solids (i.e., FOG deposits) were discussed. Fourier Transform Infrared (FTIR) spectral analysis was used in identification and quantification of the fractions of saponified solids. The EPA 200.7 method for trace elements in water, solids, and biosolids was used in measuring the minerals and metals present in saponified solids. The fatty acid profiles of the saponified solids were determined using an official method, AOCS Ce 2-66. The method related to the determination of the rheological properties of saponified solids is also presented. Finally, the modeling methods are discussed in detail later in this chapter.

1 Research Design

1.1 Materials

Two kinds of fats were used in this research study: a) Pure Wesson Canola Oil (total fat 14g, 22%; saturated fat 1g, 5%; trans fat 0g; poly unsaturated fat 3.5g; mono unsaturated fat 8g, cholesterol 0%, sodium 0%, total carbohydrate 0%, and protein 0%) made by ConAgra Foods, Omaha, NE and b) Finest quality Beef Tallow (rendered tallow; Acid-Less 43.5 Grade; Saponification(SAP) Number 195; FFA 0.30%; Essential Depot, Florida).

Three types of calcium sources were introduced in anhydrous form to perform the cold saponification process. These calcium sources are: a) Calcium chloride ($CaCl_2$, $\geq$ 93.0%, granular, 110.99 g/mol; Sigma-Aldrich, USA); b) Calcium hydroxide ($Ca(OH)_2$, 98+%, extra pure, 74.09 g/mol; Acros Organics, USA), and c) Calcium sulfate (>95%, 136.14 g/mol, powder; Fisher scientific, USA).

Sodium hydroxide (NaOH) and hydrochloric acid (HCl) were used for pH adjustment. Sodium hydroxide also acted as a catalyst for the alkali driven hydrolysis processes. Aqueous alkali solutions were prepared with de-ionized (DI) water.

1.2 Material Synthesis and Experimental Setup

A room-temperature-based saponification process was performed in preparing the calcium-based saponified solids. A 1:3 approximate molar ratio of liquid/solid fat and de-ionized water was used in all experiments based on the stoichiometric requirement for complete fat hydrolysis. More details of experimental conditions are presented in Table 1. The saturated fat (i.e. beef tallow) was only used for high temperature (45 °C) saponification processes and was initially melted before mixing the reaction constituents. A solution of sodium hydroxide and calcium chloride/calcium hydroxide in DI water was initially prepared and allowed to cool until the temperature of the solution reached 22-25°C. The liquid fat (i.e. Canola or melted Beef Tallow) was gradually added to the calcium chloride solution and slowly-mixed. The solution was stirred at 230 or 460 rpm using a Stir-Pak laboratory mix impeller (Cole-Parmer instrument). Figures 1a and 1b display the experimental setup under room and warm temperature conditions, respectively. A Sheldon water bath was adopted to achieve and maintain the desired temperature. Samples were mixed for eight hours for the kinetics experiments. Kinetic samples were collected from the reaction beaker every half an hour over the reaction period of eight hours. Samples at a higher frequency (every 15 minutes) were collected during the first hour to get a better understanding of the initial development of kinetic data.

Table 1 Experimental Conditions of the Saponification Experiment

Experimental conditions	*Value*	*Unit*	*Comment*
Temperature, T	22	°C	For liquid fat only
	45	°C	For both liquid and solid fat*
Canola oil/Beef tallow	74.7	%wt	
$CaCl_2$	9.8	%wt	-
Catalyst, NaOH	0.6	%wt	-
Water	14.9	%wt	-

**Beef tallow is solid under room temperature condition and therefore was used in high temperature condition only.*

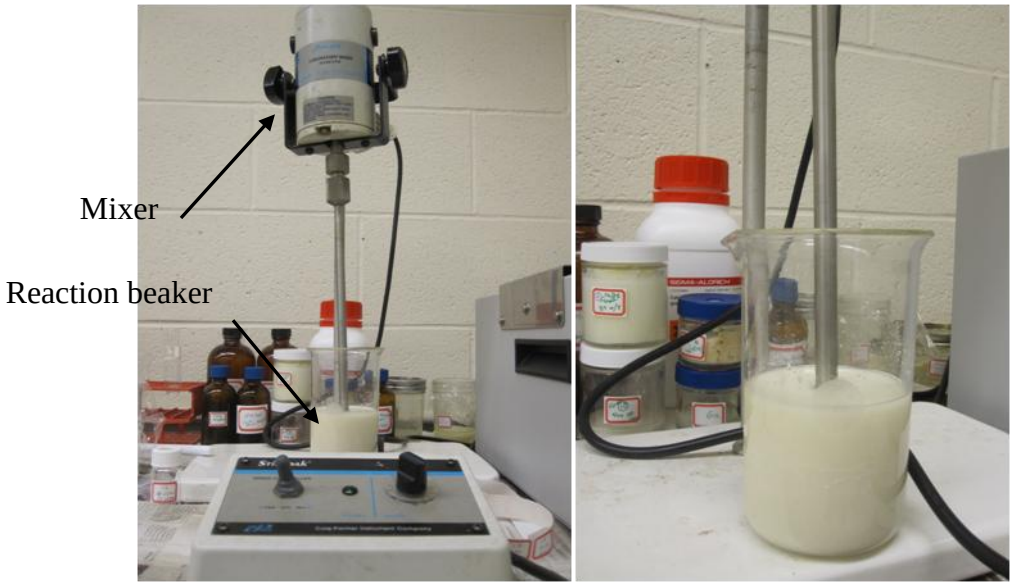

Figure 1a Experimental Setup under room temperature condition

Figure 1b Experimental set up under high temperature condition (45±0.5 °C), Front View (*left*) and Top View (*right*)

2 Methods

2.1 Fourier Transform Infrared-Attenuated Total Reflection (FTIR-ATR)

2.1.1 Instrumentation

Infrared absorption spectra of the saponified samples were obtained with a Digilab FTS-6000 Fourier Transformed Infrared (FTIR) spectrometer mounted with a crystallized Zinc Selenide (ZnSe) sampling attachment (4000-520 cm^{-1}; Pike Technologies Inc., MIRacle^{TM} Single Reflection ATR). Attenuated Total Reflection (ATR) measurement technique was adopted in determining the absorption spectra of the saponified sample. The ATR crystal characteristics used in this FTIR sampling process are shown in Table 2. The data were computed with the Bio-Rad Win-IR Pro software version 2.97 and then imported and analyzed using a data analysis and graphing software OriginPro 8.1 SRO (Pro, O. 8, 2007). The margin of error of the FTIR method is ±5%. The underlying principles of this method are presented in the following sub-section.

Table 2 ATR Crystal Characteristics for FTIR Sampling

Crystal type	ZnSe
Refraction index of the crystal, n_1	2.4
Depth of penetration, d_p, for n_2=1.5, refractive index = 1000 cm^{-1}, 45 degree, microns	2.01
Water solubility, g/100g	Insoluble
pH range	5-9
Hardness, kg/mm^2	120
Cutoff cm^{-1}, Spectral Range	520

2.1.1.1 Principles of the ATR Approach

In the ATR approach, an IR beam is directed into a crystal of relatively higher refractive index. An evanescent wave is created from the IR beam's internal reflection with the crystal. This wave then transmits orthogonally into the sample in intimate contact with the ATR crystal. Some of the energy of the evanescent wave is absorbed by the sample and the reflected radiation (some now absorbed by the sample) is returned to the detector. This ATR phenomenon is shown graphically in Figure 2.

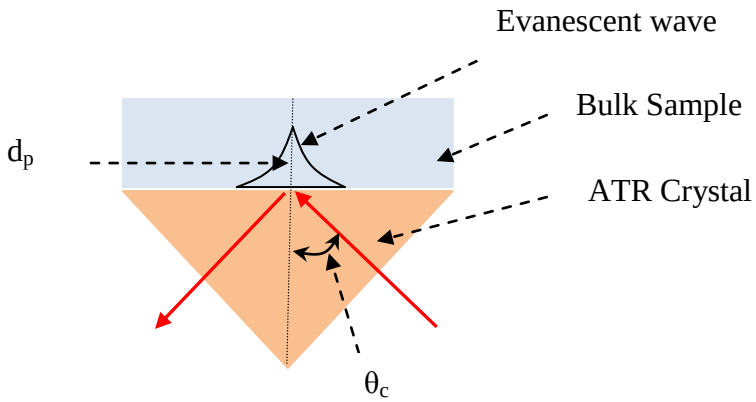

Figure 2 Graphical Representation of a single reflection ATR

Equation 1 displays the relationship between the refractive indices of the crystal and the sample, n_1 and n_2, respectively, with the critical angle, θ_c for internal reflection:

$$\theta_c = \sin^{-1} {}^{n_2}/_{n_1} \quad (1)$$

2.1.2 ATR Sampling phase

Configuration for Liquid/semi-solid sampling: A trough insert was placed on top of the reflection plate and a knurled mounting ring was used to bind the trough with the plate. The sample has then been placed inside the shallow well created around the crystal and scanning was performed subsequently. For the semi-solid samples, approximately 40 ksi (kilo-pounds per square inches) pressure was applied on the sample using a pressure clamp to ensure the best contact and highest sample sensitivity.

The sample was then carefully removed from the trough at the conclusion of the ATR analysis. Both the trough and the crystal surface were cleaned twice subsequently with ethanol and distilled water. After each cleaning, a background spectrum was taken before analyzing the new sample to eliminate cross contamination with the previous sample.

2.1.3 ATR Data Analysis Phase

OriginPro 8.1 was used in analyzing the FTIR-ATR absorbance spectra data to obtain percent saponification at each time interval. The data analysis included baseline correction followed by peak analysis. The analysis steps are as follows-

a) **Data Import**: FTIR data was first imported into OriginPro interface through Microsoft Excel 2007 for baseline correction. A line plot was performed with wave numbers (cm^{-1}) defined on the X-axis and corresponding absorbance values defined on the Y-axis. The range of interest was approximately set between 520 cm^{-1} to 4000

cm^{-1} wave numbers, the operating range of ZnSe crystal used in ATR analysis, as shown in Figure 3.

b) **Baseline Correction**: Eight data points were selected by OriginPro by default for baseline correction. The location of baseline points were modified based on two guidelines, a) original shape of the absorbance spectrum does not change significantly, and b) the baseline should include only the lowest points of a spectrum distribution. The modified data point locations for baseline correction and the final baseline corrected data are shown in Figure 4 and Figure 5, respectively.

c) **Peaks Finding**: A minimum height of twenty percent of the maximum absorbance in a single spectrum was used in finding peaks using local maximum method, a default method in OriginPro. Savitzky-Golay smoothing was performed to the spectrum data before the peak finding. Figure 6 displays the spectrum data showing the peaks at the end of the OriginPro analysis.

Peaks of the zone of interests are then selected for further computation of percent saponification using Equation 2 according to the literature reviewed in Chapter 1. Equation 2 presents relative formation of saponified solids, with the saponified solids indicator bands in the numerator, and both saponified solids and TAG indicator bands in the denominator.

$$\%\, soap = \frac{Absorbance\ in\ (670\ cm^{-1} + between\ 1300\ and\ 1420\ cm^{-1} + between\ 1550\ and\ 1610\ cm^{-1})}{Absorbance\ in\ (670\ cm^{-1} + between\ 1300\ and\ 1420\ cm^{-1} + between\ 1550\ and\ 1610\ cm^{-1} + 1745\ cm^{-1})} \quad (2)$$

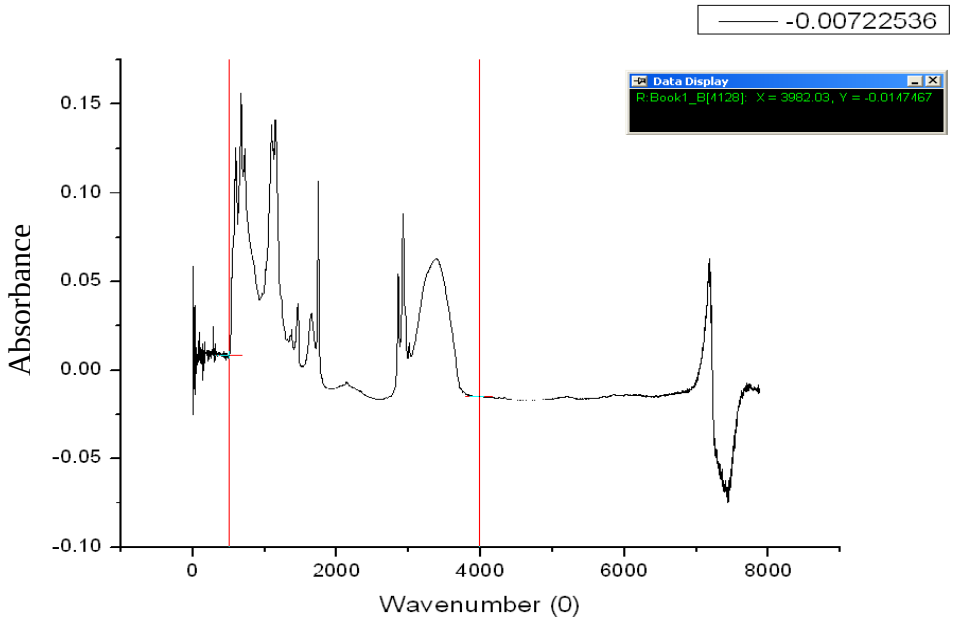

Figure 3 Selection of lower and upper ranges

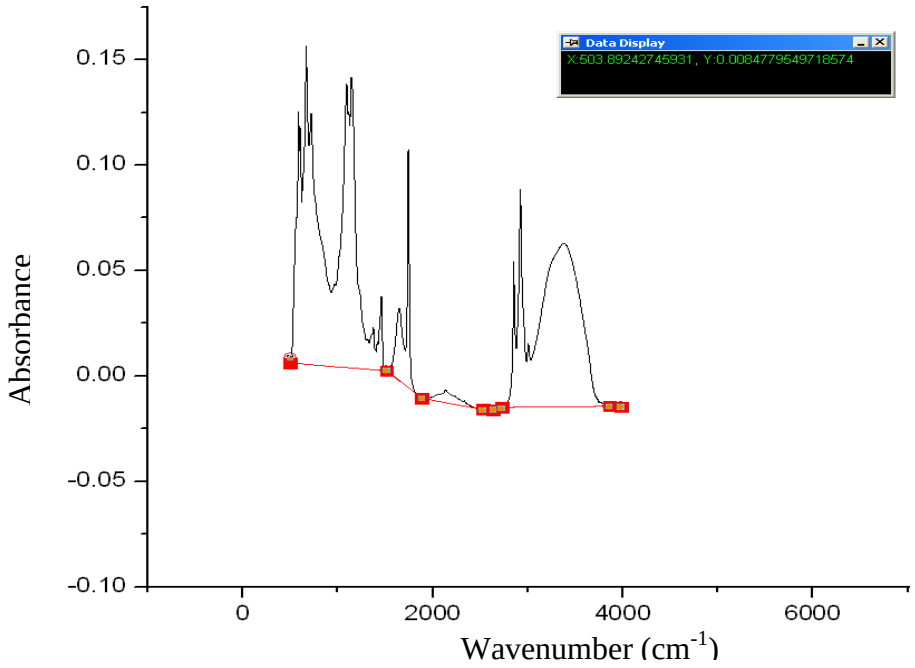

Figure 4 Spectrum showing the modified point locations for baseline correction

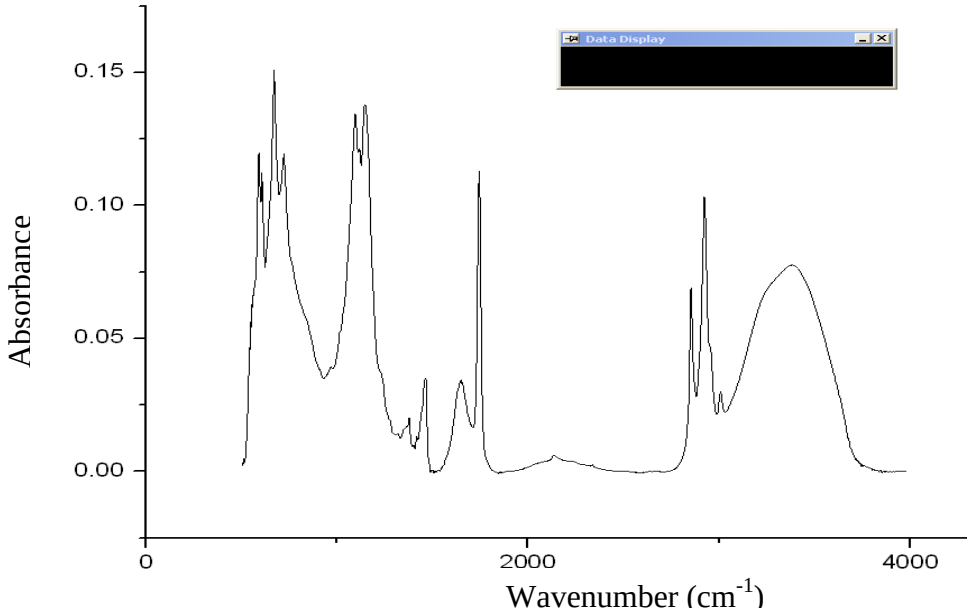

Figure 5 Baseline corrected and auto-scaled data

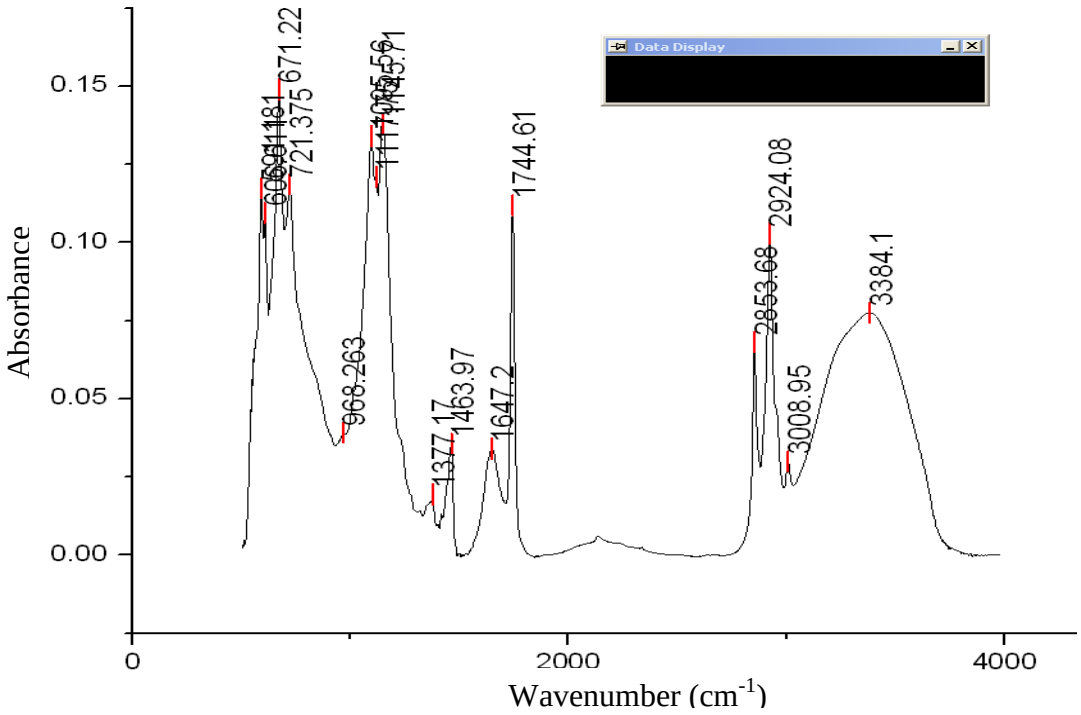

Figure 6 Spectrum showing peaks at the end of Origin analysis

2.2 Minerals and Metals Analysis

The final saponified solids were analyzed for the presence of several metals such as calcium (Ca) and sodium (Na) following the method documented in EPA 200.7 Trace elements in water, solids, and biosolids using Inductively Coupled Plasma- Atomic Emission Spectrometry (ICP-AES) (EPA, 2001). In brief, a dried, ground sample of saponified solids was acidified using a concentrated nitric acid. The sample was digested at 95 °C for approximately 60 min. Hydrogen peroxide was then added and the sample is heated for an additional 15 minutes. The sample was then delivered into an ICP-AES.

2.3 Fatty Acid Profiling

Fatty acid profiles of saponified solids were determined according to the official method, AOCS Ce 2-66 (AOCS, 2004). In brief, 0.5 to 1.0 g of sample were weighed in triplicate into glass screw topped tubes. Each tube was spiked with 0.5 mg of tridecanoin (C13:0) in ethanol to serve as an internal standard. One mL of 0.5 N NaOH in methanol was added to each, and the tubes were heated for 10 min at 85°C in a water bath. After cooling, 1 mL of 14% boron trifluoride in methanol was added to each tube. The tubes were recapped, vortexed, and returned to the water bath for 10 min. After cooling, 1 mL of water followed by 1 mL of hexane was added to each tube. The tubes were vortexed at top speed for 30s and then allowed to stand to form layers. The top (organic) layer containing the fatty acid methyl esters was removed and dried over sodium sulfate. The fatty acid methyl esters were analyzed with a Perkin-Elmer Autosystem XL GC (Sheldon, CT) fitted with a capillary BPX-070 column (SGE Inc., Austin, TX) using Gas chromatography-flame ionization detector (GC-FID). The temperature gradient was 60°C with a 2 min hold time, increased at 4°C per min to 180°C, and then increased at 10°C to a final temperature of 235°C. The run time was 27.7 min. The carrier gas used was helium. The injection was split at 150 mL/min. The results were reported as percent of the total fatty acids based on peak areas as per the official method (AOCS Ce 1f-96), and the total fatty acids were calculated based on the ratio of

internal standard to the fatty acid peaks present when compared to a standard mixture (Kel Fir Fame 5 Standard Mix, Matreya, Pleasant Gap, PA). The standard mixture of fatty acid methyl esters was run with each sample set to determine retention times and recoveries.

2.4 Determination of Rheological Properties

The physical states of calcium-based saponified solids freshly prepared in the laboratory indicated some flow characteristics and gel-like consistencies. Therefore, the determination of the rheological properties was attempted to understand the possible flow behavior and/or the deformation behavior of these solids.

The fundamental rheological parameters related to the present study can be explained by the Two-Plates-Model as shown in Figure 7 (Mezger, 2006). The saponified solids samples were sheared between these two plates with a shear gap, h. Shear velocity, v was measured with the upper plate (with a shear area A) being set in motion by the shear force, F. The samples were sheared in a way so that a laminar flow condition was maintained. The samples were also assumed not to adhere to both plates without any slipping or sliding at the plate surface.

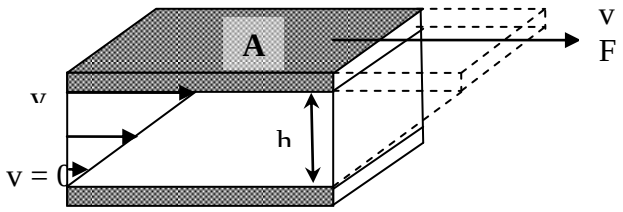

Figure 7 Flow velocity of a fluid using the Two-Plates-Model for shear tests

StressTech, a REOLOGICA instrument (ATS RheoSystems, New Jersey, US) was adopted to determine the rheological properties of calcium based saponified solids produced in the

laboratory. Oscillation stress sweep (0.1 to 100 Pa) was performed on soap samples at 10 rad/s with the analysis conditions shown in Table 3.

Table 3 Settings of REOLOGICA Instrument

Parameter	*Details*
Gap	1 mm or 0.75 mm
Sample loading method	To gap
Maximum loading force	1.273E+5 Pa; proceed when force is below 3.183E+4 Pa or when waiting more than 1.000E+1 s
Gap control	Passive
Limit loading speed	Below 3.00 mm to 0.3 mm/s
Pause for sample trimming	At 0.1 mm above target gap
Rotor release	Prompted (manual)
Control	Manual
Number of measurements	2
Measurement interval	3.000E+1 s
Frequency table	Frequency 1.000E+1 Hz Delay time 1.000E+1 s Integration periods 3 FFT size 512

The objective of these tests is to determine storage modulus G' and loss modulus G", to understand the sample's tack behavior and stickiness using the loss factor tanδ = G"/G' (Mezger, 2006). Storage modulus G' is a measure of the deformation energy stored by the sample during the shear process and represents the elastic behavior of the sample. The loss modulus G" is a measure of the deformation energy used up by the sample and therefore represents the viscous behavior of the sample. Loss factor tanδ is the ratio of the viscous and

elastic portion of the viscoelastic deformation behavior. Ideal elastic behavior can be specified in terms of $\delta = 0°$ or as $\tan\delta = 0$, where G' completely dominates G". Ideal viscous behavior can be expressed in terms of $\delta = 90°$ or as $\tan\delta = \infty$, where G" completely dominates G'. Pure water (having $\tan\delta = 0$) exhibits no tack at all, whereas a stone (showing an "infinitely high $\tan\delta$ value") which breaks with a brittle fracture. A sample shows relative stickiness if the $\tan\delta$ value is in the medium range relative to 0 and 1 (i.e., ~0.5).

2.5 Modeling methods

2.5.1 Kinetic data handling

The experimental kinetic data was studied for outlier identification using JMP Pro 9 statistical software (SAS Institute, 2001) after Origin Pro analysis (Pro, O. 8, 2007). The kinetic data was organized in an excel format and imported to JMP user interface. A multivariate analysis was performed to plot each set of experimental data with the replicates and outliers discarded manually. After the outlier elimination, the experimental kinetic data was used for the determination of kinetic parameters of the empirical and mechanistic saponification models to predict saponified solids formation using Particle Swarm Optimization (PSO) in MATLAB 2011a (Grant and Boyd, 2011).

2.5.2 Data fitting and determination of kinetic parameters using PSO

PSO is an artificial intelligence technique that can be used for wider ranges of possible applications, to find approximate solutions to extremely difficult numeric maximization and minimization problems. In this study, PSO was used to determine the optimized values of the kinetic parameters (Ebbesen et al., 2012). Gradient based optimization methods converge faster by using the derivative information to identify the search direction, but in case of multimodal function, there is a risk of the solution being stuck at a local minimum.

Alternatively, heuristic search algorithms have been successfully used in solving optimization problems in multimodal functions (Angeline, 1998; Eberhart and Shi, 2001). Since the rate equations are non-linear with potential multiple maxima and minima, the usual gradient based method failed to converge at a global minima. A hybrid optimization toolbox was utilized that is comprised of the PSO algorithm and fmincon, a gradient-based search algorithm. The objective of the hybrid scheme was to convert the global search to a local search after a number of designated iterations and therefore produce faster results than a standalone PSO technique. PSO algorithm is stochastic and therefore results in a family of solutions. A number of runs to determine a single parameter were therefore necessary to find a range of possible solutions. To determine the kinetic parameters, the kinetic models were simulated 150 times using the hybrid optimization technique. The anomalous solutions that did not fit the data were identified and discarded subsequently. After the manual search, the final ranges of solutions for kinetic parameters were obtained. Each data set was also compared with the standalone Cotte saponification and Foubert crystallization models using kinetic parameters found from PSO optimization to ensure the quality control of PSO. The objective function that was used in this study was the minimization of mean squared error between the experimental data and the results predicted by the model. The optimization problem can be summarized in Equation 3, where p represents the parameters to be estimated and n is the number of data points.

$$\min_{p \in R} \left(\frac{(y_{\exp} - y_{model}(p))^2}{n} \right) \tag{3}$$

2.5.3 Determination of relationships between model parameters and experimental conditions

To understand how the experimental conditions, i.e., pH, temperature, source fat types (canola or beef tallow), and source calcium types (i.e., calcium chloride or calcium sulfate) influence the values of the kinetic parameters in the empirical and mass-action based saponification models, relationships were determined based on the statistical analysis of the

parametric and experimental data. The statistical analyses were performed using JMP Pro 9 statistical software (SAS Institute, 2001). For each model, outliers were identified using multivariate analysis. Multiple non-linear regression analysis was subsequently performed to develop an equation for each kinetic parameter. The equation was developed based on the statistically significant relationship of each kinetic parameter with each experimental variable. The non-linear transformations for the experimental variables were constructed using the mathematical transformations available in JMP, such as square root, exponential, and Arrhenius equation. The best possible relationship or model equation with the lowest Bayesian Information Criterion (BIC) value was determined using a mixed stepwise analysis with the effects of the statistically significant experimental variables. Mixed stepwise analysis involved inclusion of the next significant experimental variable to the equation whose probability value was lower than the previous variable (i.e., $p2 > p1$ and $pi < 0.05$, where i represents each experimental variable). The fat source types and calcium source types were categorical variables, and therefore, numerical substitutions were necessary to include their effects on empirical relationships. Fatty acid compositions of source fat types and calcium contents in the final saponified solids were adopted, respectively.

The results of the current study are presented in three subsequent chapters (Chapters 4, 5, and 6).

References

Angeline, P. J. (1998). Evolutionary optimization versus particle swarm optimization: Philosophy and performance differences. In *Evolutionary Programming VII* (pp. 601-610). Springer Berlin Heidelberg.

Ebbesen, S., Kiwitz, P., & Guzzella, L. (2012, June). A generic particle swarm optimization Matlab function. In *American Control Conference (ACC), 2012* (pp. 1519-1524). IEEE.

Eberhart, R. C., and Shi, Y. (2001). Tracking and optimizing dynamic systems with particle swarms. In *Evolutionary Computation, 2001. Proceedings of the 2001 Congress on* (Vol. 1, pp. 94-100). IEEE.

Grant, M., & Boyd, S. (2011). CVX: Matlab software for disciplined convex programming, version 1.21.

Mezger, T. (2006). G. The rheology handbook: For users of rotational and oscillatory rheometers. *Vincentz Network GmbH & Co KG*

Official Methods and Recommended Practices of the American Oil Chemists Society, 5th ed. (2004). Firestone, D., Ed.; *American Oil Chemists Society*: Champaign, IL

Pro, O. 8. (2007). About Origin Pro 8 SRO, V8.0724 Software, Copyright 1991-2007, *Origin Lab Corporation*

SAS Institute. (2001). *Jmp: The Statistical Discovery Software*. Sas Inst.

CHAPTER 4 Factors that influence properties of FOG deposits and their formation in sewer collection systems

Abstract

Understanding the formation of Fat, Oil, and Grease (FOG) deposits in sewer systems is critical to the sustainability of sewer collection systems since they have been implicated in causing sewerage blockages that leads to sanitary sewer overflows (SSOs). Recently, FOG deposits in sewer systems displayed strong similarities with calcium-based fatty acid salts as a result of a saponification reaction. The objective of this study was to quantify the factors that may affect the formation of FOG deposits and their chemical and rheological properties. These factors included the types of fats used in FSEs, environmental conditions (i.e. pH and temperature), and the source of calcium in sewer systems. The results of this study showed that calcium content in the calcium based salts seemed to depend on the solubility limit of the calcium source and influenced by pH and temperature conditions. The fatty acid profile of the calcium-based fatty acid salts produced under alkali driven hydrolysis were identical to the profile of the fat source and did not match the profile of field FOG deposits, which displayed a high fraction of palmitic, a long chain saturated fatty acid. It is hypothesized that selective microbial metabolism of fats and/or biologically induced hydrogenation may contribute to the FOG deposit makeup in sewer system. Therefore, selective removal of palmitic in pretreatment processes may be necessary prior to the discharge of FSE wastes into the sewer collection system.

Keywords: Fat, oil, and grease deposit, sanitary sewer overflow (SSO), calcium based fatty acid salts

1 Introduction

Fat, oil, and grease (FOG), generated from commercial food service establishments (FSEs) can potentially accumulate in sewer systems in the form of hardened solids that are

responsible for approximately 50 to 75% of annual sanitary sewer overflows (SSOs) in the United States (Southerland, 2002; Ducoste et al., 2008). SSOs are mainly untreated discharges that can contain harmful contaminants and therefore can significantly impact both environmental and public health (EPA, 2004). Researchers have found that FOG deposits contain a large fraction of saturated fats, with palmitic being the primary fatty acid, and calcium being the primary metal in the majority of FOG deposit samples in sewer systems (Keener et al., 2008). Previously Wright (1935) also characterized grease balls in sewer systems as 25 to 45 percent free fat, 30 to 47 percent soap fat, and 7.6 to 13.4 percent lime as $CaCO_3$, based on dry weight. Keener et al. (2008) hypothesized that FOG from kitchen establishments comes into contact with calcium ions from the wastewater, leading to the formation of the calcium-based fatty acid salts or FOG deposits through a chemical reaction called saponification. However, Keener et al. lacked experimental evidence displaying the explicit similarities between calcium-based fatty acid salts and FOG deposits. In a recent study, He et al. (2011) performed experiments that demonstrated a strong similarity between laboratory-made calcium salts and laboratory-made FOG deposits using Fourier Transform Infrared Analysis-Attenuated Total Reflection (FTIR-ATR) method. He et al.'s work provided clear evidence that hardened FOG deposits were saponified solid material. However, He et al. (2013) was able to form FOG deposits not only with a pure source of palmitic, a saturated fatty acid, but also with unsaturated fatty acids: oleic, and linoleic acid. Therefore, a question still remains concerning the predominance of palmitic acid in FOG deposits found in sewer collection systems (Keener et al., 2008; He et al., 2011) or FOG deposits produced in laboratories using FSE grease interceptor waste stream (He et al., 2011).

The environmental conditions (i.e. temperature and pH) in conventional sewer systems are far different than the conditions used in industrial soap making processes. Industrial soaps are usually prepared under boiling conditions, such as 100°C (Smith, 1932). However, temperatures that are typically observed in sewer systems range from 5-25°C (Ducoste et al., 2008). FSEs also use alkaline detergents (pH >10), degreasers and sanitizers, which may perform as an oxidizer to promote saponification (Ducoste et al., 2008). Therefore,

temperature and pH conditions in sewer systems may influence the FOG deposit formation process.

The saturated fat content of FOG deposits has also been observed to be well above the values found in common cooking oils and animal fats (i.e., values for FOG deposits ranged from 20-90%; common cooking oils ranged from 7-20%; and animal fats have a range of 33-48%) (Ducoste et al., 2008). Both Keener et al. (2008) and He et al. (2011) observed palmitic as the primary fatty acids in sewer FOG deposits and laboratory produced FOG deposits with added calcium, respectively. Recently, a UK based study (Williams et al., 2012) also observed palmitic as the primary fatty acid in their samples collected from different locations in UK sewer systems. There are many types of cooking oils available that are being used in FSEs with varying degree of fatty acid compositions (saturated, mono-unsaturated, and poly-unsaturated). Therefore, a study needs to be performed that investigates the influence of the type of fat on the formation of FOG deposits.

Microbiologically induced concrete corrosion (MICC) of sewer systems can lead to leaching of significant amounts of calcium with other anions such as OH^- and SO_4^{2-} (Hermansyah et al., 2007). Research studies have shown that while exposed to bacteria, the corrosion rate of concrete can be as high as 0.208 mm/yr depending upon the type and strength of the concrete (Gutierrez-Padilla et al., 2010). Other studies have reported that the microbial acid attack can release 28 mg of calcium and 47 mg of sulfate per gm of concrete under pH 3.0 conditions (Bielefeldt et al., 2010). Keener et al. (2008) also observed that the calcium concentrations in FOG deposits were well above the wastewater concentration levels. In addition, Keener et al. showed no correlation between the hardness of the local water source and these high calcium concentrations. Moreover, the consecutive high concentrations of sulfur and iron in FOG deposits, after calcium, measured by Keener et al. may suggest concrete corrosion as a possible source of excess calcium present in FOG deposits (Keener et al, 2008; He et al., 2013). He et al. (2013)'s work suggested that calcium released due to biogenic concrete corrosion may accumulate with fatty acids and form FOG deposits due to a charged double layer type compression process. Williams et al. (2012), however, found a correlation between

water hardness and high calcium levels in FOG deposit samples and suggested biocalcification as a possible reason. Measurements of carbonate concentrations in actual FOG deposits are necessary to prove the hypothesis. Nonetheless, these studies imply that the calcium concentration in FOG deposits could be a result of multiple sources, i.e., wastewater and concrete corrosion. The literature therefore clearly suggests that a number of factors need to be explored in more detail to fully understand how they influence the FOG deposit formation in sewer collection systems.

The primary objective of this study was to assess the properties (i.e., physical, chemical, and rheological) of FOG deposits with different sources of calcium and fat under sewer environmental conditions. The physical properties included the physical appearance, i.e., color and texture. The chemical properties included fatty acid characterization and calcium content in calcium salts. The rheological properties were included in this study to understand the visco-elastic nature of the calcium based fatty acid salts to determine their stability under shear when they eventually attach the sewer pipe wall. In particular, this study explored the effects of temperature, pH, type of fat, and type of calcium source on the physical, chemical and rheological properties of calcium based fatty acid salts.

2 Materials and Methods

2.1 Materials. Two types of fats were used: a) Pure Wesson Canola Oil (total fat 14g, 22%; saturated fat 1g, 5%; trans fat 0g; poly unsaturated fat 3.5g; mono unsaturated fat 8g, cholesterol 0%, sodium 0%, total carbohydrate 0%, and protein 0%) made by ConAgra Foods, Omaha, NE; and b) Finest quality Beef Tallow (rendered tallow; Acid-Less 43.5 Grade; Saponification(SAP) Number 195; FFA 0.30%; Essential Depot, Florida). The types of fats used in this study represent the extreme end conditions (mostly unsaturated vs. highly saturated) that are potentially available for FOG deposit formation.

Three types of calcium sources in anhydrous form were used: a) Calcium chloride ($CaCl_2$, $\geq$ 93.0%, granular, 110.99 g/mol; Sigma-Aldrich, USA); b) Calcium hydroxide ($Ca(OH)_2$, 98+%, extra pure, 74.09 g/mol; Acros Organics, USA); and c) Calcium sulfate (>95%,

136.14 g/mol, powder; Fisher scientific, USA). Calcium hydroxide was only used to produce calcium-based fatty acid salts under high pH conditions.

Sodium hydroxide (NaOH) and hydrochloric acid (HCl) were used to adjust pH. Aqueous alkali solutions were prepared with de-ionized (DI) water.

2.2 Laboratory-based formation process of Calcium fatty acid salts. A room temperature based saponification process, similar to the alkali hydrolysis in Poulenat et al. (2003), was used in this study to produce the calcium-based fatty acid salts. The details of the approach can be found in He et al. (2011). In brief, an aqueous solution containing the calcium source was prepared and allowed to cool until the temperature of the solution reached 22-25°C. The liquid fat (i.e. Canola or melted Beef Tallow) was gradually added to the aqueous calcium solution and stirred at 450 rpm using a Stir-Pak laboratory mix impeller (Cole-Parmer instrument). A Sheldon water bath (SHEL LAB, Oregon, USA) was used to maintain the target temperature. Calcium soap formation samples were collected from the reaction beaker at the end of eight hours of continuous mixing. A 3:1 approximate molar ratio of liquid/solid fat and de-ionized water was used in all experiments. The saturated fat (i.e. Beef Tallow) was introduced at high temperature (45 °C) saponification only and was initially melted prior to mixing the reaction constituents. Each experiment was performed in triplicates. Details of the experimental conditions are shown in Table 1.

Table 1 Experimental Conditions of the Saponification Experiment

Experimental conditions	*Value*	*Unit*	*Comment*
Temperature, T	22	°C	For liquid fat only
	45	°C	For both liquid and solid fat*
Canola oil/Beef Tallow	74.7	%wt	-
$CaCl_2$ or $CaSO_4$	9.8	%wt	-
Catalyst, NaOH	0.6	%wt	-
Water	14.9	%wt	-

**Beef Tallow is solid under room temperature and therefore was used in high temperature condition only.*

2.3 FTIR analysis for fat saponification. FTIR-ATR data of calcium soaps were obtained with a Digilab FTS-6000 Fourier Transformed Infrared (FTIR) spectrometer with a mounted crystallized Zinc Selenide (ZnSe) sampling attachment (4000-520 cm-1; Pike Technologies Inc., MIRacleTM Single Reflection ATR). The data was computed with the Bio-Rad Win-IR Pro software version 2.97. OriginPro 8.1 SR3 was used in baseline correction and for resolving the peaks. Percent soap was computed following Equation 1, a modified version of the relative soap formation used by Poulenat et al. (2003). Poulenat et al. used only the carboxylate ion asymmetric stretching vibration band (between 1550 and 1610 cm-1) since it was the strongest of all the characteristic soap bands for sodium, lithium, and calcium soaps made with high-oleic sunflower oil. Characteristic soap bands include the carboxylate ion symmetric stretching vibration, between 1300 and 1420 cm-1, the carboxylate ion asymmetric stretching vibration, between 1550 and 1610 cm-1, and the metal-oxygen bond vibration, around 670 cm-1. Carbonyl band (around 1745 cm-1) represents the presence of un-reacted fat in the sample. In this study, a combined effect of all the characteristic bands was determined since all the bonds appeared to be relatively strong with time in calcium based soaps.

$$\%\ saponification = \frac{Absorbance\ in\ (670\ cm^{-1} + between\ 1300\ and\ 1420\ cm^{-1} + between\ 1550\ and\ 1610\ cm^{-1})}{Absorbance\ in\ (670\ cm^{-1} + between\ 1300\ and\ 1420\ cm^{-1} + between\ 1550\ and\ 1610\ cm^{-1} + 1745\ cm^{-1})} \quad (1)$$

2.4 Fatty Acid characterization. Fatty acid profiles of calcium based fatty acid salts were determined as per the official method, AOCS Ce 2-66 (AOCS, 2004). In brief, samples were weighed in triplicate into glass screw topped tubes. Each tube was spiked with tridecanoin (C13:0) in ethanol to serve as an internal standard. Sodium hydroxide in methanol was then added and the tubes were heated for 10 minutes at 85 °C in a water bath. After cooling, boron trifluoride in methanol was added and the tubes were recapped, vortexed, and returned to the water bath for 10 minutes. After cooling, water was added followed by hexane to each tube. The tubes were vortexed at maximum speed for 30 s and then allowed to stand to form layers. The top (organic) layer containing the fatty acid methyl esters (FAMEs) was removed

and dried over sodium sulfate. The FAMEs were analyzed with a Perkin-Elmer Auto-system XL GC (Sheldon, CT) fitted with a capillary BPX-070 column (SGE Inc., Austin, TX) using Gas chromatography-flame ionization detector (GC-FID). The results were reported as percent of the total fatty acids based on peak areas according to the official method (AOCS Ce 1f-96), and the total fatty acids were calculated based on the ratio of internal standard to the fatty acid peaks present when compared to a standard mixture (Kel Fir Fame 5 Standard Mix, Matreya, Pleasant Gap, PA). The standard mixture of FAMEs was run with each sample set to determine retention times and recoveries.

2.5 Minerals and metals analysis. Calcium based soaps were analyzed for the presence of Calcium (Ca) following the method documented in EPA 200.7 Trace elements in water, solids, and biosolids using Inductively Coupled Plasma- Atomic Emission Spectrometry (ICP-AES) (EPA, 2001). In brief, a dried, ground sample of the calcium based soaps is acidified using a concentrated nitric acid. The sample is digested at 95 °C for approximately 60 minutes. Hydrogen peroxide is then added and the sample is heated for an additional 15 minutes. The sample is then delivered into an ICP-AES.

2.6 Determination of Rheology. StressTech, a REOLOGICA instrument (ATS RheoSystems, New Jersey, US) was used to determine the rheological properties of calcium-based fatty acid salts. An oscillation stress sweep (0.1 to 100 Pa) was performed on calcium salt samples at 10 rad/s with the analysis conditions displayed in Table 2. The objective of this stress sweep was to determine storage modulus, G' and loss modulus G", to understand the flow behavior (Mezger, 2006) of calcium-based fatty acid salts.

Table 2 Settings of REOLOGICA Instrument

Parameter	*Details*
Gaps	1 mm or 0.75 mm (Calcium soap); 2 mm (FOG deposit)
Sample loading method	To gap
Maximum loading force	1.273E+5 Pa; proceed when force is below 3.183E+4 Pa or when waiting more than 1.000E+1 s
Gap control	Passive
Limit loading speed	Below 3.00 mm to 0.3 mm/s
Pause for sample trimming	At 0.1 mm above target gap
Rotor release	Prompted (manual)
Control	Manual
Number of measurements	2
Measurement interval	3.000E+1 s
Frequency table	Frequency 1.000E+1 Hz Delay time 1.000E+1 s Integration periods 3 FFT size 512

3 Results and Discussion

3.1 Fat saponification and Roles of calcium sources. The room temperature based saponification, initiated with three different forms of calcium (i.e. calcium chloride, calcium hydroxide, and calcium sulfate), produced significant amounts of calcium-based fatty acid salts (calcium soaps) within eight hours of rapid-mixing under near-stoichiometric conditions. Minute granules of soaps were immediately observed at the beginning of the mixing process and may be attributable to some initial free fatty acid present in the source fats and/or instantaneous saponification due to rapid mixing of reactants. The soap globules later disappeared in the continuous mixing of water-in-oil type emulsion.

Salted out calcium soaps, made with Canola and calcium chloride, seemed to dissolve in the liquid fat while undergoing mixing (image not shown here), but became phase-separated when mixing ceased (Figure 1). The separation occurred with water-containing glycerol phase in the lower layer, the semi-solid soap in the middle and clear oil in the upper layer. These observations were consistent with Smith (1932) for the cold saponification process and therefore indicate that these soaps have an affinity towards both the aqueous layer and oil layer. Anhydrous calcium sulfate, being highly hygroscopic, absorbed moisture and produced a soft mass once mixed with water. Experiments initiated with manual mixing of the constituents followed by high mixing for eight hours displayed a quick agglomeration of calcium sulfate forming a soft white ball above the impeller surface. This soft white ball had a qualitative marsh-mallow-like consistency. However, saponification was still hypothesized to have occurred at the interface of the calcium sulfate ball and liquid fat as well as between the entrapped liquid fat and calcium sulfate inside the white ball. Calcium hydroxide and calcium chloride displayed no such properties. These observations suggest that calcium sulfate (gypsum), a product of concrete corrosion (Mori et al., 1992; Atsunori and Terunobu, 1999; Gutierrez-Padilla et al., 2010), may aggregate and stick to sewer walls when the un-reacted liquid fat reaches the sewer crown section due to the wave action of water. It is important to mention that Keener et al. (2008) also found sulfur to be one of the highest mineral present in FOG deposits after calcium.

Figure 4 displays differences in colors and appearances of calcium soaps under different source and reaction conditions. All the soaps were semi-solid and of consistent mass. Canola soaps made with both calcium sulfate and calcium hydroxide appeared granular and rough in texture compared to those with calcium chloride. The granular soap formation could be attributed to the solubility of the respective calcium sources under the prescribed environmental conditions. The colors of these soaps were also significantly different, i.e. whitish with calcium chloride, significantly white with calcium sulfate, and brown with calcium hydroxide. Soaps left undisturbed for a period of time appeared denser with time due to gravitational settling of fine soap particles in the oil solution. The soap produced with

calcium hydroxide was significantly hard after a month. The hardening of soap may be attributable to the vaporization of moisture from soap with time by changing the semi-solid phase to solid phase. The observations here suggest that the visual characteristics, such as, color and texture of the laboratory made calcium based fatty acid salts can be compared with fresh FOG deposit samples in sewers and a qualitative idea on the possible calcium sources involved in the formation process can be made.

3.2 Role of Fat type. Previous studies (Keener et al., 2008; He et al., 2011) found palmitic, a saturated fatty acid, as the primary fatty acid present in FOG deposits. However, in the present study under alkali driven hydrolysis, the fatty acid compositions of the final soap samples were similar to the source fats introduced at the beginning of the saponification process (Table 3, Figure 2, and Supplemental Figure 1). Moreover, Beef Tallow, the primarily saturated fat used in this study, also produced less calcium soaps compared to Canola, the liquid fat, under the same pH and temperature conditions for the same calcium source (Table 4). Beef Tallow, which was studied only under warm temperature (45 °C) conditions, also solidified above the solid soap matrix when cooled down to room temperature. Although a fraction of Beef Tallow and other similar solid fats may transport down to the sewer system beyond grease interceptor (GI), the present study suggests the fatty acid compositions in the fresh FOG deposit are primarily related to the source fat conditions. Fresh FOG deposits prepared by He et al. (2011) using wastewater field samples (GI effluents) clearly showed that the largest fatty acid constituent in the GI effluent contains primarily palmitic (Figure 2 and Supplemental Figure 1). Therefore, generation of palmitic acid in wastewater and hence its preferential accumulation in FOG deposits may be possible through several mechanisms: a) preferential generation of saturated fatty acid fractions during the cooking process (Duckett and Wagner, 1998) and b) preferential breakdown of unsaturated fatty acids such as oleic or linoleic by lipolytic enzymes, present in food residuals in grease interceptors, leaving palmitic to readily react to form calcium-based fatty acid salts (Ghosh et al., 1996; Matsui et al., 2005, Montefrio et al., 2010). Research (He et

al., 2013) also suggests that significant formations of FOG deposits are possible with unsaturated fatty acids and calcium released from concrete in sewer system. FOG deposits produced from unsaturated fats (i.e. oleic) may convert to saturated fractions with time due to the possible chemical and/or biological activity of anaerobes in sewer system (Oppenheimer, 1960; Rhead et al., 1971; Zobell and Upham, 1944). While it's not known if any or all of these mechanisms are involved in producing a waste stream that predominantly contains saturated fatty acid, the results of this study clearly shows that FOG deposits created with pure oils or fats will have fatty acid contents similar to that pure fat or oil.

Table 3 Fatty acid compositions of calcium-based fatty acid salts

Fat type	Calcium type	pH ± 0.5	Temp ± 0.5 (°C)	Palmitic	Stearic	Oleic	Linoleic
Canola	Calcium chloride	7	22	5.0±0.1	1.8±0.5	68.9±1.0	18.0±1.0
		10	22	5.7±0.3	2.3±0.5	73.1±1.9	9.1±0.7
		14	22	4.5±0.1	1.4±0.3	63.2±1.9	20.6±1.1
	Calcium sulfate	7	22	4.3±0.1	1.7±0.3	65.0±0. 5	18.9±0.4
		10	22	4.3±0.0	2.0±0.1	65.7±0.5	18.1±0.1
		14	22	4.2±0.1	1.9±0.0	64.9±0.6	18.0±0.3
	Calcium chloride	7	45	4.1±0.0	1.9±0.0	64.2±0.3	18.3±0.2
		10	45	4.2±0.1	1.9±0.1	64.1±0.5	18.4±0.3
		14	45	4.4±0.1	2.0±0.1	63.3±0.6	19.3±0.5
	Calcium sulfate	7	45	4.2±0.0	1.9±0.0	62.7±0.3	19.2±0.2
		10	45	4.2±0.1	1.8±0.0	62.5±0.2	19.6±0.4
		14	45	4.5±0.1	1.9±0.0	62.3±0.4	19.4±0.2
Beef Tallow	Calcium chloride	7	45	24.4±0.2	18. 8±0.4	38.0±0.8	2.0±0.1
		10	45	24.7±0.2	19.5±0.2	34.1±0.3	1.6±0.1
		14	45	24.0±0.2	18.8±0.2	36.3±1.2	2.3±0.0
	Calcium sulfate	7	45	24.3±0.1	19.3±0.2	38.2±1.1	1.7±0.1
		10	45	24.0±0.1	18.7±0.2	36.9±1.6	1.8±0.1
		14	45	23.5±0.2	18.4±0.2	40.3±0.2	2.3±0.1

Samples also contained minor fatty acids: Palmitoleic: 0-2.9%, Margaric: 0-1.7%, Alpha-linoleic: 0.1-8.7%, Arachidic: 0.1-0.7%, Eicosenoic: 0.1-1.4%, Behenic: 0-0.4%. Source fat compositions: a) Canola: Palmitic, 4.2±0.0%, Stearic, 2.0±0.0%, Oleic(cis), 62.5±0.1%, and Linoleic, 18.9±0.1%; b) Beef Tallow: Palmitic, 23.4±0.2%, Stearic, 19.9±0.5%, Oleic(cis), 41.4±0.6%, and Linoleic, 2.5±0.1%

Table 4 Percent saponification after eight hours of reaction

Fat type	Calcium type	pH ± 0.5	Temperature ± 0.5 (°C)	Percent saponification (mean)
Canola	Calcium chloride	7	22	42.9
		10	22	43.4
		14	22	37.7
	Calcium sulfate	7	22	21.4
		10	22	60.1
		14	22	71.9
	Calcium chloride	7	45	20.1
		10	45	24.0
		14	45	57.4
	Calcium sulfate	7	45	87.8
		10	45	87.3
		14	45	41.7
Beef Tallow	Calcium chloride	7	45	19.1
		10	45	21.4
		14	45	18.5
	Calcium sulfate	7	45	31.6
		10	45	28.7
		14	45	51.6

3.3 Role of pH. The pH conditions changed the solubility of calcium in aqueous solution and therefore changed the amount of free calcium ions as well as hydroxyl ions available for fat hydrolysis and saponification. The pH of the final soaps was found to decrease, which is attributable to the release of H+ ions during the saponification reaction (Equation 2). The undocumented data showed that the decrease was somewhat proportional to the initially available OH- ions for hydrolysis, i.e. the rate of decrease in pH increased with higher initial pH.

$$\underset{(FFA)}{2\,R-COOH} + \underset{(Calcium\ ions)}{Ca^{2+}} \rightarrow \underset{(Calcium\text{-}based\ fatty\ acid\ salts)}{(R-COO)_2Ca} + \underset{(Protons)}{2\,H^{+}} \quad (2)$$

With the increase in initial pH conditions, a significant change in color and texture was also observed in calcium soaps, both in case of calcium chloride and calcium hydroxide, as can be seen in Figure 3. Calcium sulfate, however, always produced significantly whitish solid soap irrespective of the initial pH condition. An actual FOG deposit sample collected from a manhole in Cary, North Carolina displayed brownish color on the outside and whitish color on the inside. It is hypothesized that the brownish color of the outer core may be due to natural oxidation (i.e. age) and/or microbial activities inside the manhole (Williams et al., 2012). The whitish inner core, however, could be primarily the calcium sulfate based fatty acid salts with the presence of debris in layers, which was also observed by Keener et al. (2008).

3.4 Role of temperature. Beef Tallow is a solid fat at room temperature having a congealing temperature between 29-31 °C (88-85 °F) (Dawson and Kalinske, 1944). Beef Tallow was melted first (under 45°C) to facilitate its participation in the saponification reaction following alkali hydrolysis. According to recent investigations performed by Aziz et al. (2012), the temperature in the grease interceptor is typically 30 to 45 °C (86 to 113 °F), which is suitable for congealing common fats, such as Butter fat, Beef Tallow, Mutton tallow, and Pork lard (Dawson and Kalinske, 1944). However, depending on the efficiency of the grease interceptors, a fraction of un-reacted melted fat can pass through GIs and discharged into sewer systems (Dawson and Kalinske, 1944). These fats may congeal and contribute to growth of FOG deposits in the sewer crown portion, when wastewater hydraulics permits its contact in sewer systems. Rheological properties of the calcium based fatty acid salts and FOG deposit samples will be discussed later in this research.

3.5 ATR results. The characteristic bands in calcium soaps were identified and divided into four regions (part 1 at 4000-2800 cm^{-1}; part 2 at 1800-1350 cm^{-1}; and part 3 at 1350-1180 cm^{-1} and near 720 cm^{-1}, and part 4 at 670-440 cm^{-1}) according to Poulenat et al. (2003).

Supplemental Table 1 displays the comparison among the calcium-based fatty acid salts and their group frequencies. In Supplemental Table 1, FTIR-ATR analysis displayed the signature bands of calcium-based fatty acid salts, strong metal-oxygen bonds (closer to 670 cm^{-1}) and hydroxyl bonds (closer to 3400 cm^{-1}) in final soap samples, as also observed by He et al. (2011). A qualitative visual comparison between calcium soap formed in solution and its spectral data, however, indicated that a significant amount of soap needs to be formed to observe the appearance of metal oxygen band using the FTIR method. Growth of carboxylate bands (between 1300 and 1420 cm^{-1}, and between 1550 and 1610 cm^{-1}) in these cases may represent the stage of intermediate soap formation since visual solid formations were observed. These observations were especially evident in samples with Canola and calcium chloride under neutral pH and room temperature condition. Figure 4 displays the ATR spectral analysis of a typical calcium soap made with Canola and calcium chloride obtained in the laboratory. Besides the existence of a strong signal in part 1 O-H bands, in part 2 spectral region (1800-1350 cm^{-1}), the presence of the C=O stretching vibration (near 1745 cm^{-1}) is attributed to the ester bond in triacylglycerol (TAG) due to the presence of un-reacted liquid fat in the soap matrix. For Canola based soaps in which the source fats primarily consist of oleic and linoleic acid, the appearance of the asymmetric stretching vibration of the carboxylate group, however, was observed closer to 1640 cm^{-1} that was not consistent (between 1550 and 1610 cm^{-1}) with Poulenat et al. (2003). This phenomenon of band shifting was also present in He et al. (2013) results with FOG deposits prepared under laboratory conditions. Supplemental Figure 2 displays the growth of ~1640 cm^{-1} band with time, which suggests the progression of saponification reaction. Conjugation of carboxylate bands from oleic acid (1704 cm^{-1}) and oleic acid metal salts may have resulted in this significant shift in absorption frequency (Hsu, 1997; He et al., 2011). The conjugation may also suggest the stage of intermediate soap formation where both oleic acid and oleic acid metal salts are present.

The appearance of the symmetric and asymmetric carboxylate group bands in the Canola soap with calcium hydroxide was consistent with the results in Poulenat et al. The

asymmetric and symmetric stretching vibrations were split into two absorption band pairs (1570, 1541 cm^{-1}, and 1462, 1419 cm^{-1}), respectively, in Canola soap with calcium hydroxide and three symmetric stretching vibrations (1463, 1420, and 1404 cm^{-1}) in Beef Tallow soap with calcium chloride at 22 °C. A single stretching vibration (1456 cm^{-1}) was observed in Canola soap with calcium chloride and another single stretching vibration (1461 cm^{-1}) in Beef Tallow soap with calcium chloride at 45 °C. A single symmetric stretching vibration (1313 cm^{-1}) for Canola soap with $Ca(OH)_2$, a double stretching vibration (1385 and 1353 cm^{-1}) for Beef Tallow at 22 °C, and another single 1380 cm^{-1} were observed for Beef Tallow at 45°C. Bending vibrations were observed only in Beef Tallow soaps prepared with $CaCl_2$ at both 22 and 45 °C (Supplemental Table 1). The appearance of these carboxylate group bands indicates the ionized structure of the calcium soap (Mehrotra et al., 1994; Mehrotra and Upadhyaya, 1987). Hence, the structure of the calcium soap molecules would be more like type I than type II as XY_2-type molecule and is consistent with Poulenat et al. (Supplemental Figure 3).

The part 3 spectral region between 1350 and 1180 cm^{-1} represents the presence of aliphatic chains. The skeletal C-C vibrations were observed in each of the calcium soaps in Supplemental Table 1. The presence of weak glycerin absorption bands was also observed between 1150 and 850 cm^{-1} (1107, 1103, 1101, 1066, 1046, 965, and 914 cm^{-1}), which indicates the formation of crude soap. Crude soap is a mixture containing soap, glycerine, residual alkali, and triacylglycerols (Varma et al., 2000; Mehrotra et al., 1994). In the vicinity of 720 cm^{-1}, absorption bands (722, 720, and 712 cm^{-1}) representing rocking vibrations of successive methylene, $-CH_2-$, groups were observed in all crude soaps. The part 4 spectral observation in the vicinity of 670 cm^{-1} represents the presence of Ca-O bonds. The strength of Ca-O bond coincides with the strength of the absorption bands in calcium soaps. The calcium soaps produced with Canola oil and all the calcium sources used in this study at very high pH and room temperature displayed very strong absorption bands in this region (674 or 675 or 680 cm^{-1}). The Beef Tallow soap produced with calcium chloride under very high pH and warm conditions (45 °C) displayed a weak metal oxygen band (685 cm^{-1}), which is

consistent with visual observation of saponification. Beef Tallow, a solid fat under room temperature, may have slower alkali hydrolysis kinetics compared to Canola oil, a liquid fat under room temperature (Dawson and Kalinske, 1944).

FTIR analyses of calcium soaps, made in laboratory with different calcium and fat sources, displayed characteristic bands similar to actual FOG deposits in sewers (He et al., 2011 and 2013). However, exact locations of the characteristic bands in the designated regions may vary due to possible band shifting occurrence. Presence of significant amount of solid soap in the FOG deposit matrix is also necessary for the visibility of metal oxygen band in FTIR spectrometry. Therefore, COO^- bands, present in FOG deposits, may represent an intermediate saponification reaction and/or un-reacted excess FFA that could contribute to FOG deposit formation following DLVO theory as suggested by He et al. (2011).

3.6 Mineral and metal analysis. Tables 5 and 6 display results of mineral and metal analyses performed with the final calcium based fatty acid salts. Calcium soaps in Table 6 were prepared with double the reactant amounts compared to the samples in Table 5. When the saponification reaction was performed using double the reactant amounts for Canola oil and calcium chloride, under the same pH and temperature conditions, the calcium amount in the calcium soap matrix increased. This increase may be due to possible coagulation of calcium ions in the calcium based salt matrix based on charged double layer compression as suggested by He et al. (2011). In Table 6, keeping other conditions the same, soaps prepared with calcium sulfate seemed to have lower calcium concentration than soaps prepared with calcium chloride. The difference in calcium concentration in final soaps may be due to difference in solubility of the calcium sources in solution resulting in different amounts of available calcium ions for saponification. Calcium content of the calcium soaps also changed with the changes in pH and temperature conditions for different calcium sources. Although it is hard to differentiate the effects of pH and temperature on calcium sulfate based soaps, calcium chloride based soaps displayed the highest calcium content under neutral pH conditions, irrespective of the fat sources. Therefore, the availability of free calcium in the

mixture to form fatty acid salts can be related to the solubility of the calcium source introduced at the beginning of the saponification reaction. However, more research is needed to confirm this hypothesis. Overall, the results of mineral and metal analyses suggest that the agglomeration of excess calcium is possible in FOG deposits and supports He et al.'s (2011) results.

Table 5 Calcium content of the fatty acid salt samples at high pH conditions

Fat type	Calcium type	pH ± 0.5	Temp ± 0.5 (°C)	Initial, $\frac{\text{mg calcium}}{\text{mg calcium salt}}$	Final, $\frac{\text{mg calcium}}{\text{mg calcium salt}}$	% reaction/ coagulation
Beef Tallow				0.0000713	-	
Canola				0.0000295	-	
Canola	Calcium chloride	14	22	0.098	0.061	62.2
Canola	Calcium hydroxide	14	22	0.098	0.071	72. 5
Beef Tallow	Calcium chloride	14	45	0.098	0.040	40.8

Table 6 Calcium content of the fatty acid salt samples: Impact of pH and temperature

Fat type	Calcium type	pH ± 0.5	Temp ± 0.5 (°C)	Initial, $\frac{\text{mg calcium}}{\text{mg calcium salt}}$	Final, $\frac{\text{mg calcium}}{\text{mg calcium salt}}$	% reaction/ coagulation
Canola	Calcium chloride	7	22	0.196	0.148	75.5
		10	22	0.196	0.101	51.4
		14	22	0.196	0.116	59.3
	Calcium sulfate	7	22	0.196	0.106	54.1
		10	22	0.196	0.104	53.3
		14	22	0.196	0.103	52.3
	Calcium chloride	7	45	0.196	0.128	65.3
		10	45	0.196	0.107	54.4
		14	45	0.196	0.115	58.6
	Calcium sulfate	7	45	0.196	0.100	50.8
		10	45	0.196	0.075	38.4
		14	45	0.196	0.059	30.3
Beef Tallow	Calcium chloride	7	45	0.196	0.096	48.9
		10	45	0.196	0.075	38.2
		14	45	0.196	0.080	40.9
	Calcium sulfate	7	45	0.196	0.053	27.1
		10	45	0.196	0.080	40.7
		14	45	0.196	0.045	23.0

3.7 Rheological properties

3.7.1 Flow behavior of calcium soap

Figure 5 and Supplemental Figure 4 display shear modulus (G', G") vs. shear stress of a calcium chloride based fatty acid salt analyzed twice under two gap conditions (gap = 1 mm and 0.75 mm; ω = 10 Hz). Calcium-based fatty acid salts displayed behavior similar to viscoelastic gel or solid with G' being slightly higher than G" with increasing shear stress. A gel point was observed where G' crossed G", indicating a transition from viscous to elastic properties with increasing shear. In each case, Figure 5 and Supplemental Figure 4, the second experiment was performed with all samples under constant shear with a delay of 10 seconds. Two back to back runs for both gap conditions were performed to understand the flow and separation behavior of the calcium soaps. In all the calcium chloride based soaps, a steady decrease of G" was followed by an abrupt increase indicating a possible rearrangement of the particles near the end was observed. G' followed a similar trend as G" in run 1 for each sample. However, in run 2, a steady decrease in G' followed by a chaotic increase may be due to the possible rearrangement of the particles in run 1. Two gap conditions for calcium chloride based soaps did not make a significant difference in G' and G" values as they all lie between 10^{-1} and 10^{3} Pa. However, the minor changes in their trends may be attributed to the soap crystal sizes of the calcium soap samples. The calcium sulfate based soaps displayed a steady decreasing trend in G' and G" with G' being slightly higher than G" as more shear was applied (Figure 6). The values of G' and G" was higher in calcium sulfate based fatty acid salts (between 10^{2} and 10^{5} Pa) than in calcium chloride based fatty acid salts. Above all, replicable results for both types of lab based soaps indicate a certain stability in the produced soap system suggesting limited flow properties of soaps if they came in contact with the sewer wall. In the current study, stickiness of the calcium salts was recognized using qualitative sensory measurements. However, more rheological studies (i.e., oscillatory frequency sweeps) can be performed in the future to determine the adhesive properties of calcium based fatty acid salts and therefore of FOG deposits.

3.7.2 Rheology of FOG deposit

Fresh FOG deposit collected from a manhole in the Cary sewer collection system, displaying a strong metal oxygen band around 670 cm^{-1} as shown in Figure 7, was analyzed for its rheological properties. Two sub-samples (FOG deposit (1) and FOG deposit (2)) were chosen from the fresh FOG deposit mass based on their visual differences in color and surface texture. FOG deposit (1) was less granular, but seemed stickier compared to the FOG deposit (2) sample. The visual observation of layers was also consistent with observations by Keener et al. (2008). The deposit displayed no movement with a gap = 1 mm. This lack of movement may be attributed to the large crystals in a significant portion of debris in the deposit, which was also visible to the naked eye. An increased gap (2 mm) was introduced under the same frequency and the nature of G' and G" was observed to follow similar trend as calcium chloride based fatty acid salts (Figure 8, FOG deposit (1) sample compared to Figure 5). However, replicable results were not observed with another sample from the same FOG deposit (FOG deposit (2) in Figure 8) and can be attributable to the layering effects of FOG deposits (Keener et al., 2008). The G' and G" values of the first FOG deposit sample lie in the range of 10^{-1} and 10^{3} Pa, and in the second sample, between 10^{2} and 10^{8} Pa. The comparable values of storage and loss moduli in FOG deposit (1) sample that was previously attached to the manhole wall and calcium chloride based soaps indicate similar visco-elastic nature in both solids. A transition from viscous to elastic phase in both solids also displayed similar stability while experiencing the same range of shear stresses (Figures 5 and 8).The moduli values and the visual comparison also indicate that FOG deposit (2) sample could be a composition of calcium sulfate based soaps (Figure 8) and unknown components such as debris. Rheology of gypsum was also obtained to better understand the properties of FOG deposit (Supplemental Figure 5). Gypsum showed significantly higher G' and G" values (10^{3} to 10^{10} Pa) similar to FOG deposit (2) sample. The nature and range of G' and G" variation in FOG deposits therefore confirm that FOG deposits are layered combinations of debris and calcium based fatty acid salts with several possible sources of calcium. As calcium based salts may harden with time as discussed in section 3.1, the storage modulus of the FOG deposits that are similar to calcium chloride based soaps are expected to increase with time

indicating increased elastic nature. However, more rheological measurements are needed to confirm this hypothesis.

4 Conclusions

The change in calcium content in the calcium based salts with the use of different calcium sources suggests a dependence upon the solubility limit of the calcium sources with different pH and temperature conditions. Calcium chloride, having the highest solubility among the three calcium sources studied, produced a soft, gel-like soap mass. Calcium hydroxide and calcium sulfate, on the other hand, displayed a granular texture. These semi-solid masses may harden and gain significant strength with time leading to maintenance challenges for their removal from the sewer pipe wall. Calcium based fatty acid salts displayed a certain level of stability indicating their limited flow properties when adhered to the sewer wall. The rheology of FOG deposits when compared to the calcium salts also validated results from previous studies and indicated that FOG deposit matrix could be layered combinations of debris and calcium based fatty acid salts with several calcium sources. Calcium-based fatty acid salts produced under alkali driven hydrolysis conditions displayed the same FFA profile as its fat chemical precursor and deviated significantly from the FFA profile of sewer based FOG deposits that contained a large fraction of palmitic. This deviation in FFA profile indicates alternate fate pathways of fatty acids leading to the accumulation of palmitic in FOG deposits. Therefore, selective removal of palmitic in pretreatment processes prior to the discharge of FSE wastes may be necessary to reduce the FOG deposit formation in sewer collection systems.

Acknowledgments

We would like to thank the United States Environmental Protection Agency (EPA STAR grant: 83426401) for funding this research. The authors would also like to thank Donald Smith of the Town of Cary for the assistance in collection of FOG deposits from manhole.

References

Atsunori, N., and Terunobu, M. (1999). A repair system of concrete corroded by bacteria using HDPE sheets and mortar admixed with inhibitor. Paper presented at the *Reunion*

Internationale des Laboratoires et Experts des Materiaux Symposium on Adhesion between Polymers and Concrete, pp. 497-510

Aziz, T.N., Holt, L.M., Keener, K.M., Groninger, J.W., and Ducoste, J.J. (2012). Field characterization of external grease abatement devices. *Water Environment Research, 84(3),* 237-246

Bielefeldt, A., Gutierrez-Padilla, M. G. D., Ovtchinnikov, S., Silverstein, J., and Hernandez, M. (2010). Bacterial kinetics of sulfur oxidizing bacteria and their biodeterioration rates of concrete sewer pipe samples. *Journal of Environmental Engineering, 136,* 731

Dawson, F., and Kalinske, A. (1944). Design and operation of grease interceptors. *Sewage Works Journal, 16*(3), 482-489

Duckett, S., and Wagner, D. (1998). Effect of cooking on the fatty acid composition of beef intramuscular lipid. *Journal of Food Composition and Analysis, 11*(4), 357-362

Ducoste, J. J., Keener, K. M., Groninger, J. W., and Holt, L. M. (2008). Fats, roots, oils, and grease (FROG) in centralized and decentralized systems. *Water Environment Research Foundation.* IWA Publishing, London

Ghosh, P.K., Saxena, R.K., Gupta, R., Yadav, R.P., and Davidson (1996). Microbial lipase: production and applications. *Science progress,* 79(2), 119-157

Gutiérrez-Padilla, M. G. D., Bielefeldt, A., Ovtchinnikov, S., Hernandez, M., and Silverstein, J. (2010). Biogenic sulfuric acid attack on different types of commercially produced concrete sewer pipes. *Cement and Concrete Research, 40*(2), 293-301

He, X., Iasmin, M., Dean, L. O., Lappi, S. E., Ducoste, J. J., and de los Reyes III, F. L. (2011). Evidence for fat, oil, and grease (FOG) deposit formation mechanisms in sewer lines. *Environmental science and technology, 45*(10), 4385-4391

He, X. de los Reyes III, F.L., Leming, M., Lappi, M., Ducoste, J. (2013). Mechanisms of Fat, oil, and grease (FOG) deposit formation in Sewer Lines. *Water Res.,47(13),4451-4459*

Hermansyah, H., Kubo, M., Shibasaki-Kitakawa, N., and Yonemoto, T. (2006). Mathematical model for stepwise hydrolysis of triolein using Candida rugosa lipase in biphasic oil–water system. *Biochemical engineering journal*, *31*(2), 125-132

Keener, K.M., Ducoste, J.J., Holt, L.M. (2008). Properties influencing fat, oil, and grease deposit formation. *Water Environ. Res*. 80, 2241-2246

Koga, Y., and Matuura, R. (1961). Studies on the structure of metal soaps. *Mem. Fac. Kyushu Univ., Series 4*(1), 1-62

Matsui, T., Miura, A., Iiyama, T., Shinzato, N., Matsuda, H., and Furuhashi, K. (2005). Effect of fatty oil dispersion on oil-containing wastewater treatment. *Journal of Hazardous Materials*, 118(1–3), 255-258

Mezger, T. G. (2006). *The rheology handbook: For users of rotational and oscillatory rheometers.* Vincentz Network GmbH and Co KG.

Mehrotra, K., Rani, L., and Kumar, A. (1994). Physico-chemical properties of lithium soap. *REVUE ROUMAINE DE CHIMIE*, 39, 517-517

Mehrotra, K., and Upadhyaya, S. (1987). Thermal, IR and X-ray analysis of calcium soaps. *Tenside Detergents, 24*(2), 90-91

Montefrio, M. J., Xinwen, T., and Obbard, J. P. (2010). Recovery and pre-treatment of fats, oil and grease from grease interceptors for biodiesel production. *Applied Energy*, *87*(10), 3155-3161

Mori, T., Nonaka, T., Tazaki, K., Koga, M., Hikosaka, Y., and Noda, S. (1992). Interactions of nutrients, moisture and pH on microbial corrosion of concrete sewer pipes. *Water Research, 26*(1), 29-37

Norris, M. H., and McBain, J. W. (1922). CLXII.—A study of the rate of saponification of oils and fats by aqueous alkali under various conditions. *J.Chem.Soc., Trans., 121*, 1362-1375.

Official Methods and Recommended Practices of the American Oil Chemists Society (2004). 5th ed.; Firestone, D., Ed.; *American Oil Chemists Society*: Champaign, IL

Oppenheimer, C. H. (1960). *Geochim. Cosmochim. Acta*, **19**, 244.

Poulenat, G., Sentenac, S., and Mouloungui, Z. (2003). Fourier-transform infrared spectra of fatty acid salts—Kinetics of high-oleic sunflower oil saponification. *Journal of Surfactants and Detergents*, 6(4), 305-310

Rhead, M., Eglinton, G., Draffan, G., and England, P. (1971). Conversion of oleic acid to saturated fatty acids in severn estuary sediments. *Nature*, Volume 232, Issue 5309, pp. 327-330

Smith, L. (1932). The kinetics of soap making. Transactions and Communications. *Journal of the Society of Chemical Industry*, pp 337-348

Southerland, R. (2002). Sewer fitness: Cutting the fat. *American City and Country*, 117(15), 27-31

USEPA (2001). Method 200.7: Trace elements in water, solids, and biosolids by inductively coupled plasma-atomic emission spectrometry. Rev. 5. EPA-821-R-01-010. *U.S. Environmental Protection Agency*, Washington, DC.

USEPA (2004). Report to Congress: Impacts and Control of CSOs and SSOs. *U.S. Environmental Protection Agency*

Varma, R., Kumar, U., and Sangal, P. (2000). Characterisation of sodium soaps and their refractive index studies in methanol. *ASIAN JOURNAL OF CHEMISTRY*, 12(3), 659-662.

Williams, J., Clarkson, C., Mant, C., Drinkwater, A., and May, E. (2012). Fat, oil and grease deposits in sewers: Characterisation of deposits and formation mechanisms. Water Research, 46(19):6319-28

Wright, E. (1935). Disposal of sewage from the south essex sewerage district, salem, massachusetts. *Sewage Works Journal*, 7(4), 663-672

Zobell, C. E., and Upham, H. C. (1944). Bull. Scripps Inst. Oceanog., 5, 239

Figures

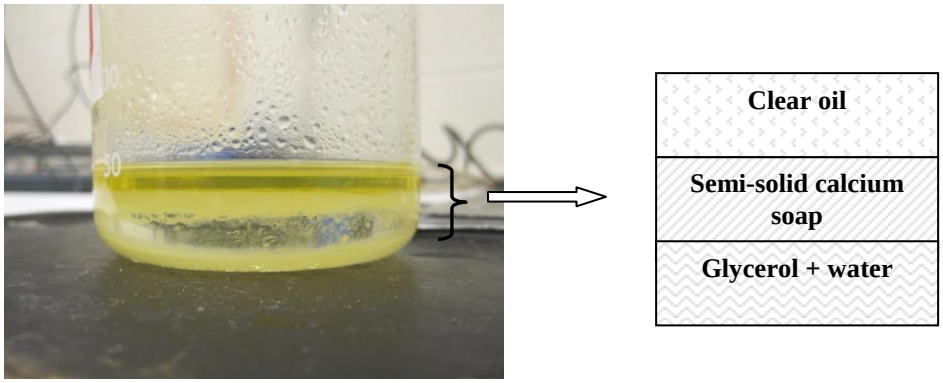

Figure 1 Phase separation in calcium based saponification (Canola, calcium chloride, pH 7, 22 °C)

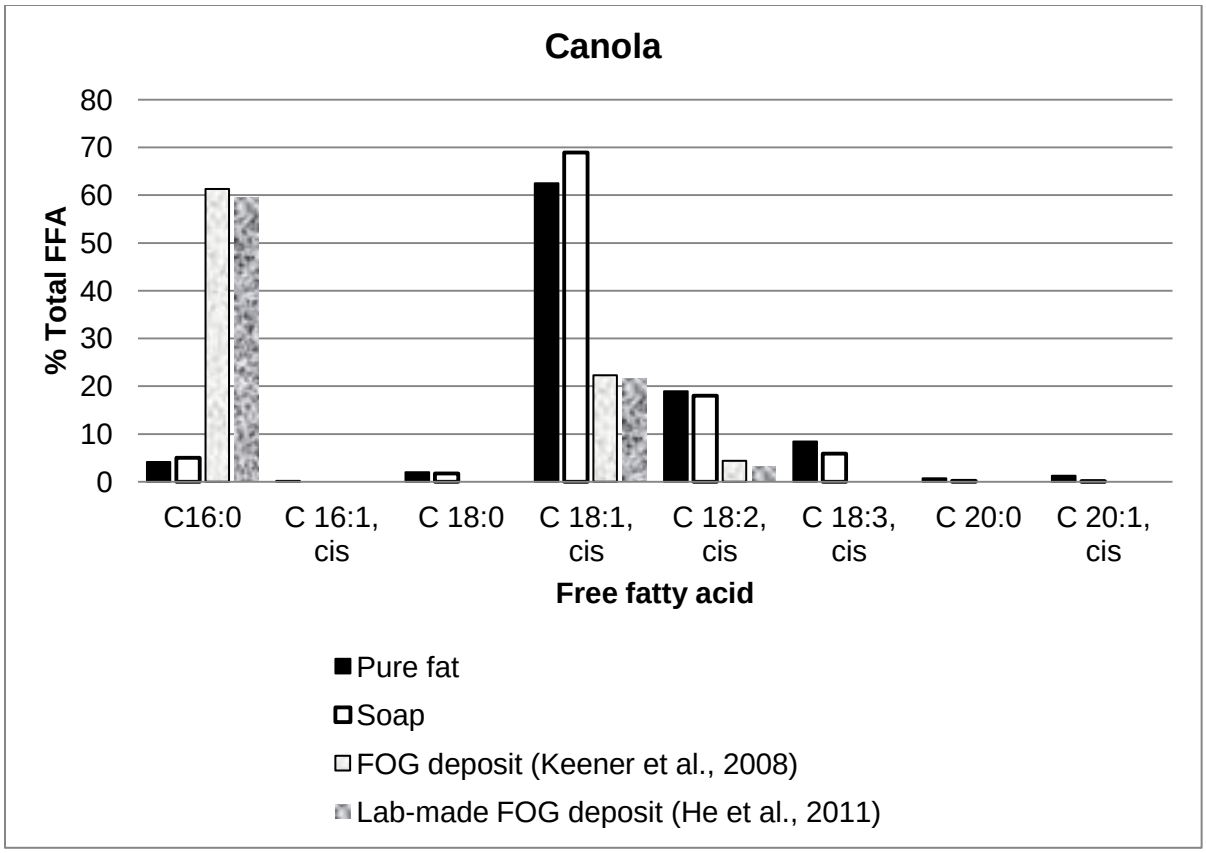

Figure 2 Fatty acid profile comparisons between canola based soaps and FOG deposits

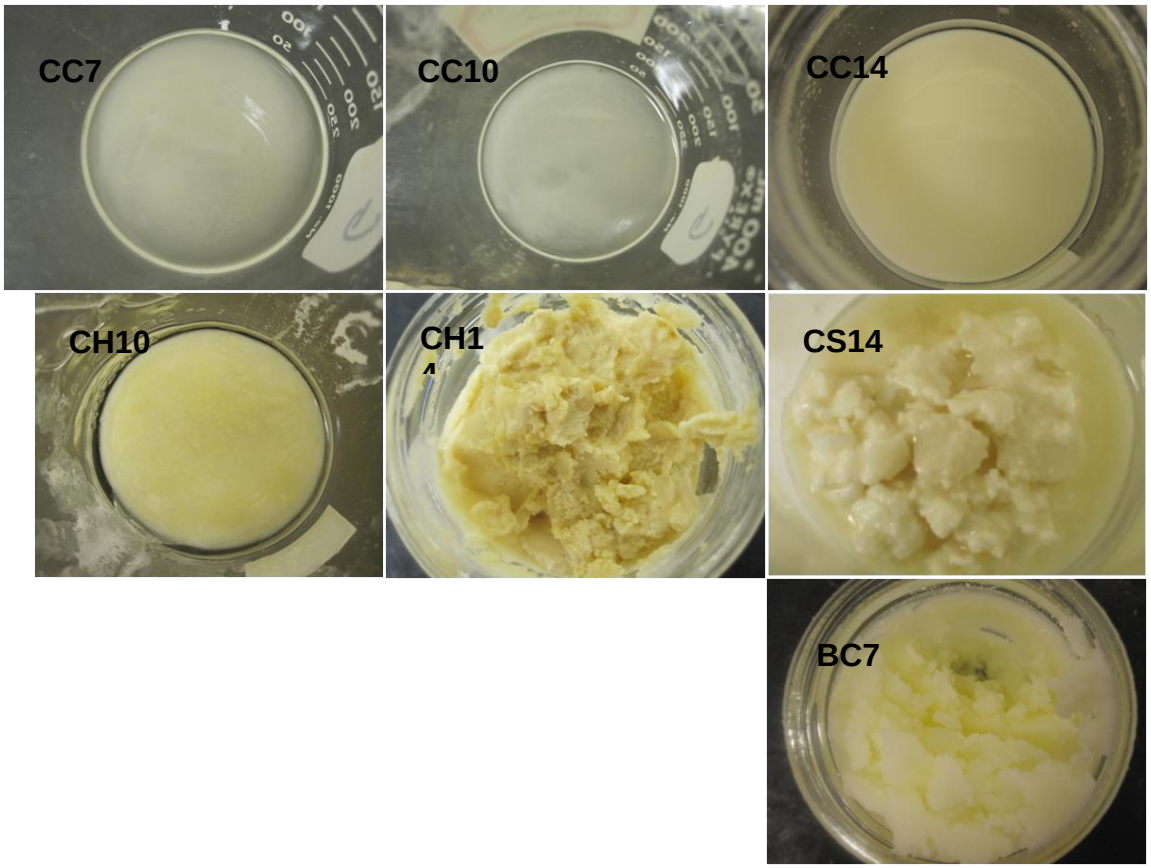

Figure 3 Physical appearances of calcium-based fatty acid salts (***CC = Canola and calcium Chloride; BC = Beef tallow and calcium Chloride; similarly in the second letters, S = calcium Sulfate, and H = calcium Hydroxide; the numbers indicate pH values.***)

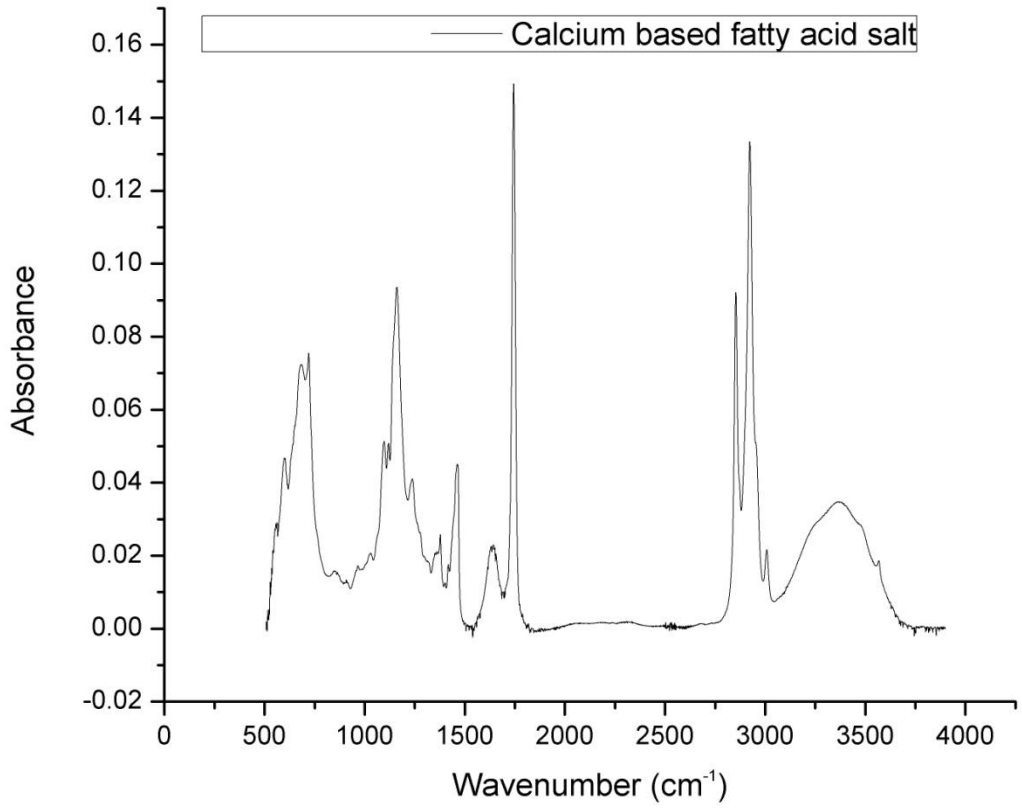

Figure 4 Lineplot of calcium chloride based soap showing peak locations

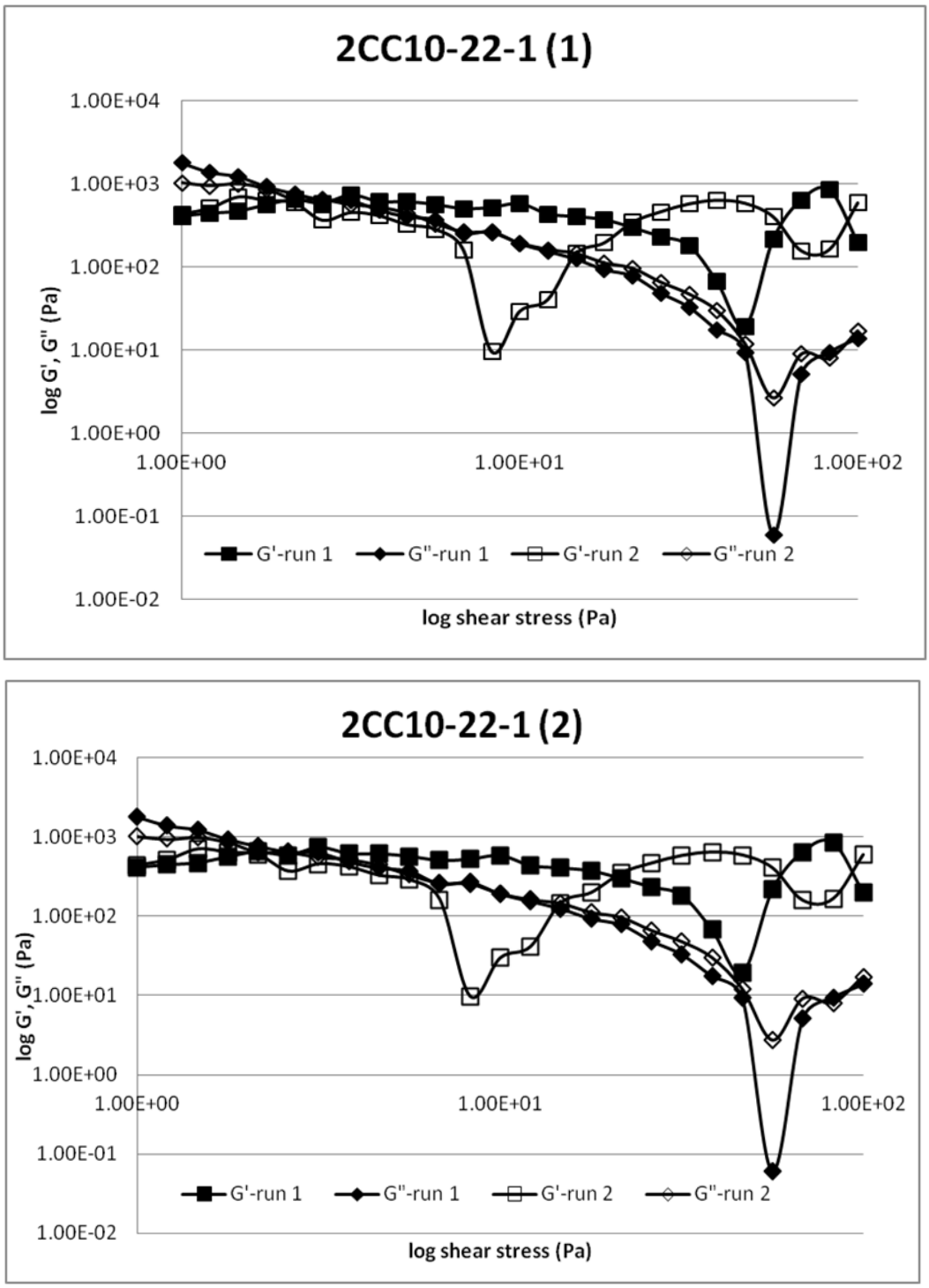

Figure 5 Shear stress dependence of calcium soap (Experiment 2, Canola, calcium chloride, pH 10, 22 °C; analysis-1 (top) and analysis-2 (bottom); ω = 10 Hz, gap 1.00 mm)

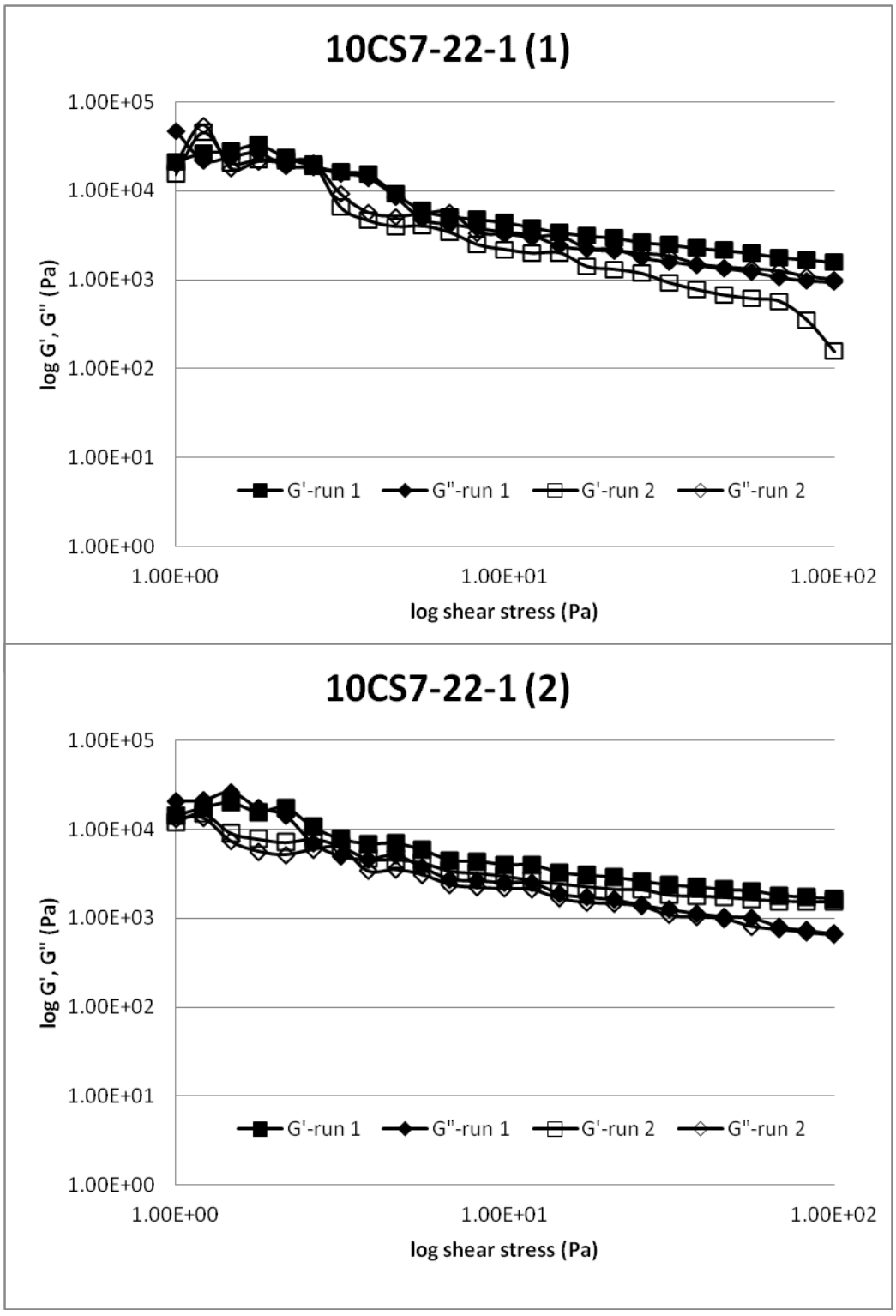

Figure 6 Shear stress dependence of calcium soap (Experiment 10, Canola, calcium sulfate, pH 10, 22 °C; analysis-1 (top) and analysis-2 (bottom); ω = 10 Hz, gap 1.00 mm)

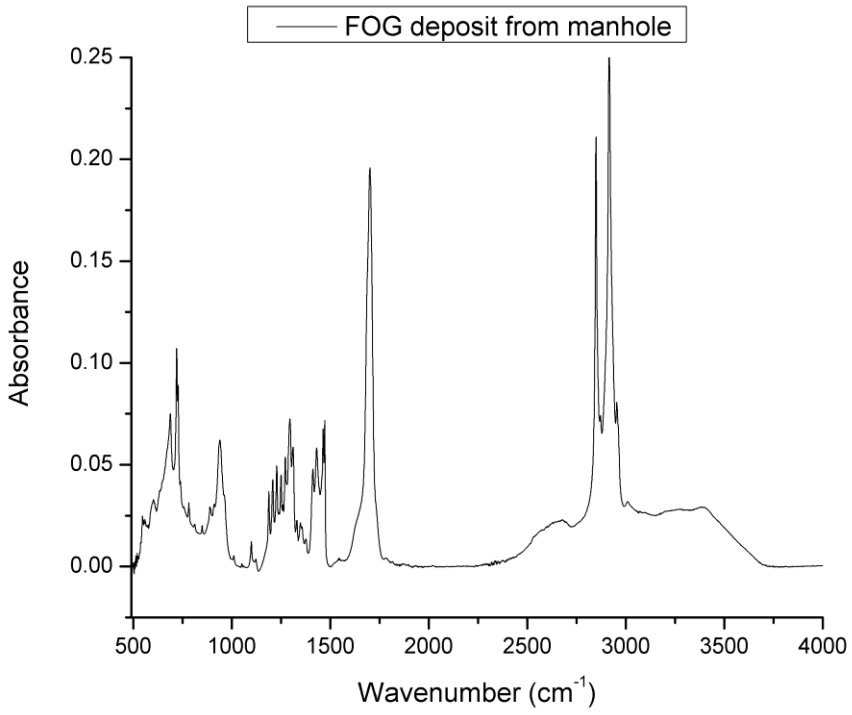

Figure 7 Baseline corrected data of FOG deposit collected from manhole (Cary, NC)

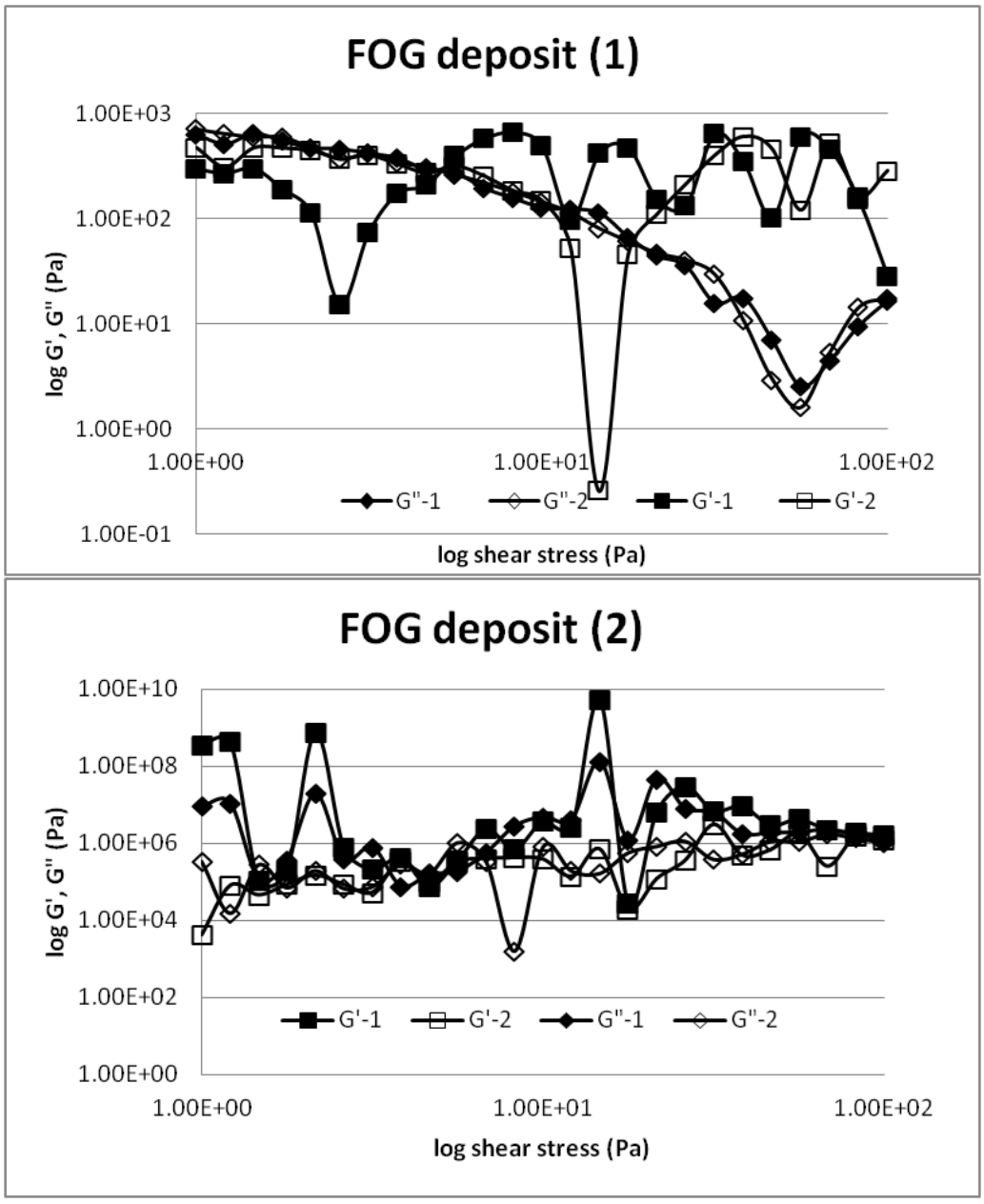

Figure 8 Shear stress dependence of FOG deposit (collected from a manhole beside a pizza restaurant; analysis 1 (top) and analysis 2 (bottom); gap = 2 mm)

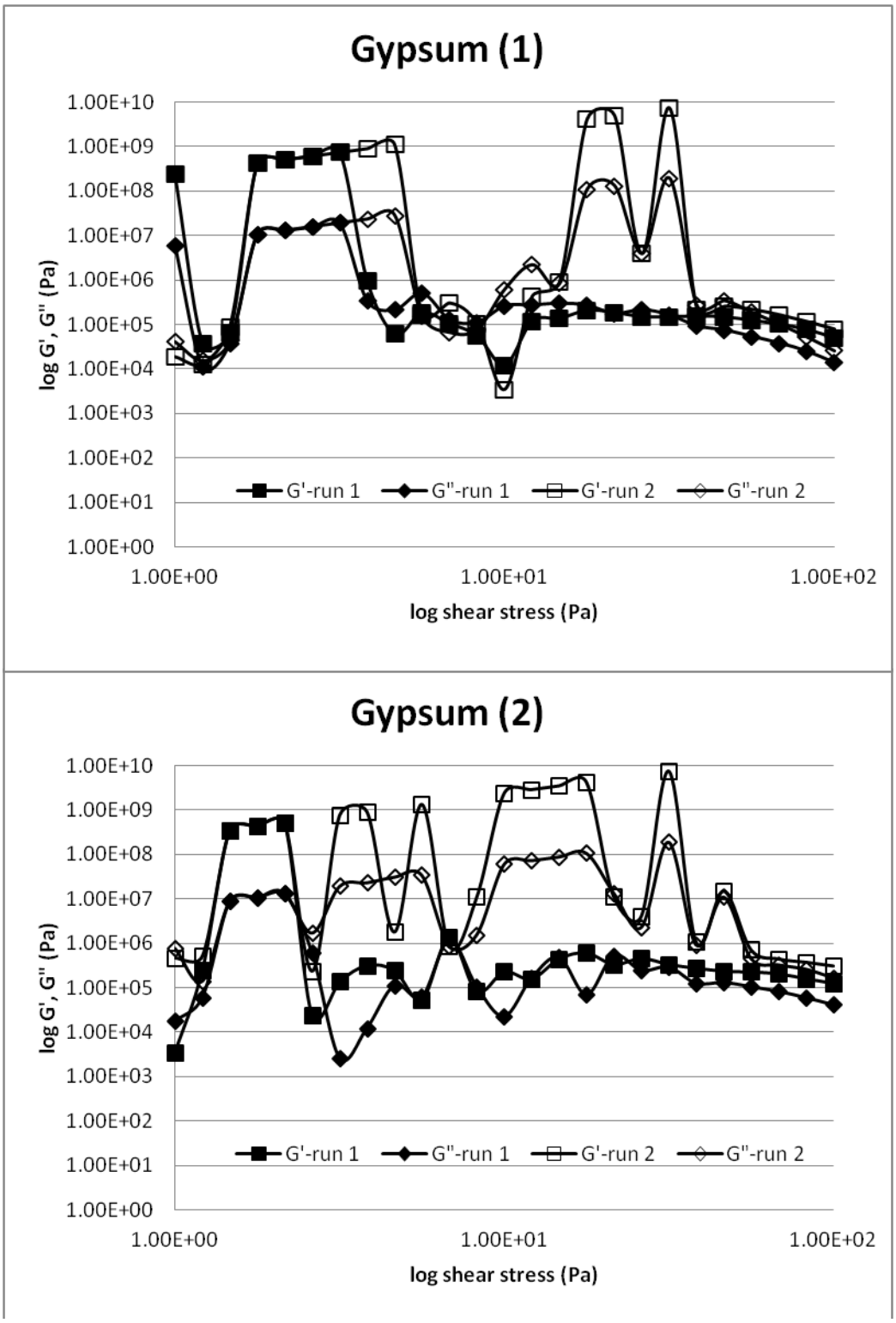

Figure 9 Shear stress dependence of Gypsum (*analysis-1 (top) and analysis-2 (bottom);* ω = 10 Hz, gap =1.00 mm)

APPENDIX

Appendix S

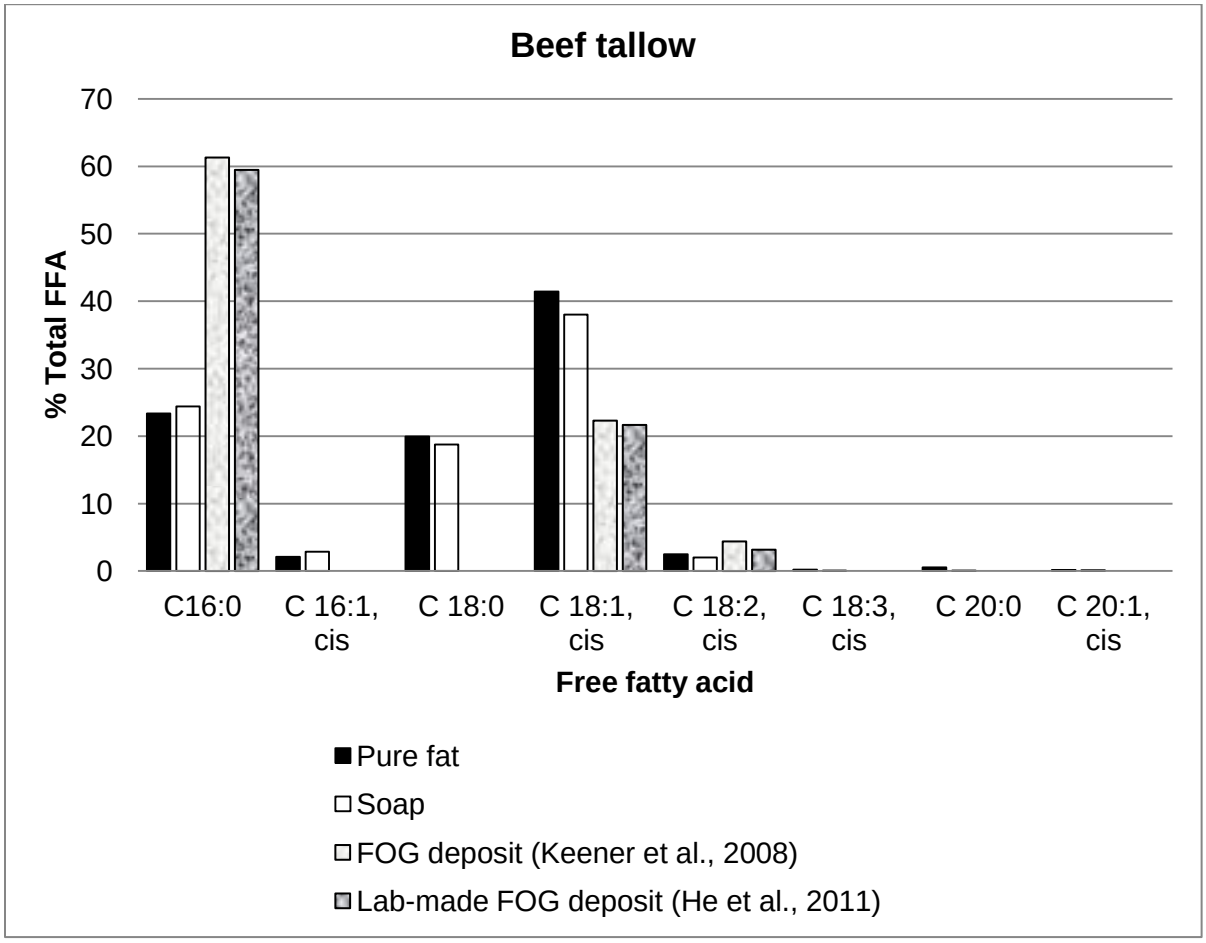

Supplemental Figure 1 Fatty acid profile comparisons between beef tallow based soaps and FOG deposits

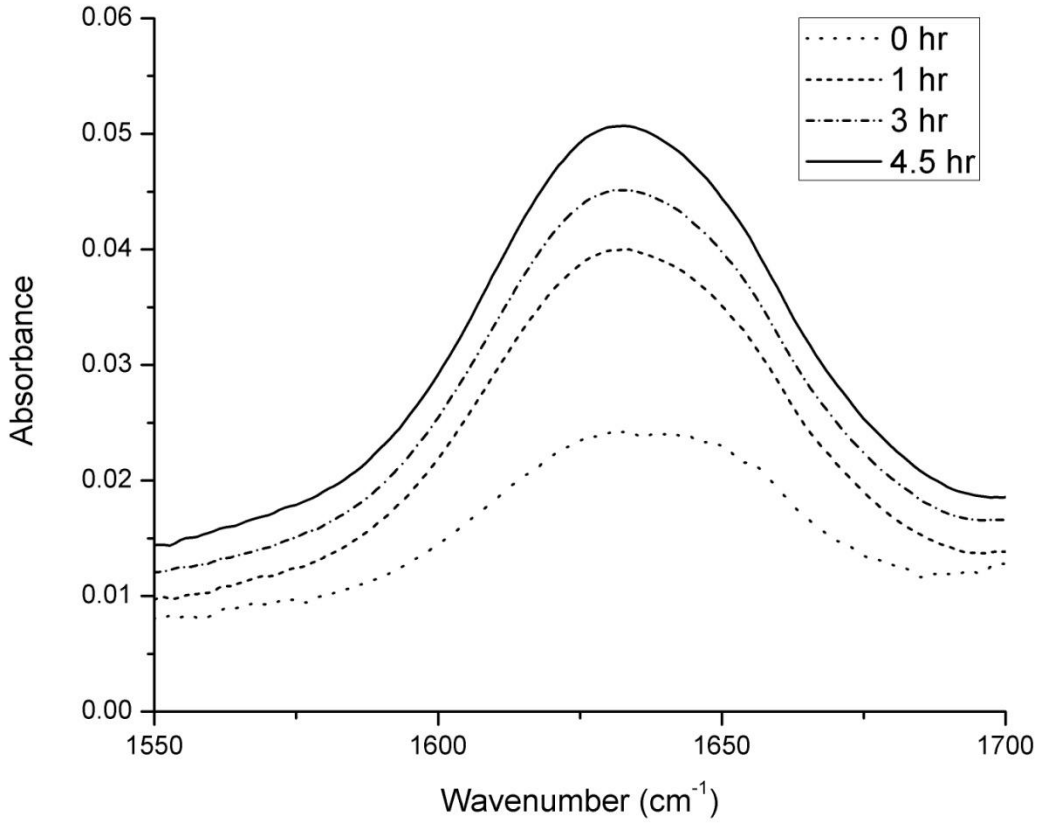

Supplemental Figure 2 Growth of ~1640 cm^{-1} waveband with time (2CC10-22: Experiment 2, Canola, Calcium Chloride, pH 10, 22 °C)

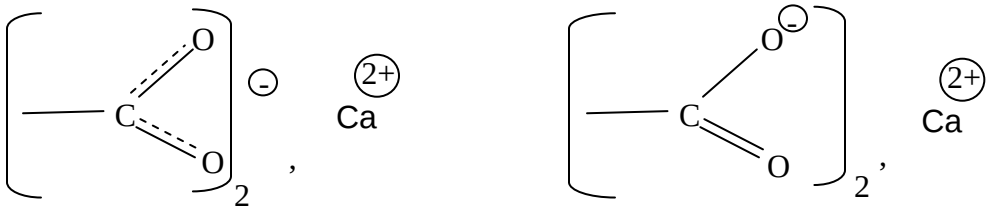

Supplemental Figure 3 Structure of soap molecule displaying the ionized carboxyl group (Koga and Matuura, 1960)

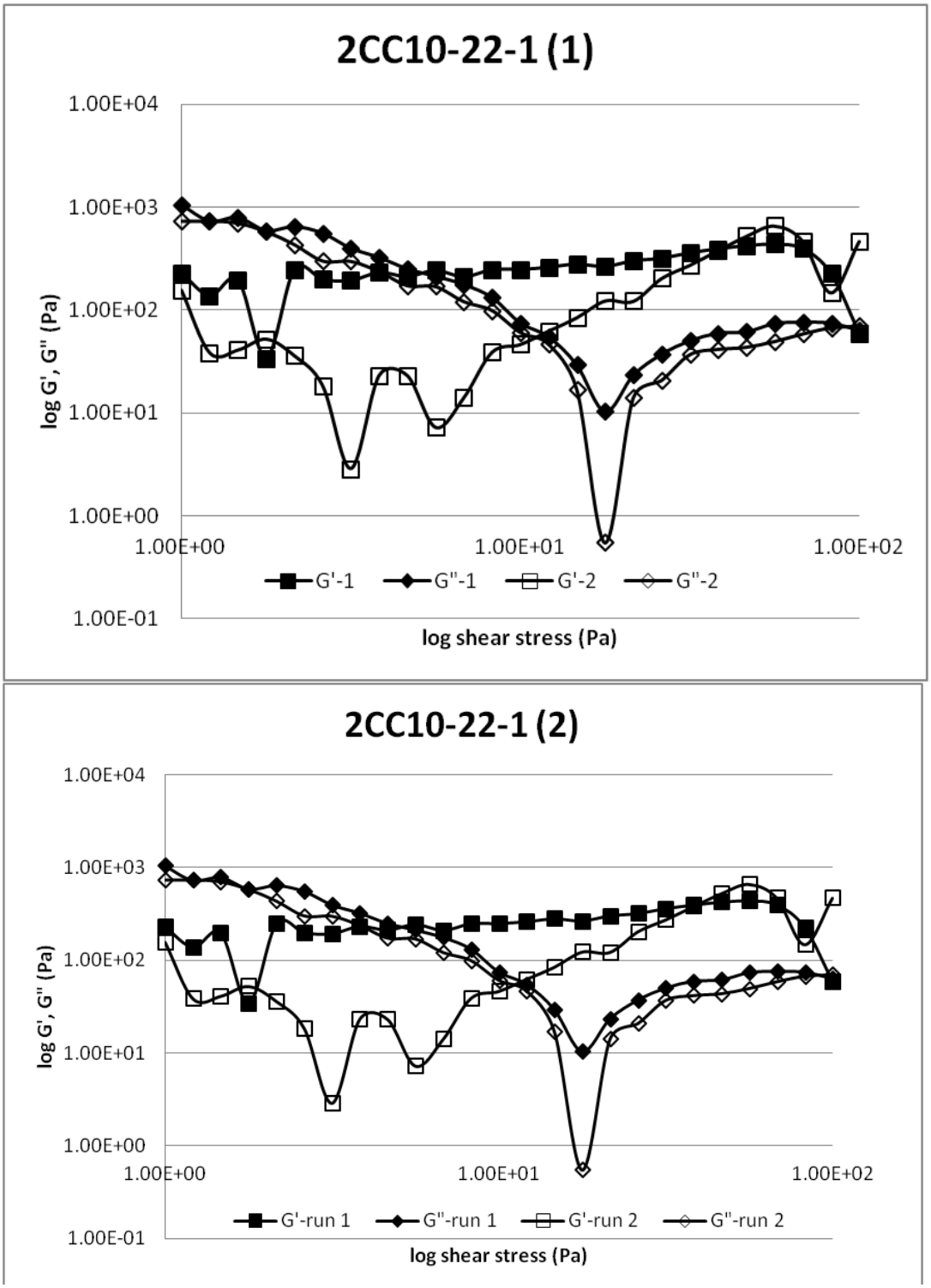

Supplemental Figure 4 Shear stress dependence of calcium soap (Experiment 2, Canola, calcium chloride, pH 10, 22 °C; analysis-1 (top) and analysis-2 (bottom); ω = 10 Hz, gap 0.75 mm)

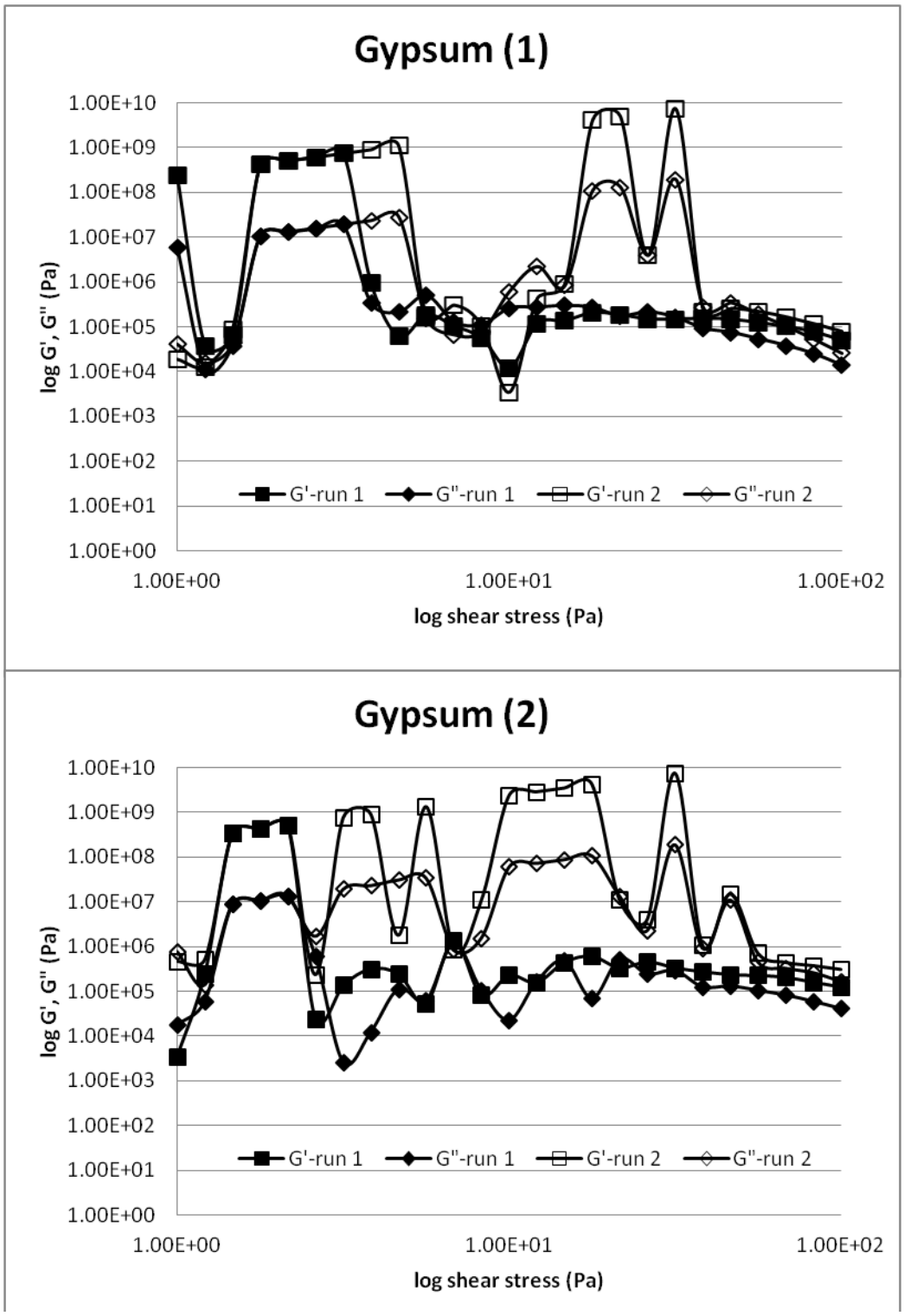

Supplemental Figure 5 Shear stress dependence of gypsum (analysis-1 (top) and analysis-2 (bottom); ω = 10 Hz, gap =1.00 mm)

Supplemental Table 1 Comparisons of observed wave frequencies among calcium soaps

Frequencies (cm^{-1})					
Canola with $CaCl_2$	Canola with $CaSO_4$	Canola with $Ca(OH)_2$	Beef Tallow with $CaCl_2$	Beef Tallow with $CaCl_2$ @45°C	Assignments
		3639 (n, w)			Non bonded hydroxyl group, OH^- stretch
				3558 (n, vw)	Tertiary alcohol, OH^- stretch
3367 (b, ms)	3331 (b, ms)	3381 (b, ms)	3464 (b, vw)	3390 (b, vw)	Hydroxyl group. H-bonded OH^- stretch
3010(vw)		3011 (vw)	3001 (vw)		Stretching =CH-H
2924 (s)	2923 (vs)				Asymmetric stretching CH_2, C-H
2857 (w)	2853 (s)				Symmetric stretching CH_2, C-H
1744 (s)	1744 (vs)	1744 (w)	1739 (vs)	1741 (vs)	Stretching C=O (ester)
			1702 (vw)	1696 (vw)	C=C stretching
1637 (s)	1650 (w)	1641 (w)		1640 (vw)	
		1570 (ms)			Asymmetric stretching COO^-, C-O (ω_2)
		1541 (ms)			
1456 (w)	1463 (w)	1462 (s)	1463 (w)	1461 (w)	
		1419 (s)	1420 (vw)		
			1404 (vw)		
					Symmetric stretching COO^-, C-O (ω_1)
			1385 (vw)	1380 (vw)	
	1377 (vw)	1313 (w)	1353 (vw)		
		1279 (w)			Twist and wag CH_2
1234 (w)	1236 (w)	1240 (w)	1243 (w)	1232 (w)	Skeletal C-C vibrations
			1231 (w)		Rocking CH_3
1159 (s)	1154 (vs)	1164 (w)	1171 (vs)	1169 (ms)	Deformation COOR
1103 (w)	1117 (vs)	1107 (w)	1101 (w)	1103 (w)	Glycerin
	1096 (vs)	1046 (w)	1066 (vw)		Glycerin

Supplemental Table 1 Continued

	967 (vw)		965 (vw)	964 (vw)	Glycerin
					Bending deformation COO^- (ω_3)
		914 (w)			or glycerin
			837 (vw)		
	721 (vs)	713 (vs)	722 (w)	720 (s)	Rocking $(CH_2)_n$, n > 4
			697 (vw)		
675 (vs)	673 (vs)	674 (vs)		685 (w)	Ca-O bond
			645 (vw)		OH^- out-of-plane bend
599 (vs)	593 (vs)	601 (vs)		591 (w)	

Abbreviations are explained in Supplemental Table 2.

Supplemental Table 2 Abbreviations

Abbreviations:		% Range/guideline
vs	very strong	>80
S	strong	>60 & <=80
Ms	medium strong	>40 & <=60
Vw	very weak	>20 & <=40
W	weak	<=20
B	broad	from visual appearance
n	narrow	from visual appearance

CHAPTER 5 Quantifying Fat, Oil, and Grease deposit formation kinetics in Sewer Collection Systems

Abstract

Fat, oil, and grease (FOG) deposits formed in sanitary sewers are calcium-based saponified solids that are responsible for a significant number of nationwide sanitary sewer overflows (SSOs) across United States. In the current study, the kinetics of lab-based saponified solids were determined to understand the kinetics of FOG deposit formation in sewers for two types of fat (Canola and Beef Tallow) and two types of calcium sources (calcium chloride and calcium sulfate) under three pH (7±0.5, 10±0.5, and ≈14) and two temperature conditions (22±0.5 and 45±0.5 °C). The results of this study displayed quick reactions of a fraction of fats with calcium ions to form calcium based saponified solids. Results further showed that increased palmitic fatty acid content in source fats, the magnitude of the pH, and temperature significantly affect the FOG deposit formation and saponification rates. The experimental data of the kinetics were compared with two empirical models: a) Cotte saponification model and b) Foubert crystallization model and a mass-action based mechanistic model that included alkali driven hydrolysis of triglycerides. Results showed that the mass action based mechanistic model was able to predict changes in the rate of formation of saponified solids under the different experimental conditions compared to both empirical models. The mass-action based saponification model also revealed that the hydrolysis of Beef Tallow was slower compared to liquid Canola fat resulting in smaller quantities of saponified solids. The mass-action based mechanistic saponification model, with its ability to track the fundamental chemical components, may provide an initial framework for its incorporation in system wide sewer collection modeling software to predict the spatial formation of FOG deposits in municipal sewers.

1 Introduction

Fat, oil, and grease (FOG) deposit formations have been implicated in 50 to 60% of the SSOs across the United States (EPA, 2004). Municipalities are facing increased challenges to establish cleaning maintenance requirements in their Sewer System Management Plans (SSMP) based on identifying collection system pipes that are subjected to frequent accumulation of FOG deposits (Tupper, 2010). The difficulty in specifying an appropriate cleaning maintenance requirement is due to the inability to clearly associate the formation of FOG deposits with a specific food service establishment (FSE) facility. Therefore, a detailed study is needed to clearly identify how different source and environmental factors in sewer systems and/or FSEs may affect the rates of FOG deposit accumulations. Once these rates have been quantified, a model can be developed that can capture the kinetics of FOG deposits and can potentially be incorporated in system wide municipal sewer collection system models.

He et al. (2011) demonstrated that FOG deposits are similar to calcium-based saponified solids as hypothesized by Keener et al. (2008). Calcium-based saponified solids are products of a chemical reaction where free fatty acids released during fat hydrolysis react with calcium ions. Sodium and potassium alkalis have traditionally been used by researchers in fat saponification (Smith, 1932). However, calcium has been found as the predominant metal in FOG deposits of sewer systems (Keener et al., 2008; He et al., 2011; 2013, Iasmin et al., 2014). Conventional fats that are associated with the cooking process in food service establishments (FSE) range from saturated (palm oil and animal derived fats such as beef tallow, butter, and chicken fats) to mono-unsaturated/poly-unsaturated fats (cooking oils such as canola oil, corn oil, olive oil, soybean oil, and vegetable oils). It was expected that such fat sources would produce a range of fatty acids within these saponified solids. However, Keener et al. found palmitic as the predominant fatty acid (i.e., saturated) in FOG deposits which was later observed by He et al (2011) while producing laboratory based FOG deposits with grease interceptor (GI) effluent wastewater and the addition of calcium chloride. Recently, Iasmin et al. (2014) determined that some source and environmental factors, i.e.,

types of fats used in FSEs (saturated vs. unsaturated), types of calcium sources available in sewer systems, and the environmental conditions, i.e., pH and temperature in sewer systems affect the physical, chemical, and rheological properties of FOG deposits. Iasmin et al. results showed that fatty acid profiles of the calcium-based saponified solids produced under alkali driven hydrolysis were identical to the fatty acid profiles of the source fats. Iasmin et al. results also suggest that calcium content in the FOG deposits may depend upon the solubility limits of the calcium sources that are influenced by the pH and temperature conditions in the sewer system. These different source and environmental conditions may have a significant impact on the rate of FOG deposit formation, which was not assessed in Iasmin et al (2014). Therefore, to identify potential susceptible locations for FOG blockages in sewer collection systems, the kinetics of FOG deposits are needed and based on variable source and environmental factors uncovered in Iasmin et al (2013).

Literature reviews on model development that relates to saponification reactions have reported an autocatalytic nature of the reactions and that their kinetics tend to follow an "S"-shaped curve (Smith, 1932; Jones, 1958; Poulenat et al., 2003; Cotte et al., 2006). Cotte et al. (2006) proposed a saponification model that characterizes the entire experimental 'S' shape kinetics of triolein saponification by lead salts, at temperatures ranging from 100 to 180 °C. In Cotte et al.'s model, a two-step reaction process for saponificaiton with Lead oxide (PbO) was proposed that involved: a) a slow dissolution of metal salt (L) in an aqueous solution and b) the reaction between the dissolved metal species (D) and the oil (O) to form saponified solids (S) and an alcohol (A) by-product (Equations 1 and 2).

$$L \rightarrow D \ (k_1) \tag{1}$$

$$D + O \rightarrow S + A \ (k_2) \tag{2}$$

The final differential equation for the formation of saponified solids was described as follows:

$$\frac{df}{dt} = k_2[r_0\{1 - exp(-k_1 t)\} - f](1 - f) \tag{3}$$

$$r_0 = k_3 \frac{m^0_{metal}/M_{metal}}{m^0_{oil}/M_{oil}} \quad (4)$$

where, k_1, k_2, and k_3 are fitting parameters, r_0 is the initial metal salt/oil molar ratio, m^0 represents the initial masses of metal salt and oil, and M represents the molar masses of metal salt and oil. k_1 represents the forward rate of dissolution of metal salt in an aqueous solution, k_2 represents the rate of forward reaction between the dissolved metal species and the oil, and k_3 represents the rate of active participation of the metal and oil ratio. Cotte et al. showed good agreement between the predicted and experimental aqueous PbO data.

Fat crystallization models were also found to follow an "S" shaped curve for crystallization kinetics. Foubert et al. (2002) developed a crystallization model based on Wunderlich (1990) phase transition chemical reaction (Equation 5). Due to its "S" shape profile uncovered by saponification processes reported in the literature, Foubert et al.'s model is a potential candidate to simulate fat saponification.

$$O(liquid) \leftrightarrow S(solid) \quad (5)$$

Wunderlich (1990) assumes that the reaction order will depend on the presence of impurities or phase distributions with different levels of perfection. In their model, Foubert et al. assumed that the crystallization process is first order and n^{th} order in the forward and reverse directions, respectively. The differential equation that described Foubert et al.'s model was written in terms of the remaining crystallizable fat content (h):

$$\frac{dh}{dt} = k_2 h^n - k_1 h \quad (6)$$

$$h = \frac{a-f}{a} \quad (7)$$

where, f represents the fraction of saponified solid and a represents the maximum solid fat content. k_1, k_2, and n are the fitting parameters.

In Equation 6, Foubert et al. did not provide any theoretical justification for the reaction to proceed in reverse, but speculated that it may be related to the re-melting of some crystals

due to the dissipation of latent heat of crystallization. Foubert et al.'s model was compared with the re-parameterized Gompertz model and Avrami model and was found to better capture the asymmetry in 'S' shaped kinetics curves, which Smith (1932) had also noted in his saponification research. It may be possible to use Wunderlich's approach to describe fat saponification as it relates to FOG deposit formation where *h* describes the remaining oil content, and *f* describes the amount of FOG deposit.

Both Cotte et al. (2006) and Foubert et al. (2002) have the potential to capture the calcium-based saponification kinetics. While these empirical models may give plausible information related to the formation rate of FOG deposits, neither model tracks the rate of fat hydrolysis (i.e., the release of fatty acids that would then participate in the saponification reaction). Therefore, an additional part of this study was also to develop a mechanistic model for the production of saponified solids. Overall, the objectives of this research were to determine the kinetics of calcium-based saponified solids, evaluate environmental conditions that influence the rate of formation, and evaluate and develop a model to capture the experimental saponification kinetics data.

2 Experimental

2.1 Formation of calcium based saponified solids under laboratory conditions. The liquid/melted-solid fat (Canola or Beef tallow) was added to aqueous solution of calcium chloride/ calcium sulfate and mixed for eight hours under three different pH (7±0.5, 10±0.5, and ≈14) and two different temperature conditions (25 and 45 °C). Kinetic samples were collected for eight hours, at 15 minute intervals for the first hour and at 30 minute intervals till the eighth hour to capture the kinetics of the calcium-based saponified solid formation. A detail description of the experimental conditions can be found in Iasmin et al. (2014).

2.2 Computation of fraction of saponification using FTIR-ATR analysis. The quantity of saponified solids was measured following a modified equation of Poulenat et al. (2003) for

relative absorbance of signature calcium-based saponified solid bands as described in Iasmin et al. (2014). Saponified solid fraction was computed following Equation 8 in which all the characteristic saponification bands (the carboxylate ion symmetric stretching vibration, between 1300 and 1420 cm^{-1}; the carboxylate ion asymmetric stretching vibration, between 1550 and 1610 cm^{-1}; and the metal-oxygen bond vibration, around 670 cm^{-1}) were incorporated.

$$Fraction\ of\ saponification = \frac{Absorbance\ in\ (near\ 670\ cm^{-1} + between\ 1300\ and\ 1420\ cm^{-1} + between\ 1550\ and\ 1610\ cm^{-1})}{Absorbance\ in\ (near\ 670\ cm^{-1} + between\ 1300\ and\ 1420\ cm^{-1} + between\ 1550\ and\ 1610\ cm^{-1} + 1745\ cm^{-1})} \quad (8)$$

2.3 Saponification model development and evaluation. A mass-action based saponification model (MASM) was developed to evaluate a fundamental alternative to the empirical saponification and crystallization models described above. MASM was developed based on fundamental alkali driven hydrolysis and saponification reactions involved in calcium based saponification process: a) formation of free fatty acids (FFAs) from hydrolysis of triglyceride (Equation 9) and b) saponification of FFAs and calcium (Ca^{2+}) available in the system (Equation 10). The reaction system is presented in Table 1 in the form of a Gujer matrix (Audenaert et al., 2011). In this matrix, the processes involved are indicated in the left column. The components shown at the top of the table represent the derived state of the variables (mol. L^{-1}) that were calculated by solving a system of differential equations. The right column contains the reaction rates of each individual process. Finally, the central matrix elements are stoichiometric factors that were used in the mass balances. The mass balance of each variable can be produced by multiplying the stoichiometric factors with the reaction rates at the same row of the variable. The summation of these products yields the time derivatives for each variable. Formation of FFAs from hydrolysis of triglyceride was assumed to follow a one-step irreversible reaction process. The rate of triglyceride hydrolysis

was assumed to follow a fourth order reaction kinetics that is proportional to the presence of un-reacted triglyceride and water in the system. FFAs produced from triglyceride hydrolysis were consumed following a third order reaction kinetics in which two moles of FFAs react with one mole of calcium ions to produce calcium-based fatty acid salts, i.e., calcium-based saponified solids. A first order reverse reaction kinetics for the possible destruction of the saponified solids was assumed in Equation (10). The rate of destruction was related to possible breakdown and/or dissolution of the saponified solids (i.e., solid phase to liquid phase) and was hypothesized to occur due to the intense mixing conditions.

$$Triglyceride + 3\ water \xrightarrow{k_T} 3\ Free\ fatty\ acid\ (FFA) + Glycerol \quad (9)$$

$$2\ FFA + Ca^{2+} \xleftrightarrow{k_s, k_d} Ca(FFA)_2 \quad (10)$$

where, k_T = Reaction rate constant for the hydrolysis of triglyceride ($L^3\ mol^{-3}\ hr^{-1}$)

k_s = Reaction rate constant for saponification of FFA and Ca^{2+} ($L^2\ mol^{-2}\ hr^{-1}$)

k_d = Reaction rate constant for breakdown and/or dissolution (solid phase to liquid phase) of the saponified solids (hr^{-1})

The empirical Cotte saponification model, Foubert crystallization model, and the mass-action based saponification model were evaluated for their performances to represent the experimental kinetics of the calcium based saponified solids. MATLAB R2011a (Grant and Boyd, 2011) was used to solve each model and to determine the optimized values of the kinetic parameters.

Table 1 Gujer Matrix presentation of the reaction system

	Components					
Process	T	W	FFA	Ca^{2+}	$Ca(FFA)_2$ or S	Reaction Rate
Hydrolysis of Triglyceride	-1	-3	+3			$k_T[T][W]^3$
Production of saponified solids			-2	-1	+1	$k_s[Ca^{2+}][FFA]^2$
Breakdown or dissolution of saponified solids					-1	$k_d[S]$
	Triglycerides (mol. L^{-1})	Water (mol. L^{-1})	Free Fatty Acid (mol. L^{-1})	Calcium ions (mol. L^{-1})	Saponified solids (mol. L^{-1})	

2.4 Particle Swarm Optimization. Particle Swarm Optimization (PSO) was used to determine the optimized values of the kinetic parameters (Ebbesen et al., 2012). Gradient based optimization methods converge faster by using the derivative information to identify the search direction, but in case of multimodal function, there is a risk of the solution being stuck at a local minimum. Alternatively, heuristic search algorithms have been successfully used in solving optimization problems in multimodal functions (Angeline, 1998; Eberhart and Shi, 2001). Since the rate equations are non-linear with potential multiple maxima and minima, the usual gradient based method failed to converge at a global minima. A hybrid optimization toolbox was utilized that is comprised of the PSO algorithm and fmincon, a gradient-based search algorithm. The objective of the hybrid scheme was to convert the

global search to a local search after a number of designated iterations and therefore produce faster results than a standalone PSO technique. PSO algorithm is stochastic and therefore results in a family of solutions. A number of runs to determine a single parameter were therefore necessary to find a range of possible solutions. To determine the kinetic parameters, the kinetic models were simulated 150 times using the hybrid optimization technique. The anomalous solutions that did not fit the data were identified and discarded subsequently. After the manual search, the final ranges of solutions for kinetic parameters were obtained. Each data set was also compared with the standalone Cotte saponification and Foubert crystallization models using kinetic parameters found from PSO optimization to ensure the quality control of PSO. The objective function that was used in this study was the minimization of mean squared error between the experimental data and the results predicted by the model. The optimization problem can be summarized in Equation 11, where p represents the parameters to be estimated and n is the number of data points.

$$\min_{p \in R} \left(\frac{(y_{\exp} - y_{\mathrm{model}}(p))^2}{n} \right) \tag{11}$$

2.5 Determination of relationships between model parameters and experimental conditions. To understand how the experimental conditions, i.e., pH, temperature, source fat types (canola or beef tallow), and source calcium types (i.e., calcium chloride or calcium sulfate) influence the values of the kinetic parameters in the empirical and mass-action based saponification models, relationships were determined based on the statistical analysis of the parametric and experimental data. The statistical analyses were performed using JMP Pro 9 statistical software (SAS Institute, 2001). For each model, outliers were identified using multivariate analysis. Multiple non-linear regression analysis was subsequently performed to develop an equation for each kinetic parameter. The equation was developed based on the statistically significant relationship of each kinetic parameter with each experimental variable. The non-linear transformations for the experimental variables were constructed using the mathematical transformations available in JMP, such as square root, exponential, and Arrhenius equation. The best possible relationship or model equation with the lowest

Bayesian Information Criterion (BIC) value was determined using a mixed stepwise analysis with the effects of the statistically significant experimental variables. Mixed stepwise analysis involved inclusion of the next significant experimental variable to the equation whose probability value was lower than the previous variable (i.e., $p2 > p1$ and $pi < 0.05$, where i represents each experimental variable). The fat source types and calcium source types were categorical variables, and therefore, numerical substitutions were necessary to include their effects on empirical relationships. Fatty acid compositions of source fat types and calcium contents in the final saponified solids were adopted, respectively.

3 Results and Discussion

3.1 Kinetics of calcium based saponified solids. The evolution of saponification was determined by plotting the relative formation of saponified solids (fraction of saponification) vs. time for all the associated absorption bands as shown in Equation 8. Calcium sulfate based saponified solids, however, displayed interference in the region of metal-oxygen band (~ 670 cm^{-1}). Figure 1 illustrates the presence of metal-oxygen band in both the hydrated calcium sulfate and calcium-based saponified solids. In the computation of saponified solid fraction for calcium sulfate based solids, the contribution of Ca=O bands may come from both the saponified solids and/or the un-reacted calcium sulfate. However, gradual reduction in ester carbonyl band at 1745 cm^{-1} and simultaneous appearance of carboxylate bands and H-bonded O-H stretches in the vicinity of ~3360 cm^{-1} were observed that suggested progressive saponification. Therefore, it is hypothesized that the interference of un-reacted calcium sulfate on the computation of fraction of saponification decreased with time as saponification progressed. Calcium chloride based saponified solids displayed no such interference as can be seen in Figure S1. Iasmin et al. (2014) also observed a quick agglomeration property associated with calcium sulfate when in contact with liquid fat during the saponified solid formation process. Therefore, it is hypothesized that, gypsum, a product of biogenic concrete corrosion, may also accumulate in FOG deposits in two ways: a) gypsum released from the concrete surface may adsorb the liquid fat attached in the sewer crown portion and adhere to the sewer wall; b) gypsum released from the concrete surface

may travel downstream of the sewer due to the flow of wastewater, undergo saponification, and contribute to the growth of the FOG deposit matrix.

Figure 2 display the kinetics of calcium based saponified solids under different pH and temperature conditions. The results showed that the calcium-based saponification did not follow an "S" shape profile for the conditions tested, as noted in previous saponification studies involving different cations, fat source, and operating conditions (Smith, L., 1932; Jones, 1958; Poulenat et al., 2003; Cotte et al., 2006). The absence of the initial lag period can be attributed to the incorporation of all the representative saponification bands compared to Poulenat et al.'s study in which only a single carboxylate absorption band was considered to compute fat saponification. The visual observations of solids formations were also consistent with the initial saponification data. Other conditions beyond the inclusion of additional wave bands such as different types of fat sources used in this study may also play a role in faster saponification. The results showed that, for calcium chloride, an average of 15-35 percent of saponified solids was formed with both types of fats within two minutes of mixing the reactants, for all temperature and pH conditions. These results suggest that there will be a fraction of fat that will undergo fast hydrolysis and react with the available calcium. An average of 15-80 percent of saponified solids was observed for calcium sulfate based saponified solids, for all temperature and pH conditions. Although it was hard to distinguish the exact quantity, a fraction of saponification in calcium sulfate based saponified solids could be from the contribution of the metal oxygen band of the un-reacted calcium sulfate, as noted above. For calcium chloride based solids after eight hours of reaction time, the maximum level of saponified solids was found to be approximately 40 percent at both the neutral pH and pH 10 under room temperature conditions. High pH conditions, however, showed higher percentage of saponified solids (i.e., 60%) under warm temperature conditions (45 °C). For calcium sulfate, the maximum level of saponified solids was approximately 90% at both the neutral pH and pH 10 under warm temperature conditions. For room temperature conditions, a maximum of 80% of the saponified solids was produced at pH 10. The results also showed that beef tallow with calcium chloride produced the lowest amount of saponified

solids for all the conditions observed. Although the exact reason for beef tallow producing lower quantities of solids is unknown, it is hypothesized that beef tallow, being a solid fat under room temperature, may require more thermal energy to produce the similar amount of solids under the same conditions. The results also suggest that both the pH and temperature in sewer systems will affect the kinetics of FOG deposit formations as can be seen in Figure 2 and Figures S2 to S3. Therefore, apart from the possible microbial driven hydrolysis mentioned in Iasmin et al. (2013), it is hypothesized that four types of alkali driven hydrolysis may influence FOG deposit formation and may depend on the location in the collection system: a) fast hydrolysis as soon as the fat comes in contact with moisture during the cooking process at the FSE; b) alkali driven hydrolysis in grease interceptor near the inlet due to the incoming high alkaline detergents; c) alkali driven hydrolysis along the sewer line due to prolonged contact and/or mixing between un-reacted fat and high moisture; d) alkali driven hydrolysis of the adsorbed/entrapped oil at the sewer crown portion due to the release of gypsum.

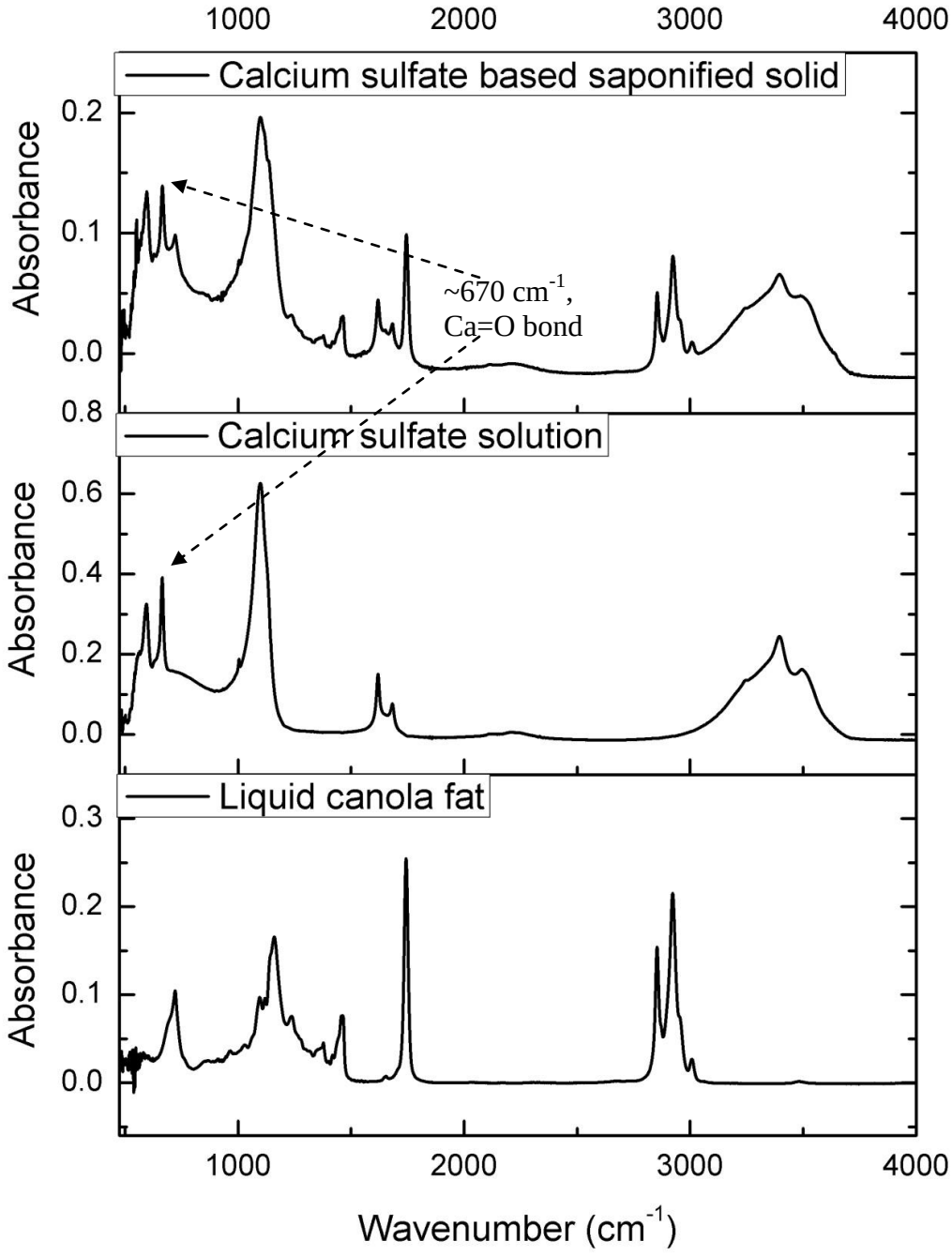

Figure 1 Spectral comparison of calcium sulfate-based saponified solids made with canola, calcium sulfate aqueous solution, and canola oil

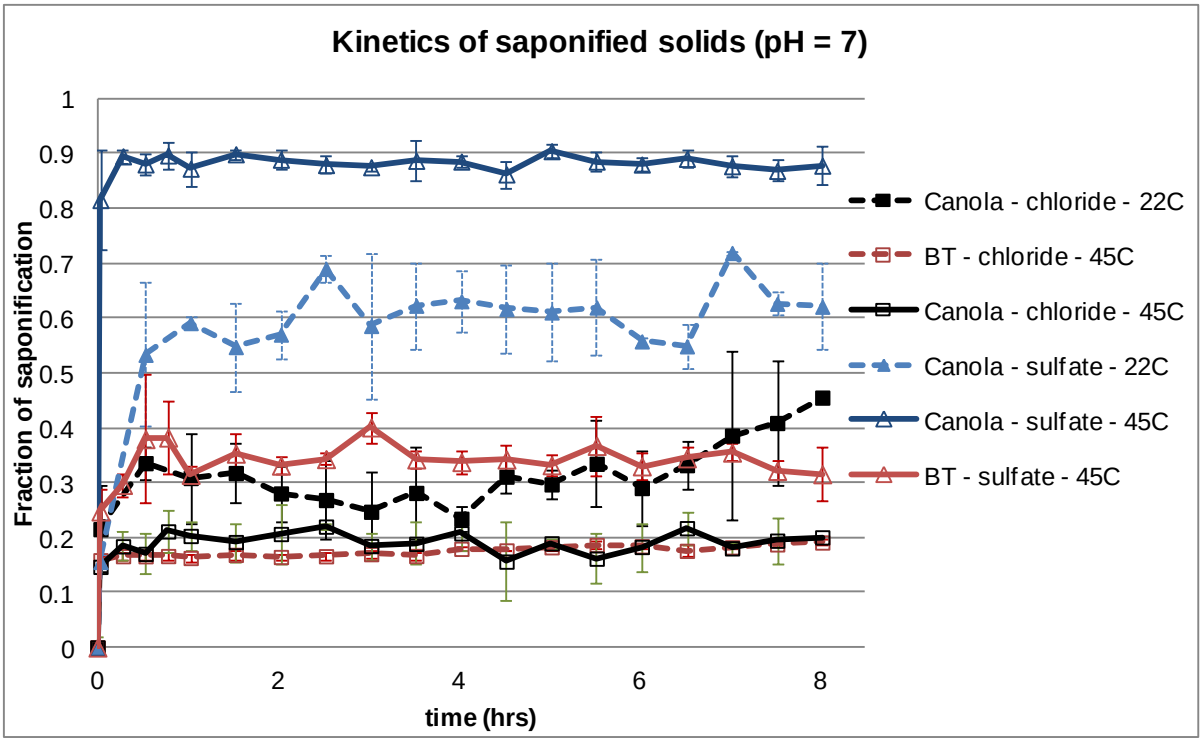

Figure 2 Graphs showing kinetics of calcium based saponified solids at pH 7 with varying temperature; for all types of fats and calcium forms

3.2 Evaluation of Kinetic models and model parameter relationships with experimental conditions

3.2.1 Performance of Cotte saponification Model

The Cotte et al. (2006) saponification model evaluations are presented in Figure 3 and Supporting Information Figures S4 to S8. Cotte saponification model seemed to fit all sets of experimental data well. Equations (12)-(14) display statistically significant effects of the experimental variables observed on the changes in Cotte saponification model kinetic parameters. The values of the kinetic parameters can be found in Supplemental Table 1.The first kinetic parameter, k_1, represents dissolution of calcium source salts (i.e., calcium chloride or calcium sulfate) in an aqueous solution. As shown in Equation (12), temperature plays a significantly positive role in the dissolution process and the result is expected as the temperature affects solubility of calcium sources. The presence of palmitic in the source fats

also seems to affect calcium dissolution. It has been hypothesized in a previous study that increased palmitic fraction in the source fat will increase the attraction of calcium into the FOG deposit matrix through double layer compression theory (He et al., 2013). The relationships in Equation (12) also show that pH had no statistically significant effect on the dissolution of calcium sources. However, when calcium chloride was used as the calcium source, the mean values of k_1 decreased with increasing pH conditions irrespective of fat source and temperature conditions, as can be seen in Supplemental Table 1. The overall statistically insignificant effect of pH on the calcium dissolution rate may be due to the fluctuations in k_1 values for calcium sulfate based saponified solids (Supplemental Table 1). These fluctuations in k_1 data for calcium sulfate based saponified solids may be due to the solubilities of different forms of calcium sulfate (i.e., anhydrous calcium sulfate and/or hydrated calcium sulfate) (Partridge and White, 1929; Messnaoui and Bounahmidi, 2006). Although relevant literature could not be found, the results suggest that pH affects the solubility of calcium chloride, and therefore, the available Ca^{2+} ions for fat saponification. The calcium content in the final saponified solids, presented in the Iasmin et al. (2014), seemed to support this hypothesis.

$$k_1 = -2834.9 + 19.8\,Palmitic(\%) + 97.3\,e^{-\frac{11605}{T(^{\circ}C)+273.15}} \quad (12)$$

The parameter k_2 represents the rate of saponification among the dissolved metal species and the available source fat. The results in Equation (13) show that temperature and pH generally play positive roles in the rates of saponification. However, for liquid canola fat and calcium chloride under room temperature, the mean rates of saponification decreased with increasing pH (Supplemental Table 1). The decreasing trend in rates of saponification may be due to the decrease in available Ca^{2+} ions with the increase in pH, as previously noted with the rates of calcium dissolution. The results in Equation (13) also suggest that a significant reciprocal relationship is present between the calcium in the final saponified solid matrix and the rate of saponification. Overall, the results suggest that slow saponification may lead to more bound (i.e. saponified) calcium in FOG deposit samples in sewer systems. Therefore, FOG deposits that are formed in slow saponification zones (e.g., zones inside grease interceptors and along

the sewer lines), where neutral pH conditions are mostly observed, will likely contain higher calcium quantity compared to FOG deposits formed at the high saponification zones, i.e., GI inlets (Aziz et al., 2012).

$$k_2 = -66205.8 + \frac{702916.4}{Calcium(\%wt)} + 1.99e^{pH} + 1846.7\, e^{-\frac{11605}{T(℃)+273.15}} - \frac{22.82\, e^{pH}}{Calcium(\%wt)} - \frac{19307.7\, e^{-\frac{11605}{T(℃)+273.15}}}{Calcium(\%wt)} - 0.054e^{pH}e^{-\frac{11605}{T(℃)+273.15}} + \frac{0.625e^{pH}e^{-\frac{11605}{T(℃)+273.15}}}{Calcium(\%wt)} \quad (13)$$

The value of k_3 represents the initial fraction of metal salt and fat molar ratio that is actively participating in the saponified solid formation process. The relationships in Equation (14) show that the quantity of palmitic in source fat has the most significant effect on the active metal-oil fraction. It suggests that the increase in palmitic fraction in the source fat will reduce the active initial fraction of metal salt and fat ratio in the saponification process. The result is consistent with the previous observations as beef tallow produced less saponified solids than liquid canola oil within the same time frame of reaction (i.e., eight hours). The results in Equation (14) also show that high pH and temperature have a negative effect on the active metal and fat ratio. An increase in pH and temperature may change the solubility of metal salts and the production of FFA due to the change in hydrolysis of triglycerides. As a result, the stoichiometric participation of Ca^{2+} and FFA to create FOG deposits may decrease. The negative relationship of k_3 with the calcium content in the final saponified solids also supports this hypothesis. Although the results show that the palmitic in source fats and high temperature and pH conditions are less suitable for stoichiometric saponification, the participation of saturated fats in saponified solids formation may increase as the fats undergo the melting process under warm temperature conditions, e.g., cooking (Duckett and Wagner, 1998). Also, attraction of excess Ca^{2+} and FFA to the FOG deposit matrix is possibly based on the DLVO theory as explained by He et al. (2011).

$$k_3 = 65.97 + \frac{93.2}{Palmitic\,(\%)} - 0.000007\, e^{Calcium(\%wt)} - 0.0000102\, e^{pH} - 1.84\, e^{-\frac{11605}{T(℃)+273.15}} \quad (14)$$

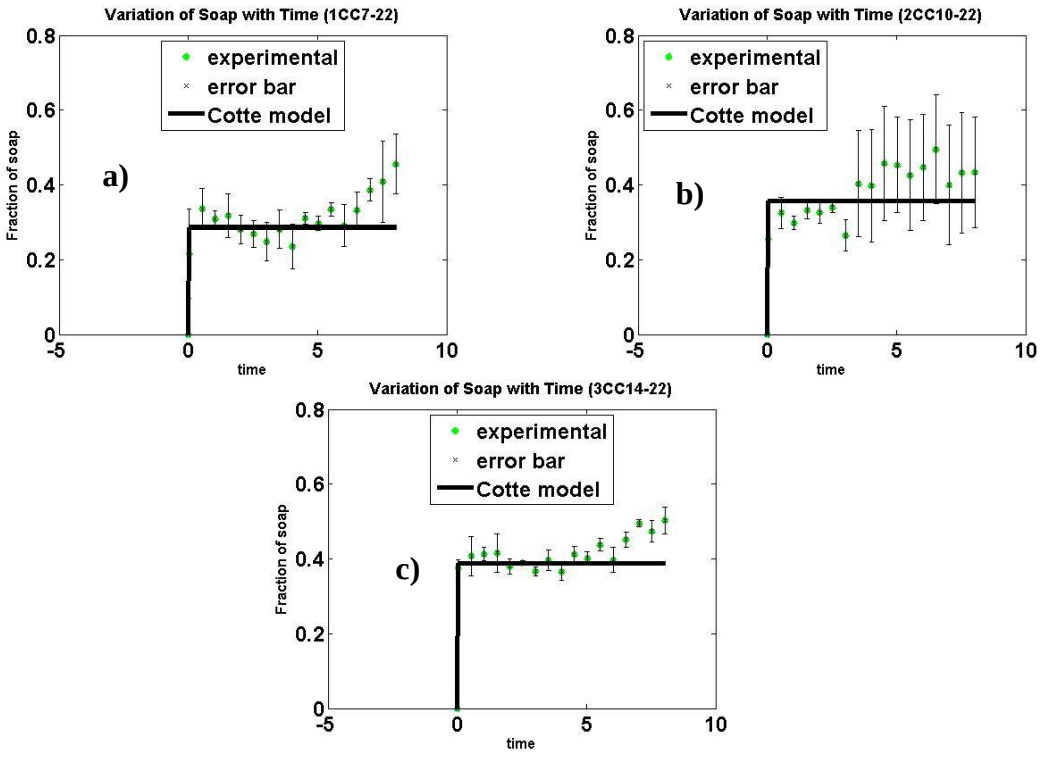

Figure 3 Cotte saponification model fits (Canola, calcium choride, 22 °C under a) pH 7±0.5; b) pH 10±0.5; and c) pH 14±0.5)

3.2.2 Performance of Foubert Crystallization Model

The Foubert et al. (2002) model evaluations are presented in Figure 4 and Supporting Information Figures S9 to S12. The values of the kinetic parameters are listed in Supplemental Table 2. These figures show that Foubert crystallization model could represent the most of the experimental data reasonably well with few exceptions associated with the early formation of solids and reactions involving beef tallow with calcium chloride. Beef tallow with calcium chloride produced the lowest quantity of saponified solids among all the tested conditions, as previously mentioned. It is hypothesized that Foubert crystallization model has limited ability to predict low saponified solids production and/or slow rate of change in saponification. It may be due to the model's structure which does not track the reactant components that are participating in the saponification reaction (i.e., availability of Ca^{2+} and FFA).

Equations (15) and (16) display relationships between Foubert crystallization kinetic parameters (k_1 and k_2) and operating conditions tested in this study. k_1 represents formation of saponified solids, i.e., saponification rate and k_2 represents breakdown of saponified solids. The third fitting parameter, n, that represents the order of the breakdown of saponified solids was set to 1. Such approximation was made to reduce complexity of the model based on Foubert et al. (2002)'s observation that any adjustments to the lag phase was performed by changing the n value and that no lag phase was noted in current study. The results of the study showed that both the formation and breakdown of saponified solids largely depend on pH and temperature, with temperature being more influential. However, temperature was more influential on the formation rate than the breakdown rate, which confirms that increased temperature will increase the quantity of saponified solids. In Supplemental Table 2, the rate of crystallization also generally increased with increasing pH for both the calcium sources and source fats under both the temperature conditions. However, a single anomaly was observed for canola and calcium sulfate under warm temperature conditions. The rate of crystallization seemed to peak at pH 10±0.5. While all the rates of calcium sulfate based saponified solids did not follow a particular trend, visual observations showed significant agglomeration property in calcium sulfate while in contact with liquid canola fat (Iasmin et al., 2014). The rates of solids breakdown, however, showed consistent trends for both the calcium sources. The breakdown rates also increases with increasing pH, especially in calcium sulfate based saponified solids (Supplemental Table 2). The presence of calcium found in the final saponified solids seemed to negatively impact the rates of saponification, as was also previously observed with Cotte saponification model.

$$k_1 = -68481 - 0.0018\, e^{Calcium\ (\%wt)} + 0.00214\, e^{pH} + 1862.3\, e^{-\frac{11605}{T(℃)+273.15}} \quad (15)$$

$$k_2 = -16155.5 + 0.00075\, e^{pH} + 437.3\, e^{-\frac{11605}{T(℃)+273.15}} \quad (16)$$

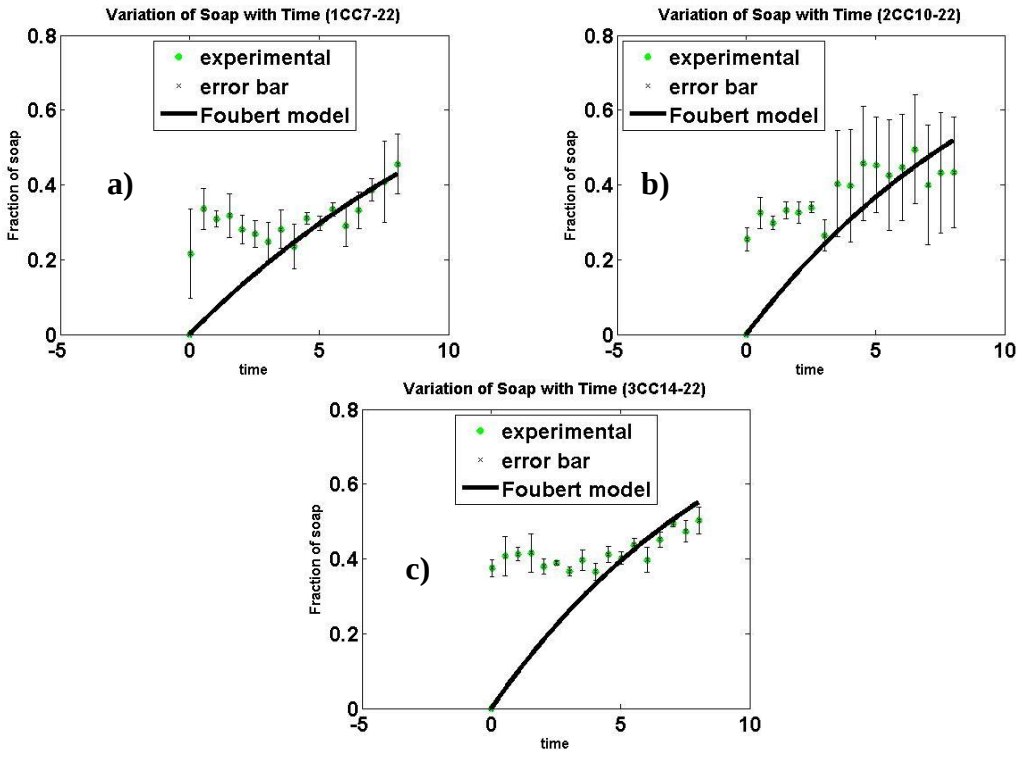

Figure 4 Foubert crystallization model fits (canola, calcium chloride, 22 °C under a) pH 7±0.5; b) pH 10±0.5; and c) pH 14±0.5)

3.2.3 Performance of mass-action based saponification model

The empirical Cotte et al. (2006) saponification and Foubert et al. (2002) crystallization models could reasonably represent the experimental data. However, a fundamental alternative was needed to better understand the FOG deposit formation chemistry. The mass-action based saponification model (MASM) was developed based on alkali driven hydrolysis and calcium based saponification, as described earlier. The MASM approach can track changes in reactants (i.e., triglyceride, FFA, and Ca^{2+}) in addition to the formation of saponified solids.

The values of kinetic parameters are listed in Table 2. The model evaluations are shown in Figure 5 and supporting Figures S13 to S16. The model fits show that mechanistic model performed well in fitting experimental kinetic data for saponified solids made with liquid

canola fat and calcium chloride. The results show that mechanistic model tries to capture both the initial rise and gradual change leading to final saponification, compared to both the Cotte saponification and Foubert crystallization models. For beef tallow and calcium chloride condition, however, the model displayed tendency to fit the saponified data only at later periods. When changes in other reaction components (i.e., triglyceride, total FFA, Ca^{2+}, and water) under the same pH and temperature conditions were compared using the MASM approach, the hydrolysis of beef tallow was slower compared to the liquid canola fat as shown in supporting Figure S17. MASM also showed that the rate of usage of total FFA (i.e., FFA concentration in the reaction system) and the rate of depletion of Ca^{2+} were slower for beef tallow compared to the liquid canola fat (Supporting Figure S17 and S18).. The trends of the auxiliary reaction components suggest that the participation of saturated beef tallow is slower compared to the unsaturated canola fat under the same pH and temperature conditions tested. This observation of fat participation is consistent with the Cotte saponification model results (kinetic parameter k_3) and is better explained with the MASM approach. The model also seemed to under-predict the kinetic data for calcium sulfate based saponified solids. However, the observation was consistent with the data obtained from Fourier transform infrared analysis (FTIR), as previously discussed. The FTIR-ATR data suggested that calcium sulfate, having similar peaks as calcium based saponified solids near 670 cm^{-1}, can contribute to metal oxide vibration band and therefore may result in false positive indicator of saponification based on the equation used to estimate the fraction of saponification.

Equations (17)-(19) display relationships between the MASM kinetic parameters and the operating conditions observed. The parameter k_T represents the rate of fat hydrolysis that seems to significantly depend upon temperature and presence of palmitic in the source fat. However, the negative relationship suggests that room temperature conditions are more conducive towards hydrolysis of fats than warm temperature (45 °C). On the other hand, saponification significantly increases with increasing temperature (i.e., the temperature coefficient is significantly higher in k_s than in k_T). Therefore, significant saponification leads to more saponified solids under warm temperature conditions, as was previously observed.

More palmitic also leads to less hydrolysis which is consistent with the previously observed results (i.e., beef tallow having more saturated fraction produces less saponified solids than liquid canola oil under the same pH and temperature conditions). The rate of saponification also seemed to have a reciprocal relationship with the calcium present in the final saponified solids. The results, therefore, suggests that slower saponification under milder temperature conditions and/or agglomeration of excess calcium, both discussed in previous studies (He et al., 2011 and Iasmin et al., 2014), are necessary to achieve the significantly high calcium content found in FOG deposit samples. The last parameter, k_d, represents possible breakdown or phase change (i.e., solid to liquid) of saponified solids. While there may not be an actual breakdown or dissolution of saponified solids present in FOG deposit formation process, the results in Equation (19) can be explained based on the possible physical changes during the solids formation. The results in Table 2 suggest that saponified solids produced with calcium chloride may experience more breakdown and/or dissolution compared to calcium sulfate based saponified solids, while comparing the k_s and k_d values under the same conditions tested.

$$k_T = 6754.54 - 30.03\ Palmitic(\%) - 151.37\ e^{-\frac{11605}{T(℃)+273.15}} \quad (17)$$

$$k_s = -41495 + \frac{26405}{Calcium(\%wt)} + 1063.2\ e^{-\frac{11605}{T(℃)+273.15}} \quad (18)$$

$$k_d = 0.475 + 0.0032\ Palmitic(\%) + 0.0101\ Calcium(\%wt) - 0.0000000086\ e^{pH} - 0.015\ e^{-\frac{11605}{T(℃)+273.15}} \quad (19)$$

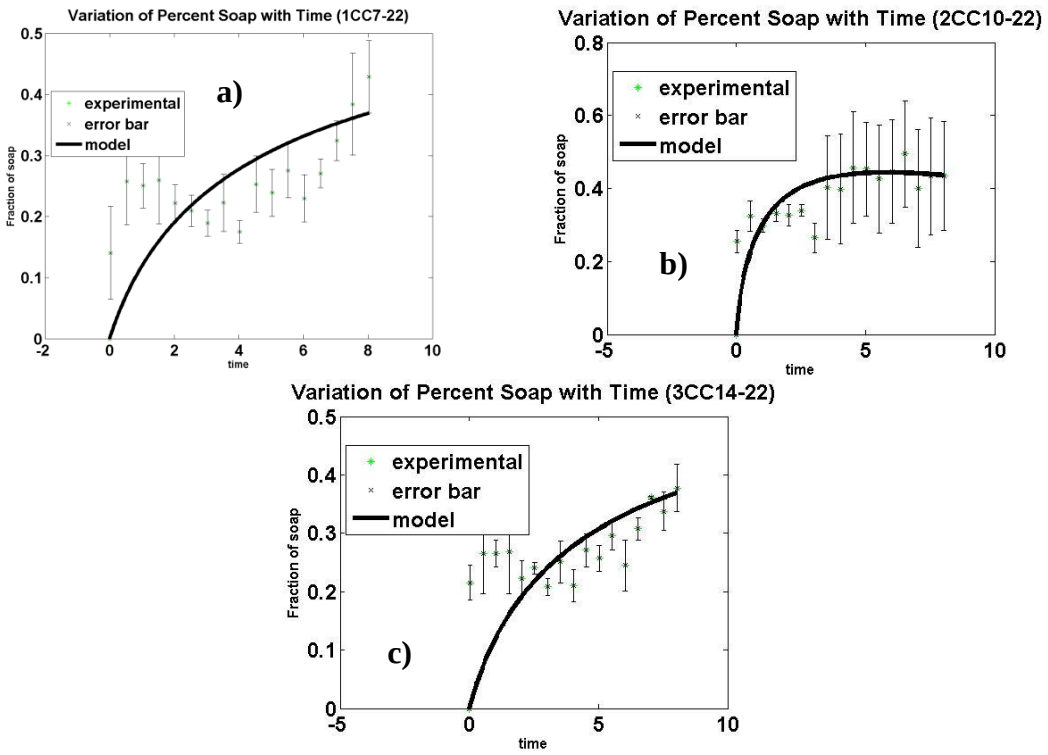

Figure 5 Mass-action based saponification model fits (canola, calcium chloride, 22 °C under a) pH 7±0.5; b) pH 10±0.5; and c) pH 14±0.5)

Table 2 Mass-action based saponification model parameters

		pH	Temp	Mechanistic model		
Fat type	Calcium type	± 0.5	± 0.5 (°C)	k_T (L^3 mol^{-3} hr^{-1})	k_S (L^2 mol^{-2} hr^{-1})	k_d (hr^{-1})
Canola	Calcium chloride	7	22	59.83 ± 24.65	1e-1 ± 2.23e-16	1e-3 ± 6.53e-19
Canola	Calcium chloride	10	22	63.74 ± 26.60	5e-1 ± 0	0.0465 ± 1.58e-6
Canola	Calcium chloride	14	22	72.16 ± 24.34	4e-1 ± 8.9e-16	1e-3 ± 6.53e-19
Canola	Calcium sulfate	7	22	92.91 ± 371.63	1525.86 ± 15964	1e-3 ± 6.53e-19
Canola	Calcium sulfate	10	22	228.65 ± 962.2	5492 ± 34815	1e-3 ± 6.53e-19

Table 2 Continued

Fat type	Calcium type	pH ± 0.5	Temp ± 0.5 (°C)	Mechanistic model		
				k_T (L^3 mol^{-3} hr^{-1})	K_S (L^2 mol^{-2} hr^{-1})	k_d (hr^{-1})
Canola	Calcium sulfate	14	22	607.38 ± 4013	9069.12 ± 55085	1e-3 ± 6.53e-19
Canola	Calcium chloride	7	45	54.88 ± 27.2	0.0856 ± 7.92e-7	1e-1 ± 2.23e-16
Canola	Calcium chloride	10	45	56.35 ± 26.9	0.0773 ± 7.63e-7	1e-1 ± 2.23e-16
Canola	Calcium chloride	14	45	98.76 ± 345.6	394.38 ± 451.98	1e-3 ± 6.53e-19
Canola	Calcium sulfate	7	45	988.95 ± 6814.3	1108.72 ± 4861.9	1e-3 ± 6.53e-19
Canola	Calcium sulfate	10	45	3932.43 ± 17460.7	1876.51 ± 7813.67	1e-3 ± 6.53e-19
Canola	Calcium sulfate	14	45	71.45 ± 293.75	204.35 ± 203.3	1e-3 ± 6.53e-19
Beef tallow	Calcium chloride	7	45	26.77 ± 14.79	0.06 ± 1.46e-16	0.096 ± 7.97e-6
Beef tallow	Calcium chloride	10	45	29.57 ± 13.88	0.07 ± 1.11e-16	0.123 ± 2.34e-6
Beef tallow	Calcium chloride	14	45	28.24 ± 13.72	0.07 ± 1.25e-16	0.134 ± 1.5e-5
Beef tallow	Calcium sulfate	7	45	55.48 ± 24.53	0.5 ± 7.04e-6	0.02 ± 1.39e-17
Beef tallow	Calcium sulfate	10	45	57.71 ± 28.98	0.25 ± 0	0.04 ±2.78e-17
Beef tallow	Calcium sulfate	14	45	34.07 ± 62.3	5330.4 ± 37599	1e-3 ± 6.53e-19

When the three kinetic models are considered, the comparison among the values of the kinetic parameters cannot be made due to the inconsistencies in units and/or dimensions. However, certain insights are found on the operating conditions that may significantly affect

the kinetics, and therefore, the mechanisms of FOG deposit formations, as shown in Figure 6. Overall, pH and temperature play a significant role suggesting high pH and high temperature conditions will lead to faster saponification, and therefore, the formation of FOG deposits. However, slower saponification is necessary for high calcium content in FOG deposits. Therefore, the high calcium content may be a result of a) FOG deposits formed in the slow saponification zones, i.e., sewer lines and zones of GIs, as mentioned earlier; and b) accumulation of excess Ca^{2+} ions due to the DLVO attraction (He et al., 2011). The results also suggest that unsaturated fat that are liquid under room temperature are more active in saponified solid formation process. Therefore, liquid fats discharged from the GI effluents have a greater potential in forming FOG deposits and reduction of their discharge into the sewer system using effective pretreatment control methods can reduce FOG deposit formation. The saturated fractions (i.e., palmitic) in FOG deposits may increase due to the following: a) the melting of the saturated fats due to high temperature cooking and/or washing resulting in their increased participation (Duckett and Wagner, 1998); b) the conversion of unsaturated fat to saturated fat due to high temperature cooking (Warner, 1999); c) the solidification of saturated fat and accumulation with the FOG deposit matrix (Iasmin et al., 2014); d) the accumulation of saturated FFA (i.e., palmitate) to the FOG deposit matrix due to the DLVO attraction (He et al., 2011); and finally e) the conversion of unsaturated to saturated fat in the layers of FOG deposits due to microbial activities (Rhead et al., 1971). While none of these conditions or hypothetical situations for saponification involving palmitic have been tested, they do provide experimental conditions that need to be investigated in future research.

While all the three models can represent the saponification process with a particular strength, the MASM approach can explain the FOG deposit formation chemistry more efficiently, knowing the basic reactant constituents. It has the most distinct ability to track the triglyceride hydrolysis that helped better explain the active participation of liquid Canola fat over solid Beef Tallow. It can also track changes in the system concentrations of the saponification reaction components (i.e., Ca^{2+} and FFA) that enhances the understanding of

FOG deposit formation chemistry with the changes in environmental conditions (i.e., pH and temperature). The MASM approach is therefore considered to be better suited to predicting the variations in saponification data and is recommended for the use in large scale FOG deposit prediction models. It is hypothesized that the performance of the MASM approach can be further improved by incorporating separate hydrolysis and/or saponification rates for the major FFAs (i.e., palmitic, oleic, and linoleic) participating in the FOG deposit formation process.

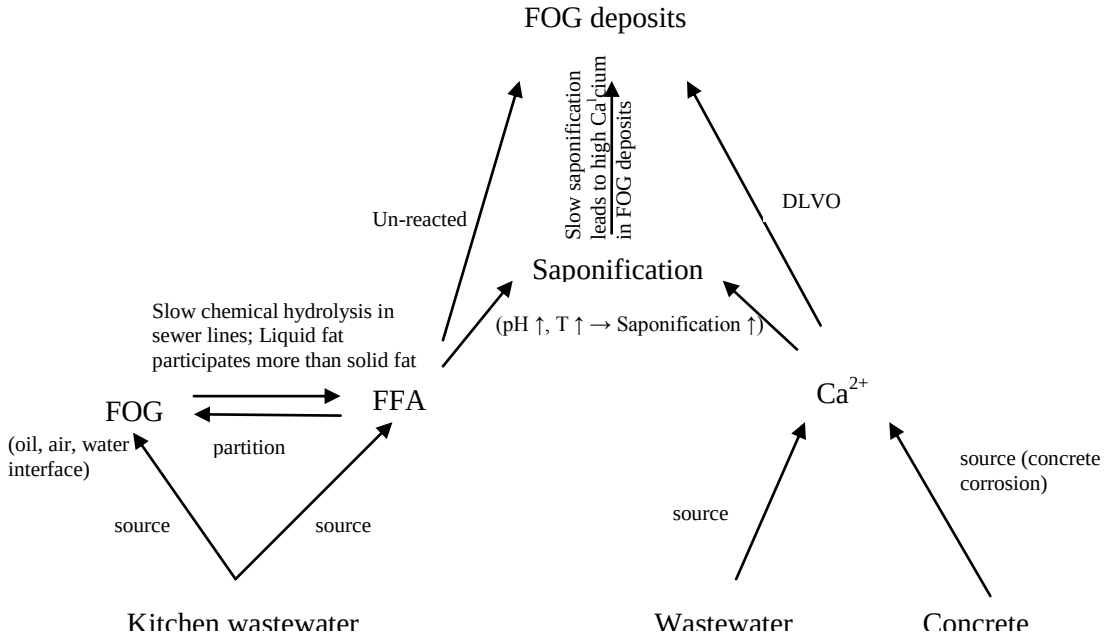

Figure 6 Modified He et al. (2013) mechanism of FOG deposit formation in sewer lines

References

Angeline, P. J. (1998). Evolutionary optimization versus particle swarm optimization: Philosophy and performance differences. In *Evolutionary Programming VII* (pp. 601-610). Springer Berlin Heidelberg.

Audenaert, W., Vermeersch, Y., Van Hulle, S. W., Dejans, P., Dumoulin, A., & Nopens, I. (2011). Application of a mechanistic UV/hydrogen peroxide model at full-scale: Sensitivity analysis, calibration and performance evaluation. *Chemical Engineering Journal*, *171*(1), 113-126.

Aziz, T. N., Holt, L. M., Keener, K. M., Groninger, J. W., & Ducoste, J. J. (2012). Field Characterization of External Grease Abatement Devices. *Water Environment Research*, *84*(3), 237-246.

Cotte, M., Checroun, E., Susini, J., Dumas, P., Tchoreloff, P., Besnard, M. (2006). Kinetics of oil saponification by lead salts in ancient preparations of pharmaceutical lead plasters and painting lead mediums.*Talanta*, *70*(5), 1136-1142

Dorner, H., and Beddoe, R. (2002). Prognosis of concrete corrosion due to acid attack 9th internat. Paper presented at the *Conf. Durability of Building Materials*

Ducoste, J. J., Keener, K. M., Groninger, J. W., and Holt, L. M. (2008). Fats, roots, oils, and grease (FROG) in centralized and decentralized systems. *Water Environment Research Foundation.IWA Publishing, London*

Ebbesen, S., Kiwitz, P., & Guzzella, L. (2012, June). A generic particle swarm optimization Matlab function. In *American Control Conference (ACC), 2012* (pp. 1519-1524). IEEE.

Eberhart, R. C., and Shi, Y. (2001). Tracking and optimizing dynamic systems with particle swarms. In *Evolutionary Computation, 2001. Proceedings of the 2001 Congress on* (Vol. 1, pp. 94-100). IEEE.

Report to Congress: Impacts and Control of CSOs and SSOs. (2004). *U.S. Environmental Protection Agency*

Foubert, I., Vanrolleghem, P. A., Vanhoutte, B., & Dewettinck, K. (2002). Dynamic mathematical model of the crystallization kinetics of fats. *Food Research International, 35*(10), 945-956

Grant, M., & Boyd, S. (2011). CVX: Matlab software for disciplined convex programming, version 1.21.

Gutiérrez-Padilla, M. G. D., Bielefeldt, A., Ovtchinnikov, S., Hernandez, M., & Silverstein, J. (2011). Biogenic sulfuric acid attack on different types of commercially produced concrete sewer pipes. *Cement and Concrete Research, 40*(2), 293-301

He, X., Iasmin, M., Dean, L. O., Lappi, S. E., Ducoste, J. J., & de los Reyes III, F.L. (2011). Evidence for fat, oil, and grease (FOG) deposit formation mechanisms in sewer lines. *Environmental Science & Technology, 45*(10), 4385-4391

He, X. de los Reyes III, F.L., Leming, M., Lappi, M., Ducoste, J. (2013). Mechanisms of Fat, oil, and grease (FOG) deposit formation in Sewer Lines. *Water Research, 47(13), 4451-4459*

Hermansyah, H., Kubo, M., Shibasaki-Kitakawa, N., & Yonemoto, T. (2006). Mathematical model for stepwise hydrolysis of triolein using candida rugosa lipase in biphasic oil–water system. *Biochemical Engineering Journal, 31*(2), 125-132.

Jones, L. D. (1958) Saponification stressing the newer methods. *Journal of the American Oil Chemists' Society, 35*(11), 630-634

Iasmin, M., Dean, L. O., Lappi, S. E., & Ducoste, J. J. (2014). Factors that influence properties of FOG deposits and their formation in sewer collection systems. *Water research, 49*, 92-102

Keener, K.M., Ducoste, J.J., and Holt, L.M. (2008). Properties influencing fat, oil, and grease deposit formation. *Water Environ. Res*. 80, 2241-2246

Messnaoui, B., and Bounahmidi, T. (2006). On the modeling of calcium sulfate solubility in aqueous solutions. *Fluid phase equilibria*, *244*(2), 117-127.

Mori, T., Nonaka, T., Tazaki, K., Koga, M., Hikosaka, Y., and Noda, S. (1992). Interactions of nutrients, moisture and pH on microbial corrosion of concrete sewer pipes. *Water Research, 26*(1), 29-37

Parker, C.D. (1945a). The corrosion of concrete I: The isolation of a species of bacterium associated with the corrosion of concrete exposed to atmospheres containing hydrogen sulfide. *Aust. J. Exp. Biol. Med. Sci.*, 23(2), 81-90

Parker, C.D. (1945b). The corrosion of concrete 2. The function of Thiobacillus-Concretivorous (Nov-Spec) in the corrosion of concrete exposed to atmospheres containing hydrogen sulfide. *Aust. J. Exp. Biol. Med. Sci.*, 23(2), 91-98

Partridge, E. P., and White, A. H. (1929). The solubility of calcium sulfate from 0 to 200. *Journal of the American Chemical Society*, *51*(2), 360-370.

Poulenat, G., Sentenac, S., and Mouloungui, Z. (2003). Fourier-transform infrared spectra of fatty acid salts—Kinetics of high-oleic sunflower oil saponification. *Journal of Surfactants and Detergents, 6*(4), 305-310

Pro, O. 8. (2007). About Origin Pro 8 SRO, V8.0724 Software, Copyright 1991-2007, *Origin Lab Corporation*

Rhead, M., Eglinton, G., Draffan, G., and England, P. (1971). Conversion of oleic acid to saturated fatty acids in severn estuary sediments. *Nature*, Volume 232, Issue 5309, pp. 327-330

SAS Institute. (2001). *Jmp: The Statistical Discovery Software*. Sas Inst.

Smith, L. (1932). The kinetics of soap making. Transactions and Communications. *Journal of the Society of Chemical Industry*, pp 337-348

Tupper, G. (2010). Pretreatment programs: EPA updates and FOG control. *CWEA North Coast Section.* w:\nab\esd\presentations\cwea\pretreatment-ncs 3-2010.ppt

Wunderlich, B. (1990). Thermal Analysis. *New York: Academic Press*

Zullaikah, S., Lai, C. C., Vali, S. R., and Ju, Y. H. (2005). A two-step acid-catalyzed process for the production of biodiesel from rice bran oil. *Bioresource Technology, 96*(17), 1889-1896

APPENDIX

Appendix S

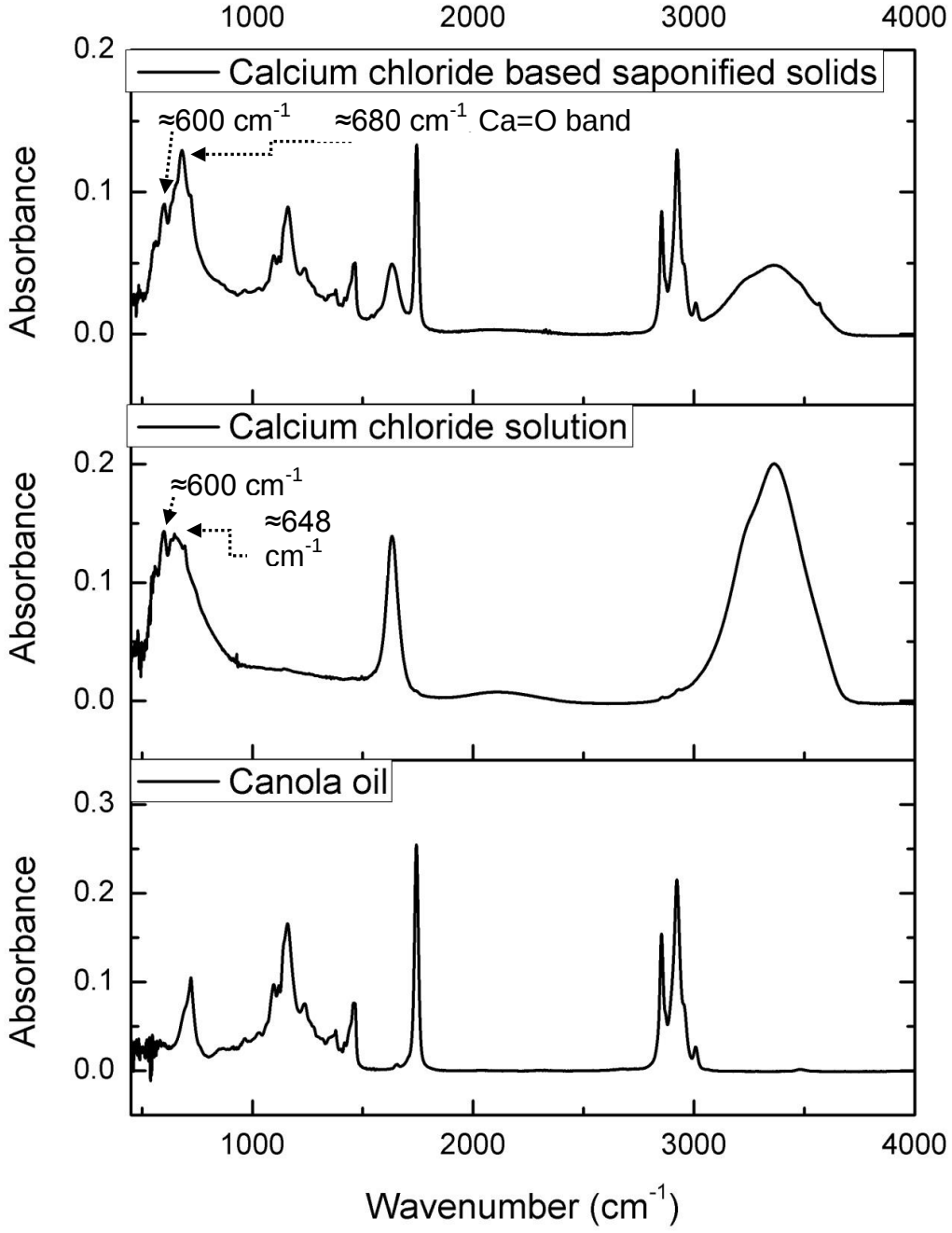

S1 Spectral comparison of calcium chloride-based fatty acid salts made with canola, calcium chloride aqueous solution, and canola oil

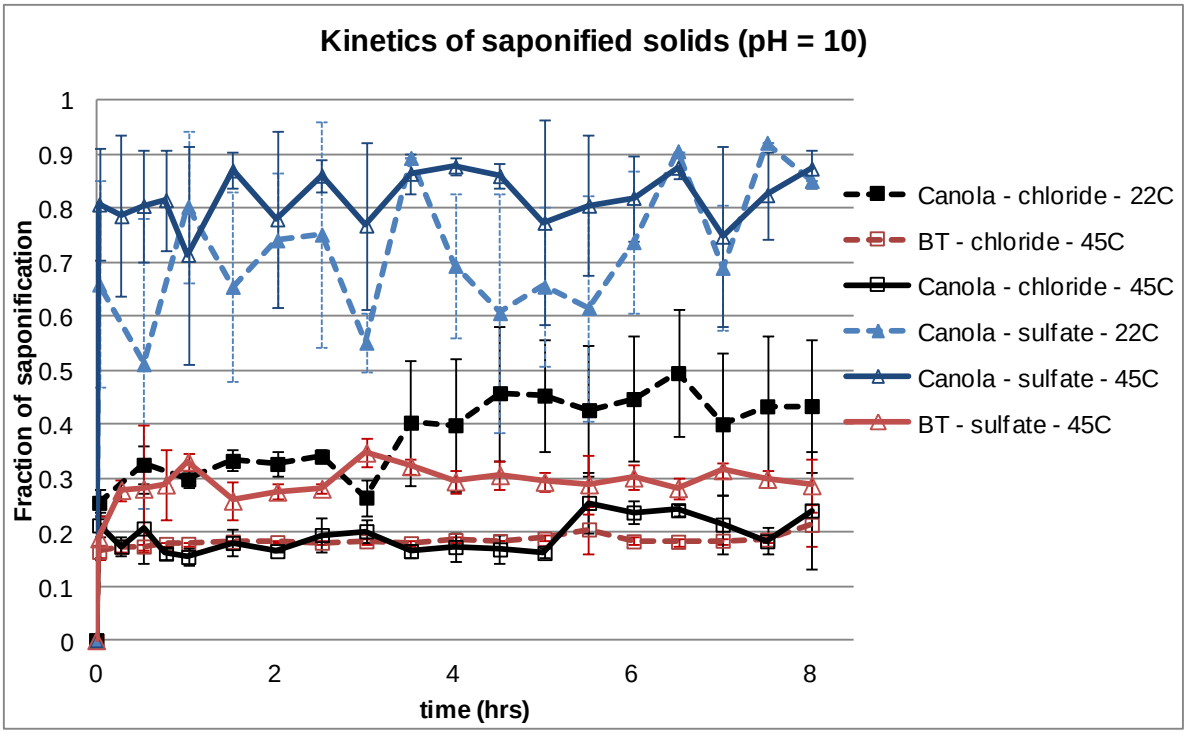

S2 Graphs showing kinetics of calcium based saponified solids at pH 10 with varying temperature; for all types of fats and calcium forms

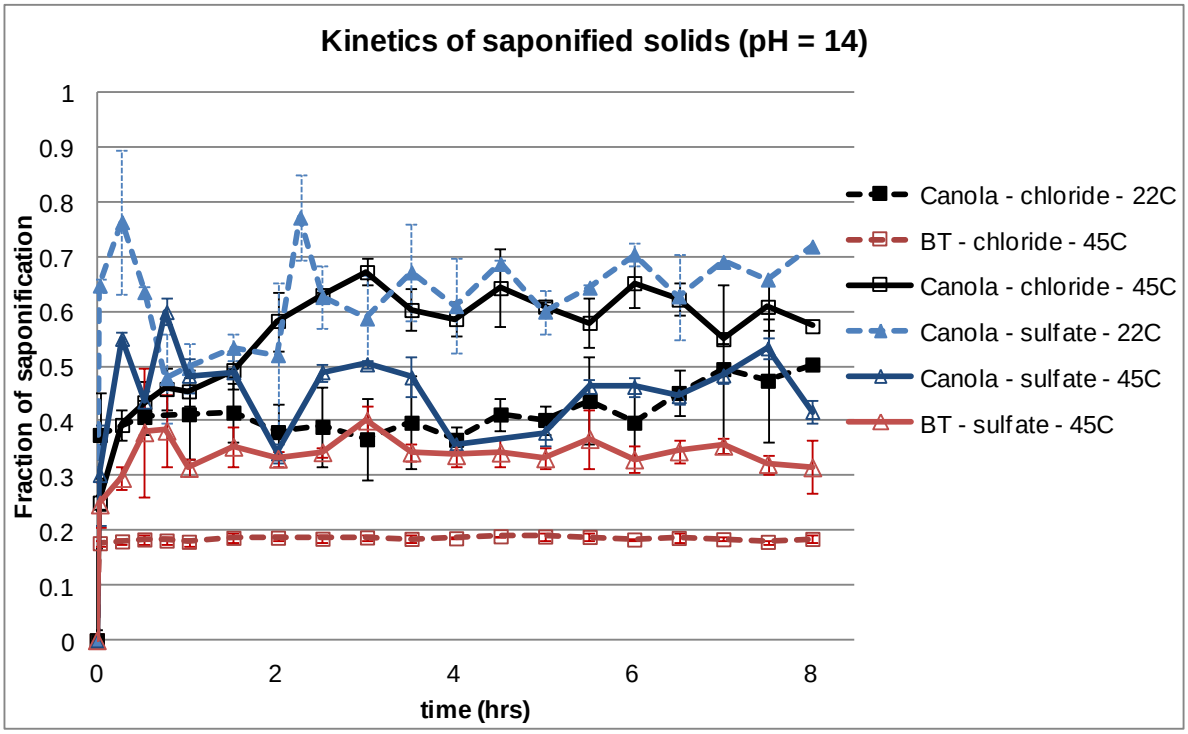

S3 Graphs showing kinetics of calcium based saponified solids at pH 14 with varying temperature; for all types of fats and calcium forms

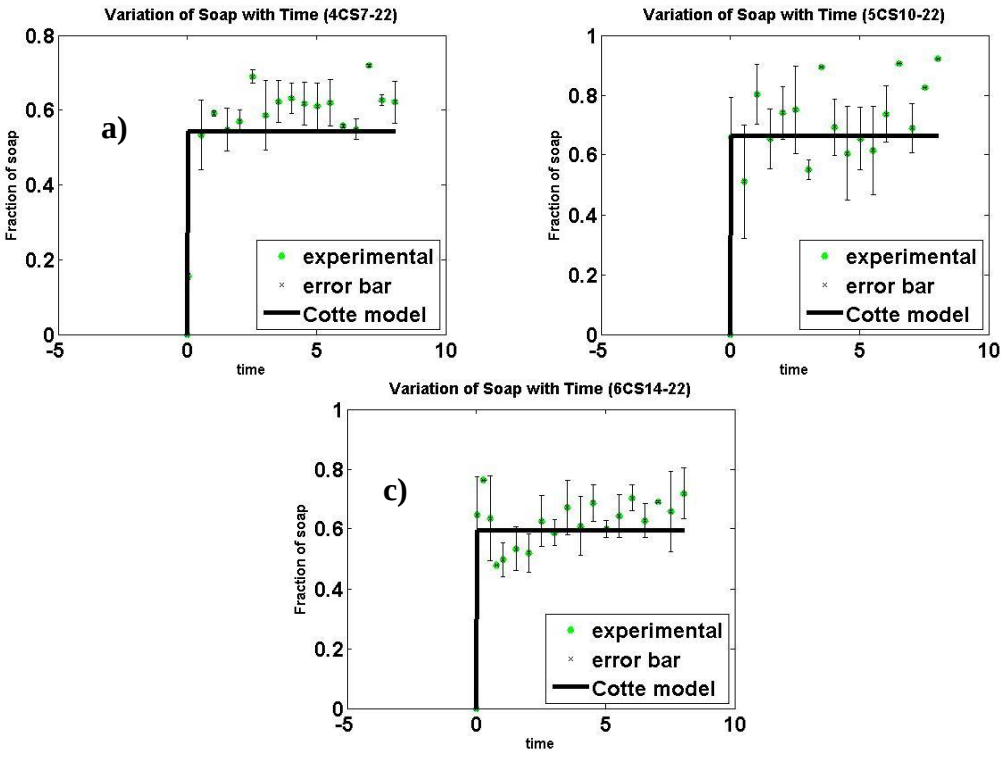

S4 Cotte saponification model fits (canola, calcium sulfate, 22 °C under a) pH 7±0.5; b) pH 7±0.5; and c) pH 14±0.5)

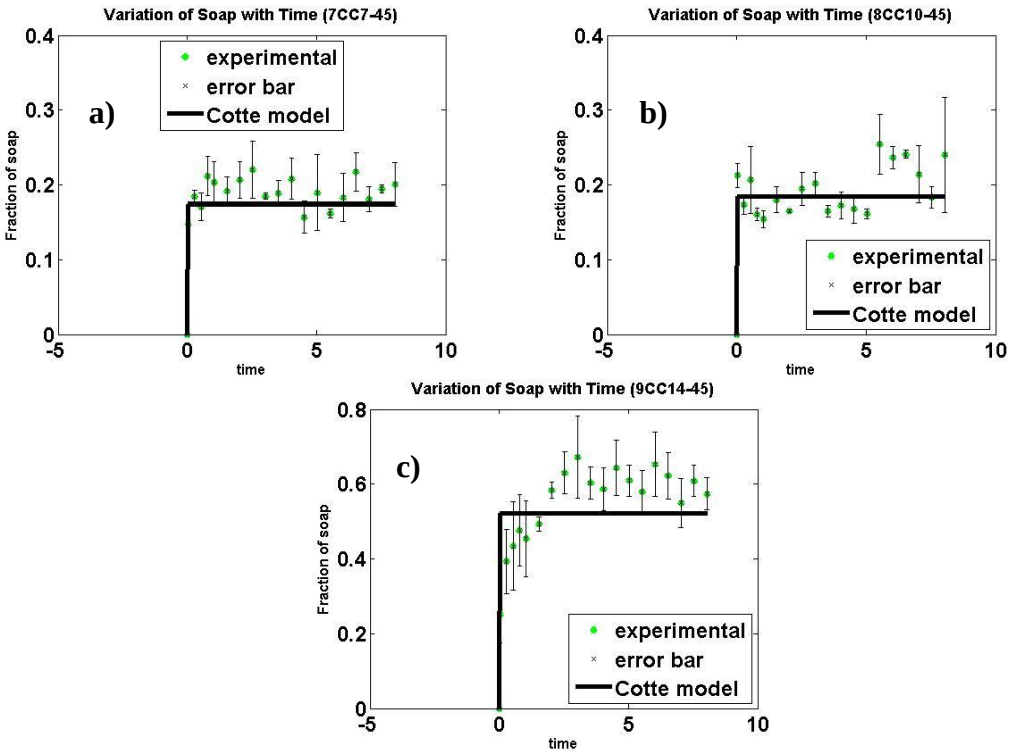

S5 Cotte saponification model fits (canola, calcium chloride, 45 °C under a) pH 7±0.5; b) pH 10±0.5; and c) pH 14±0.5)

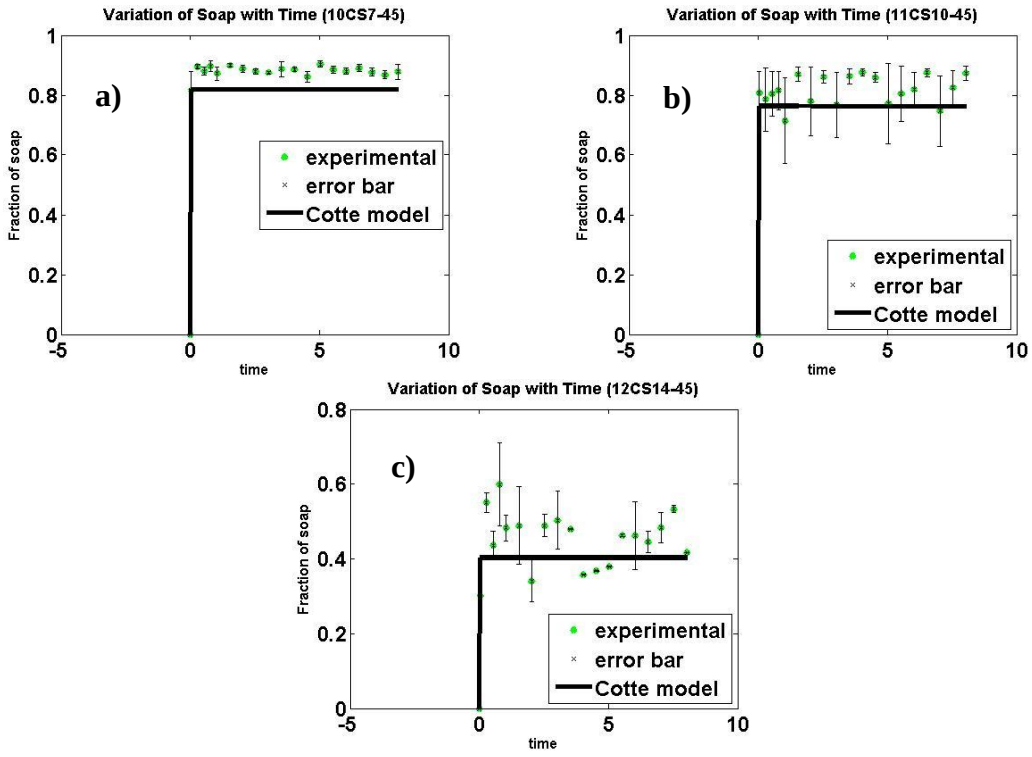

S6 Cotte saponification model fits (canola, calcium sulfate, 45 °C under a) pH 7±0.5; b) pH 10±0.5; and c) pH 14±0.5)

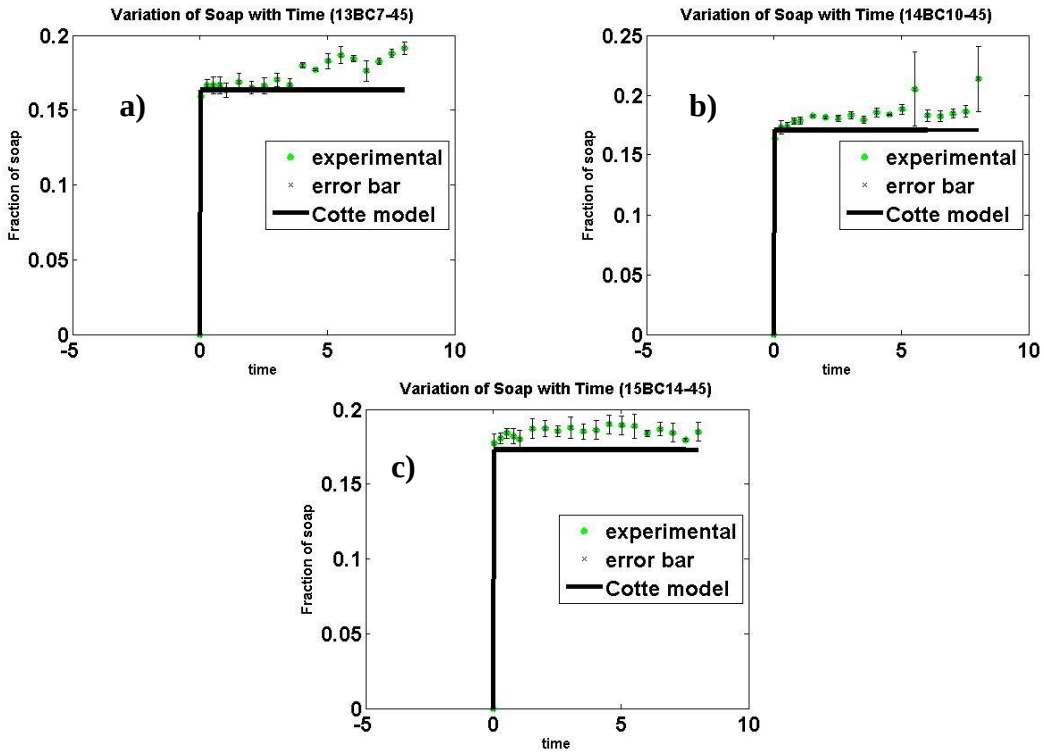

S7 Cotte saponification model fits (beef tallow, calcium chloride, 45 °C under a) pH 7±0.5; b) pH 10±0.5; and c) pH 14±0.5)

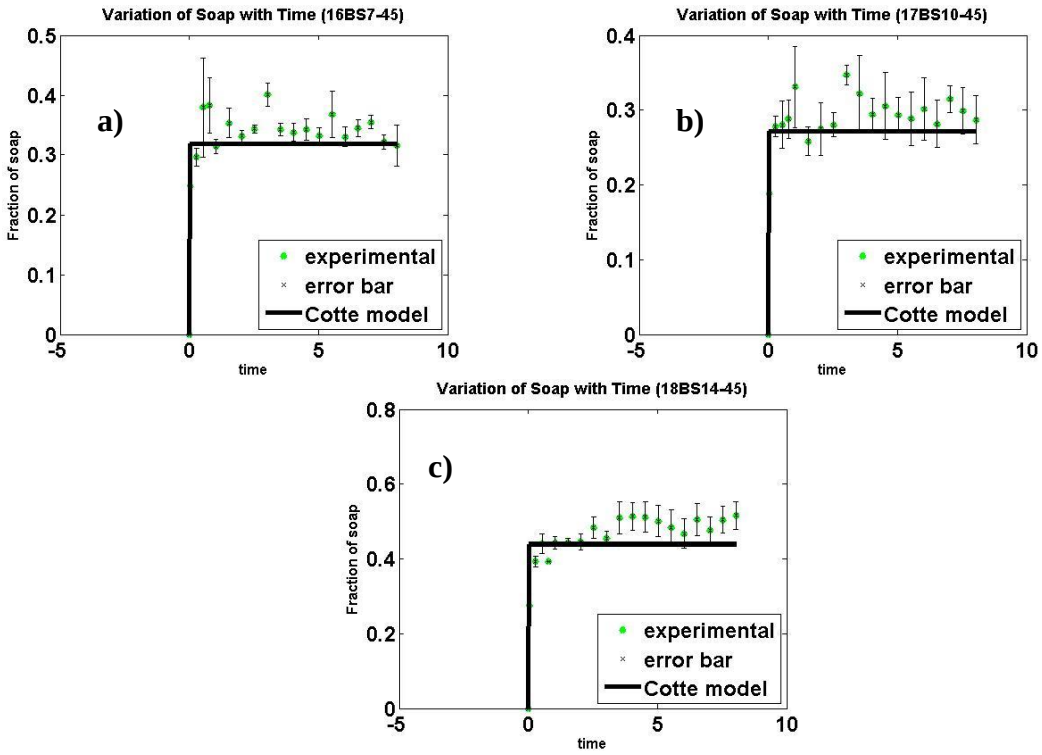

S8 Cotte saponification model fits (beef tallow, calcium sulfate, 45 °C under a) pH 7±0.5; b) pH 10±0.5; and c) pH 14±0.5)

Supplemental Table 1 Cotte saponification model parameters

Fat type	Calcium type	pH ± 0.5	Temp ± 0.5 (°C)	Saponification model		
				k_1 (hr^{-1})	$k_2(\frac{mol}{L.hr})$	k_3 (unit-less)
Canola	Calcium chloride	7	22	1270.03 ± 2370.21	2582.83 ± 8761.51	0.2732 ± 1.598e-7
Canola	Calcium chloride	10	22	1169.98 ± 1674.5	1488.66 ± 3613.92	34.11 ± 29.46
Canola	Calcium chloride	14	22	906.11 ± 780.61	839.20 ± 1057.61	0.3948 ± 0.0772
Canola	Calcium sulfate	7	22	1189.15 ± 1667.40	1198.46 ± 1554.20	3.050 ± 12.57
Canola	Calcium sulfate	10	22	458.31 ± 1170.3	1158.14 ± 4414.22	34.11 ± 29.46

Supplemental Table 1 Continued

Fat type	Calcium type	pH ± 0.5	Temp ± 0.5 (°C)	Saponification model		
				k_1 (hr^{-1})	$k_2(\frac{mol}{L.hr})$	k_3 (unit-less)
Canola	Calcium sulfate	14	22	1571.97 ± 2546.45	25293.76 ± 196259	8.72 ± 20.62
Canola	Calcium chloride	7	45	1129.20 ± 1711.41	902.69 ± 1266.3	0.165 ± 0.016
Canola	Calcium chloride	10	45	1070.57 ± 1497.31	1264.79 ± 2161.21	0.177 ± 1.917e-7
Canola	Calcium chloride	14	45	1037.96 ± 1256.92	3047.54 ± 14955	0.964 ± 3.92
Canola	Calcium sulfate	7	45	205.30 ± 570.05	289.49 ± 655.18	50.92 ± 32.84
Canola	Calcium sulfate	10	45	372.99 ± 1238.09	333.28 ± 631.7	41.51 ± 28.19
Canola	Calcium sulfate	14	45	1028.43 ± 1323.9	1031.07 ± 1297.02	0.473 ± 7.3e-7
Beef tallow	Calcium chloride	7	45	1344.64 ± 2091.77	1566.59 ± 4519.5	0.1590 ± 7.75e-8
Beef tallow	Calcium chloride	10	45	1203.1 ± 1651.55	1340.90 ± 3551	0.166 ± 1.02e-7
Beef tallow	Calcium chloride	14	45	903.53 ± 1532	1544.77 ± 2145.35	0.169 ± 1.04e-8
Beef tallow	Calcium sulfate	7	45	1150.57 ± 1397	907.67 ± 1688	0.38 ± 2.25e-7
Beef tallow	Calcium sulfate	10	45	1076.42 ± 1542.5	906.06 ± 1314.06	0.32 ± 0.033
Beef tallow	Calcium sulfate	14	45	1087.64 ± 1546.6	915.50 ± 1.32e3	0.324 ± 3.23e-7

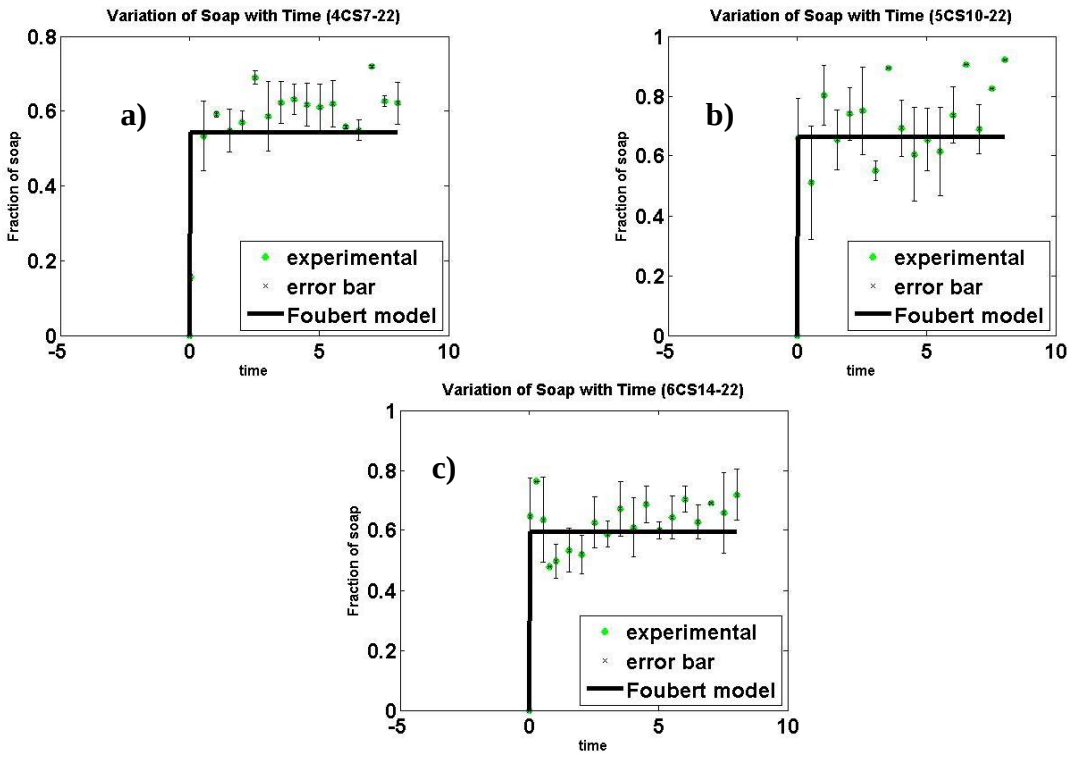

S9 Foubert crystallization model fits (canola, calcium sulfate, 22°C under a) pH 7±0.5; b) pH 10±0.5; and c) pH 14±0.5)

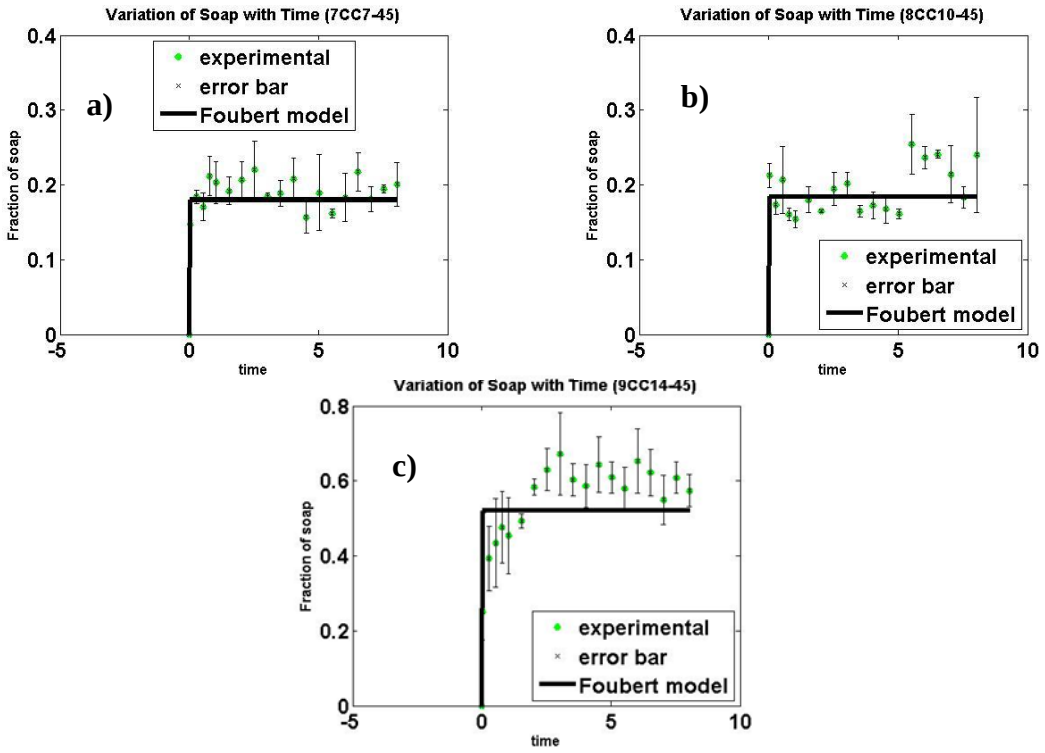

S10 Foubert crystallization model fits (canola, calcium chloride, 45 °C under a) pH 7±0.5; b) pH 10±0.5; and c) pH 14±0.5)

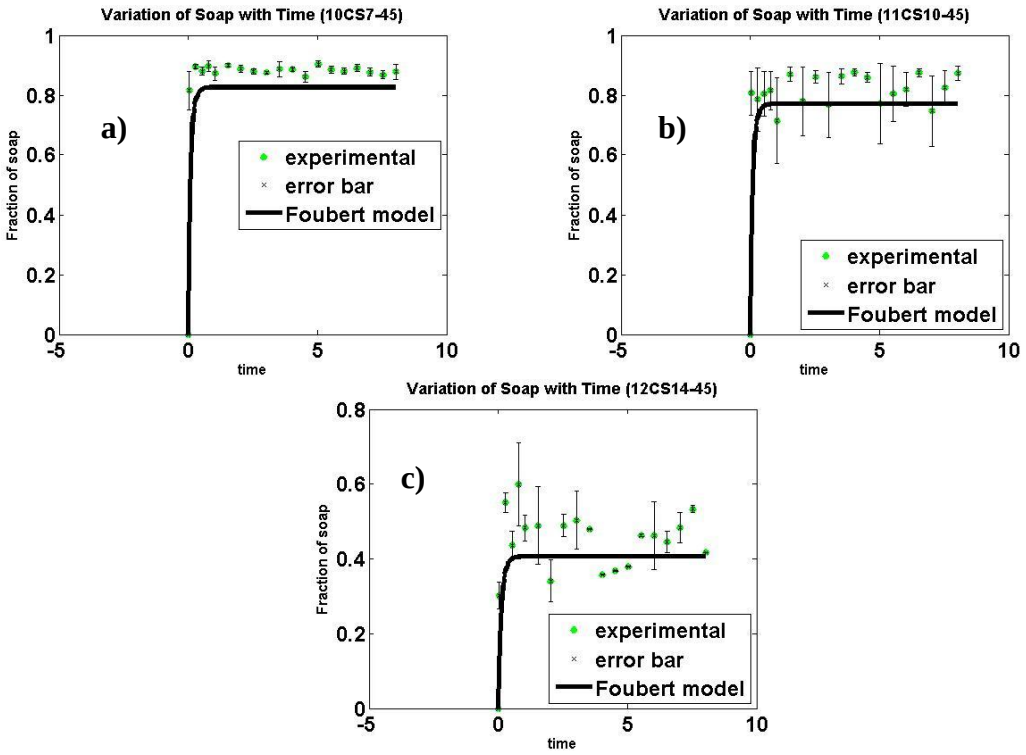

S11 Foubert crystallization model fits (canola, calcium sulfate, 45 °C under a) pH 7±0.5; b) pH 10±0.5; and c) pH 14±0.5)

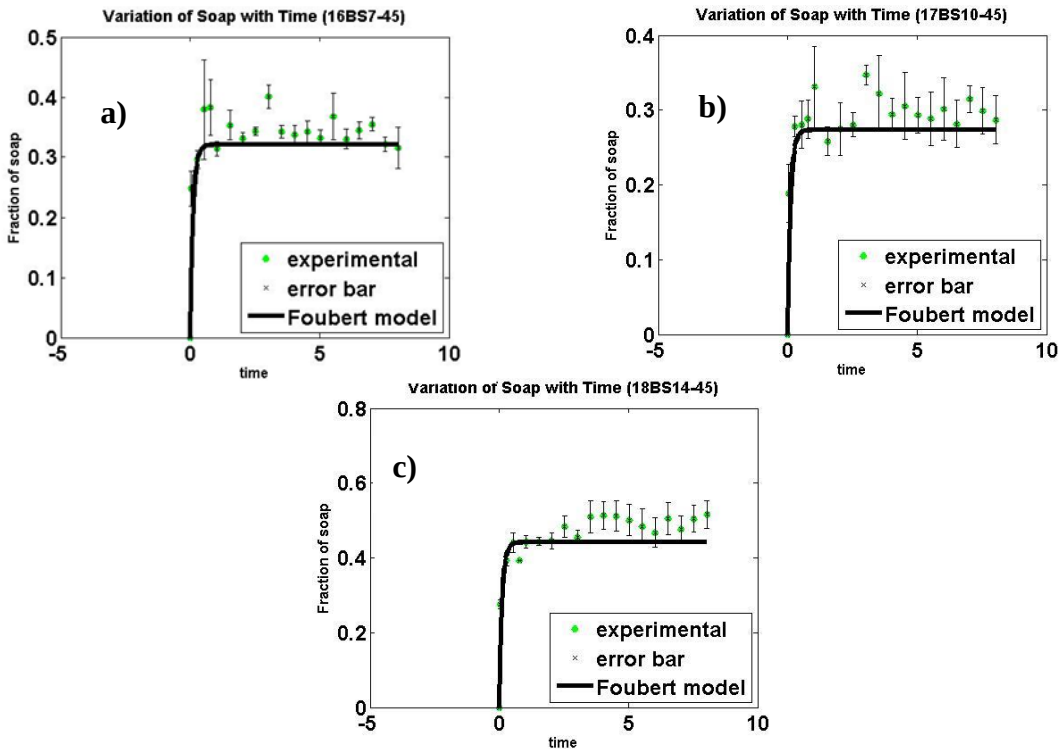

S12 Foubert crystallization model fits (beef tallow, calcium sulfate, 45 °C under a) pH 7±0.5; b) pH 10±0.5; and c) pH 14±0.5)

Supplemental Table 2 Foubert crystallization model parameters

Fat type	Calcium type	pH ± 0.5	Temp ± 0.5 (°C)	Crystallization model	
				k_1 (unit-less)	k_2 (unit-less)
Canola	Calcium chloride	7	22	0.0677 ± 7.14e-7	1e-10 ± 5.21e-26
Canola	Calcium chloride	10	22	0.0912 ± 6.22e-7	1e-10 ± 5.22e-26
Canola	Calcium chloride	14	22	0.103 ± 4.93e-7	1e-10 ± 5.22e-26
Canola	Calcium sulfate	7	22	2883.76 ± 2275.6	522.59 ± 1164.4
Canola	Calcium sulfate	10	22	3300.84 ± 2772.86	1309.63 ± 2228.6
Canola	Calcium sulfate	14	22	15789.56 ± 23134	4435.30 ± 14318
Canola	Calcium chloride	7	45	0.0382 ± 0.0087	1e-10 ± 6.71e-19
Canola	Calcium chloride	10	45	0.04 ± 5.27e-7	1e-10 ± 5.21e-26
Canola	Calcium chloride	14	45	0.179 ± 6.09e-7	1e-10 ± 5.21e-26
Canola	Calcium sulfate	7	45	97.26 ± 10.51	48.40 ± 36.71
Canola	Calcium sulfate	10	45	98.79 ± 7.003	55.52 ± 37.2
Canola	Calcium sulfate	14	45	97.26 ± 11.45	66.039 ± 41.63
Beef tallow	Calcium chloride	7	45	0.035 ± 4.6e-7	1e-5 ± 1.2e-20
Beef tallow	Calcium chloride	10	45	0.0364 ± 7.7e-7	1e-5 ± 1.2e-20
Beef tallow	Calcium chloride	14	45	0.037 ± 5.75e-7	1e-5 ± 1.2e-20
Beef tallow	Calcium sulfate	7	45	0.078 ± 4.42e-7	1e-5 ± 1.2e-20
Beef tallow	Calcium sulfate	10	45	790.64 ± 61.3	751.15 ± 58.25
Beef tallow	Calcium sulfate	14	45	3829.44 ± 2700	1583.29 ± 2422

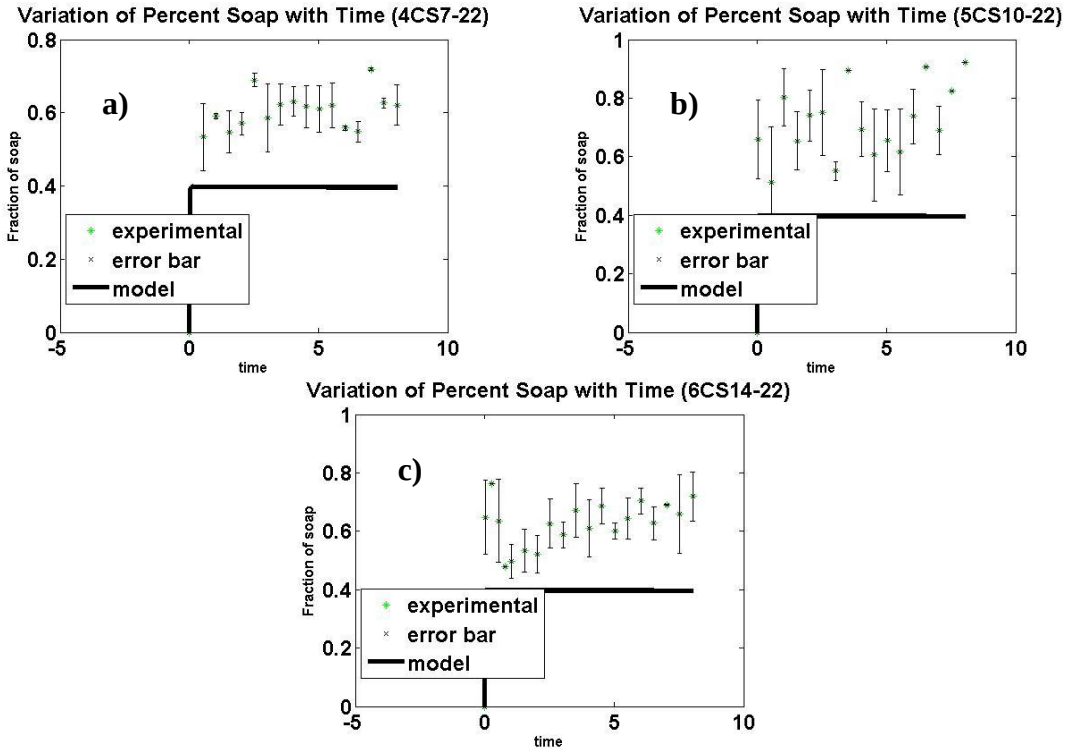

S13 Mass-action based saponification model fits (canola, calcium sulfate, 22 °C under a) pH 7±0.5; b) pH 10±0.5; and c) pH 14±0.5)

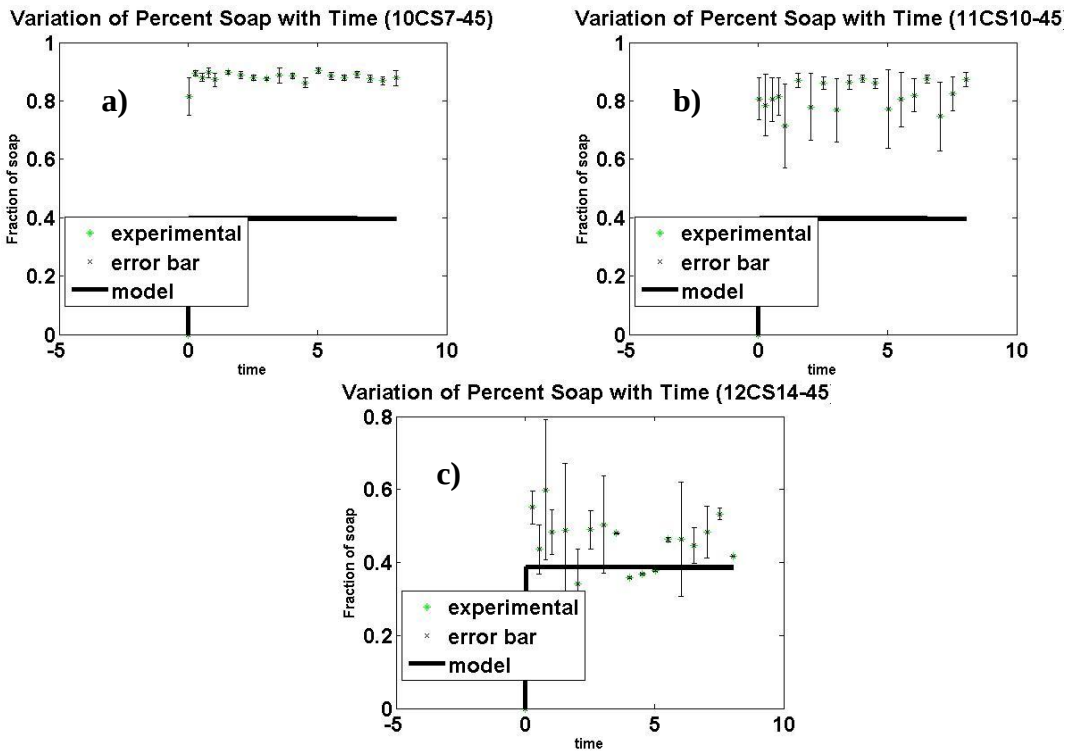

S14 Mass-action based saponification model fits (canola, calcium sulfate, 45 °C under a) pH 7±0.5; b) pH 10±0.5; and c) pH 14±0.5)

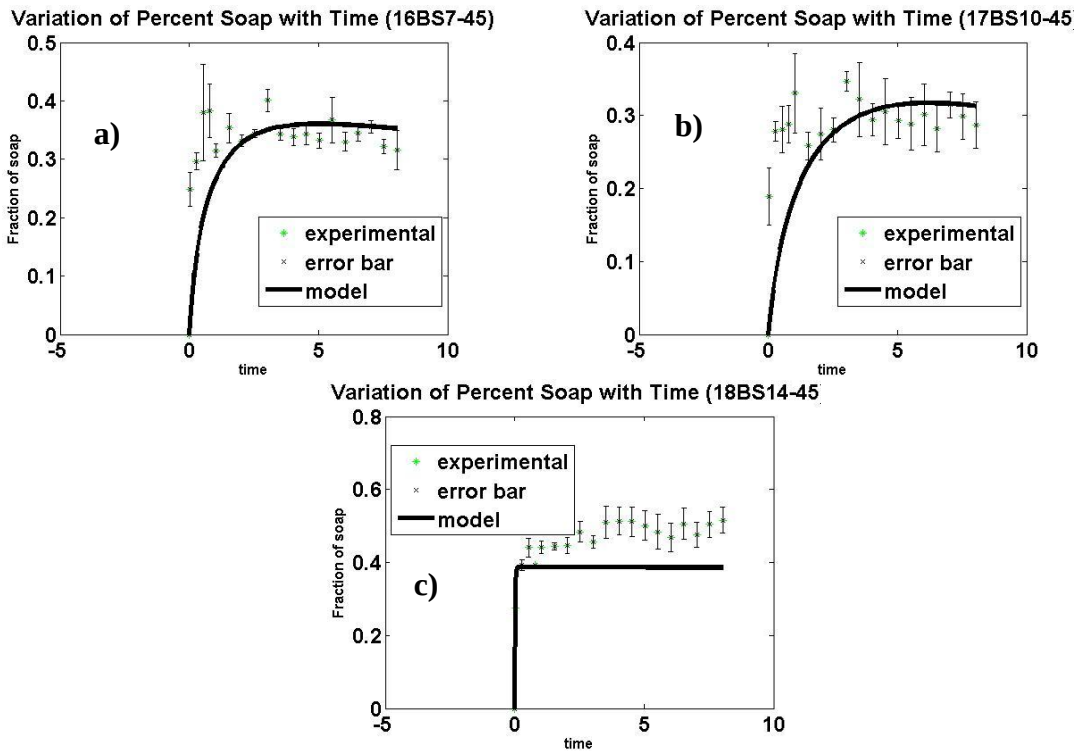

S15 Mass-action based saponification model fits (beef tallow, calcium sulfate, 45 °C under a) pH 7±0.5; b) pH 10±0.5; and c) pH 14±0.5)

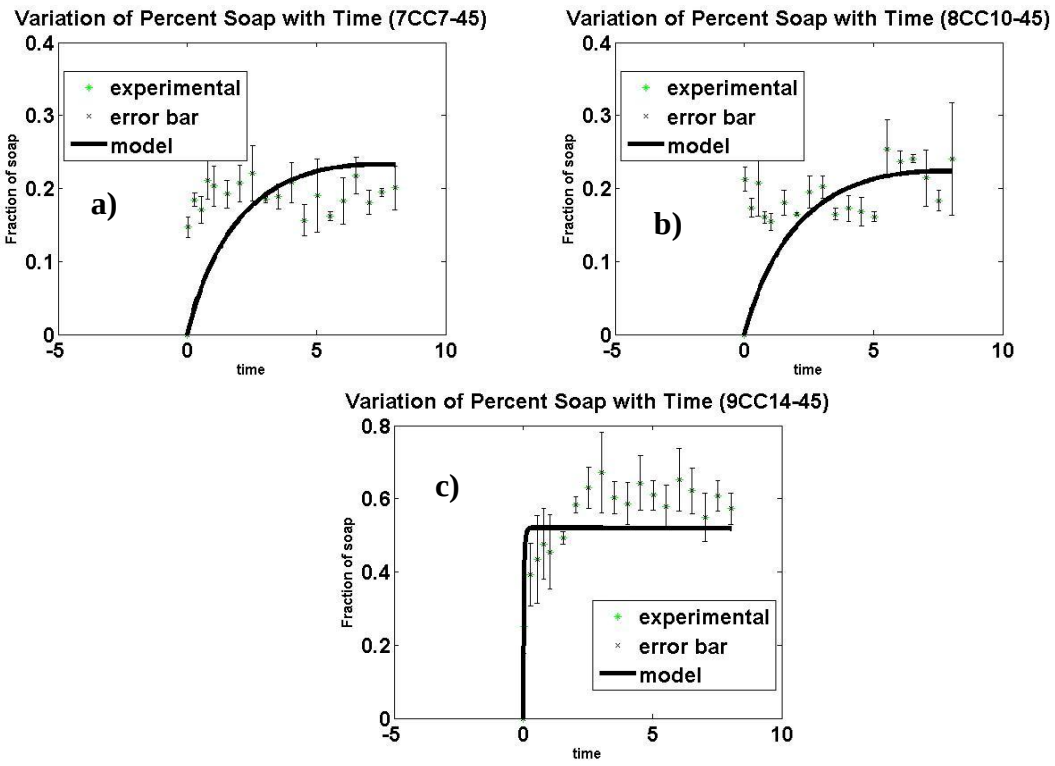

S16 Mass-action based saponification model fits (canola, calcium chloride, 45 °C under a) pH 7±0.5; b) pH 10±0.5; and c) pH 14±0.5)

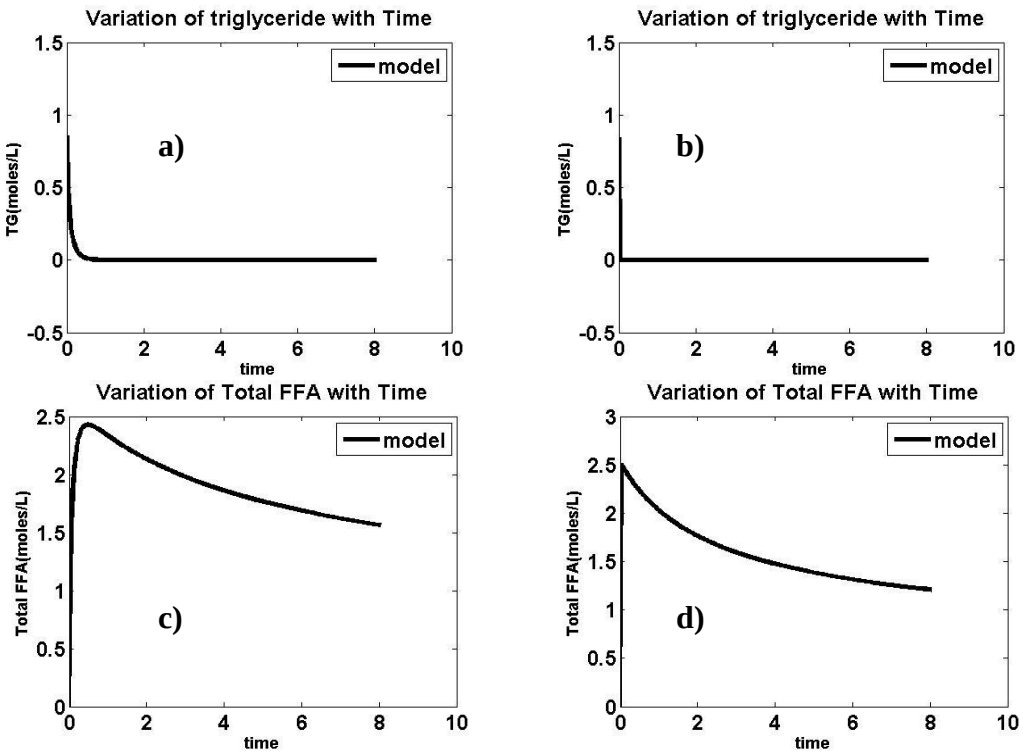

S17 Mass-action based saponification model predictions under pH 7 and 45 °C: a) Triglyceride (moles.L^{-1}) and b) Total FFA (moles.L^{-1}) for Beef tallow, and c) Triglyceride (moles.L^{-1}) and d) Total FFA (moles.L^{-1}) for Canola

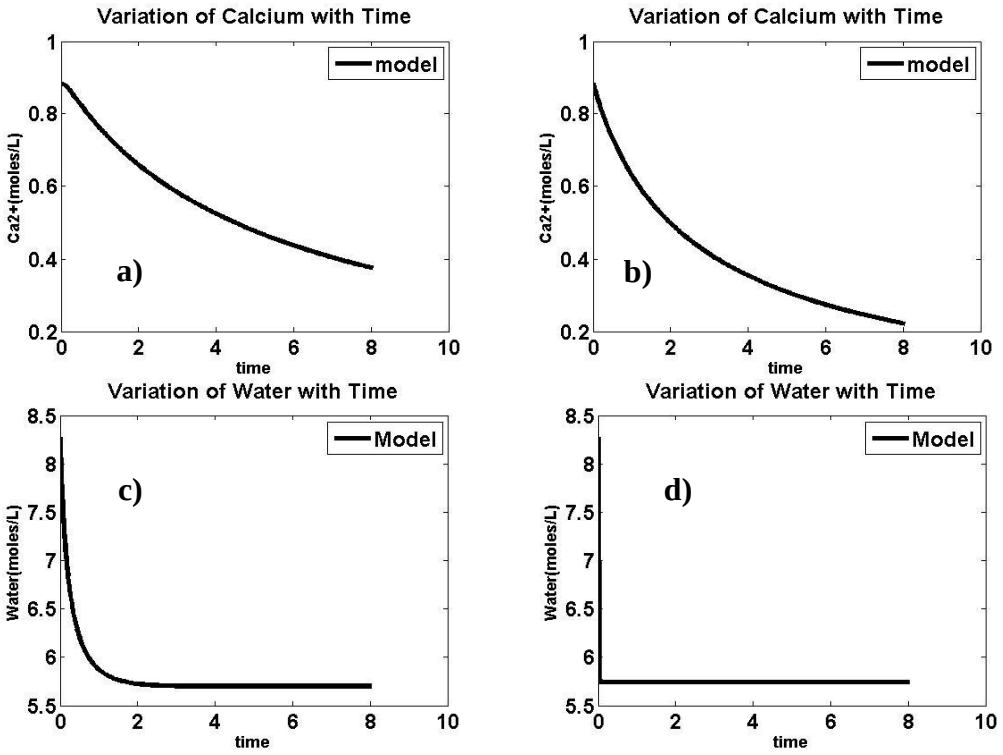

S18 Mass-action based saponification model predictions under pH 7 and 45 °C: a) Ca^{2+} (moles.L^{-1}) and b) Water (moles.L^{-1}) for Beef tallow, and c) Ca^{2+} (moles.L^{-1}) and d) Water (moles.L^{-1}) for Canola

CHAPTER 6 Effects of initial free fatty acids, detergents, and lipase on kinetics of fat, oil, and grease deposit formation in sewer collection systems

Abstract

Food service establishments (FSEs) have been implicated as major sources for fat, oil, and grease (FOG) discharge to the sewer collection system. The discharge of FOG has led to the formation of insoluble FOG deposits due to saponification reactions that result in limited conveyance of wastewater in these collection systems. While recent research studies have demonstrated that source fats and environmental conditions (i.e., pH and temperature) can play significant roles in the physical and chemical characteristics of FOG deposits, more research is needed to help elucidate the roles that FSE operation and grease interceptor maintenance plays on FOG deposit formation in sewer systems. Investigations of the FSE source conditions, i.e., presence of initial free fatty acids (FFAs) due to the cooking process, use of detergents in cleaning procedures, and lipases used in detergents and/or found in food sources are important to understanding their contribution to FOG deposit formation and their kinetics in sewer collection systems. Laboratory scale experiments were performed where FFAs (palmitic and linoleic), detergents (non-ionic and anionic), and lipases were added at two concentrations to fresh fat and calcium sources to produce calcium based saponified solids. The results showed significant increase in the formation of saponified solids with the presence of low concentrations of initial FFAs and liquid detergents. Lipase driven hydrolysis was also found to be a likely mechanism that leads to FOG deposit formation. In addition, higher temperature activities in FSEs may lead to the predominance of palmitic in FOG deposits. Apart from separate collection of yellow greases, it is recommended that FSE operations optimize the usage of detergents, and/or utilize a heat-exchange chamber prior to wastewater discharge into GIs to help reduce the risk of FOG deposit formation in sewer systems.

Keywords: Fat, oil, and grease (FOG); food service establishments (FSEs); free fatty acid (FFA); lipase

1 Introduction

Municipalities are facing increased challenges to reduce and/or control the occurrences of sanitary sewer overflows (SSOs) across United States. Fat, oil, and grease (FOG) deposits have been implicated as the primary cause of 40 to 50% of nationwide SSOs (Southerland, 2002; U.S.EPA, 2003). Much of the attention to limiting the discharge of FOG in sewer systems has been focused on Food service establishments (FSEs). Nationwide FOG control programs have been developed that requires the establishment and regular maintenance of grease control devices on FSE premises. While grease control devices have been used to limit the discharge of FOG into sewers, more assessments on the FSE source conditions are required to modify and/or improve the best management practices (BMPs) that can further help reduce the FOG deposit formations in sewer systems.

Studies performed to date have validated the influence of pH, temperature, type of fat used in FSEs, and type of calcium sources on properties of FOG deposits and their kinetics (Iasmin et al., 2014). However, Ducoste et al. (2008) mentioned that FSEs use alkaline detergents (pH >10), degreasers, and sanitizers, which may act as an oxidizer to promote saponification. Commercial detergents are commonly referred as alkylbenzenesulfonates, a family of compounds similar to soap having both polar and non-polar ends (Garcia et al., 1994). The dual nature (partly hydrophilic and partly hydrophobic) of these detergents helps facilitate the removal of FOG from FSE appliances. The addition of detergents, however, may also act as a catalyst for the saponification process similar to the auto-catalytic actions of pre-formed soaps as observed by researchers (Ducoste et al., 2008). Hence, the kinetics of FOG deposit formations in sewer systems may change due to the use of detergents in FSEs and further exacerbate the accumulation of saponified solids on pipe walls. Free fatty acids (FFAs) can also be formed due to hydrolysis of fats during high temperature cooking (Warner, 1999) and/or from microbial activity in grease interceptors (Monterfrio et al., 2010). Smith (1932) has shown that increased initial FFA concentration decreases the lag period of the auto-catalytic saponified solids formation process. Yet, no prior research has explored the impact of initial FFA or detergents on the formation of saponified solids.

Researchers have identified three predominant fatty acids in the formation of FOG deposits: a) palmitic, b) oleic, and c) linoleic, with the largest fraction coming from palmitic (Keener et al., 2008 and He et al., 2011). Recent bench scale studies performed by He et al. (2013) with grease interceptor (GI) effluent waste stream and the three types of FFA also showed significant formation of FOG deposits under pH controlled concrete corrosion conditions. However, their research did not provide clear experimental evidence on the predominance of palmitic acid in FOG deposits, as observed by Keener et al. (2008) and He et al. (2011). In a later study, Iasmin et al. (2014) showed that the fractions of saturated and unsaturated FFA in saponified solids created with pure or commercially available fats were consistent with the FFA fraction profile of the fat source. Iasmin et al. results suggest that the FFA profile of the saponified solids (i.e., FOG deposit) could be an indicator of the fats introduced at the beginning of saponification process. However, as noted earlier, all FOG deposits or saponified solids created in the lab with GI effluent wastewater or analyzed from the sewer collection system, produced an FFA fraction profile that did not resemble the pure or commercial fat source FFA profile (i.e., no pure source contained the fraction of palmitic measured in these FOG deposit samples) (Keener et al., 2008; He et al., 2011; He et al., 2013; Iasmin et al., 2014).

Matsui et al. (2005), while examining the biological treatment of wastewater from restaurant kitchens using an immobilized bioreactor, noted that unsaturated fatty acids following initial triglyceride hydrolysis by lipase may be preferentially broken down through beta-oxidation by microorganisms. The preferential consumption of these unsaturated fatty acids consequently leaves behind saturated fatty acids in wastewater that can react with calcium to form solid tacky substances, calcium di-stearate and di-palmitate. Recently, He (2011) also demonstrated lipolytic activity in the anaerobic environment of the GIs. It's possible that these biological processes may be altering the fate and transport of unsaturated FFAs in the sewer collection system and can possibly explain the significant accumulation of palmitic in FOG deposits. Exploration of lipase driven hydrolysis is needed to find its contribution in the FOG deposit formation process. Therefore, the objective of this research was to understand

the contribution of lipase enzymes, the effects of initial FFA, and the presence of detergents on the quantity, kinetics and chemical characteristics of the saponified solids..

2 Materials and methods

2.1 Materials

Pure Wesson Canola Oil (total fat 14g, 22%; saturated fat 1g, 5%; trans fat 0g; poly unsaturated fat 3.5g; mono unsaturated fat 8g, cholesterol 0%, sodium 0%, total carbohydrate 0%, and protein 0%) made by ConAgra Foods, Omaha, NE was used as the fat source and calcium chloride ($CaCl_2$, $\geq$ 93.0%, granular, 110.99 g/mol; Sigma-Aldrich, USA) was used as the source of calcium. Palmitic acid (analytical grade) and linoleic acid (technical grade) were procured from Sigma-Aldrich, USA. Two types of detergents: a) non-ionic detergent (sorbitane trioleate, analytical grade) and b) anionic detergent (sodium alkyl ether sulfate and formaldehyde, analytical grade) were obtained from Fisher Scientific and Sigma-Aldrich, USA, respectively and used as sources of detergents. In addition to these pure detergents, a household commercial dishwashing detergent (Dawn, produced by Procter and Gamble) was used to study its effect in saponified solids formation. Sodium hydroxide (NaOH) was used to adjust pH. All aqueous alkali solutions were prepared with de-ionized (DI) water.

2.2 Formation of saponified solids

All saponified solids were prepared under pH 10±0.5 following an alkali driven hydrolysis technique described in He et al. (2011). Solutions of calcium chloride and de-ionized water were added to source fat solutions with detergents or free fatty acids. These solutions were mixed under high mixing conditions using a Stir-pack laboratory impeller (Cole-Parmer instrument). Free fatty acids were added at two different concentrations (0.5% wt. of source fat, representing fresh source fat with some initial FFA and 10% wt. of source fat, representing cooked fats). Pure forms of detergents (anionic and non-ionic) were used to understand the individual effects of detergent types. Detergents were also added as weight

percentage of source fat (0.05% and 5%, representing background and high concentrations, respectively used by FSEs). Free fatty acids or detergents were first introduced to source fat solutions and mixed using a Stir-pack laboratory mixed impeller (Cole-Parmer instrument) under high mixing conditions (460 rpm) for ten minutes. Calcium solutions were later added and saponification reaction was allowed for eight hours. Two types of mixing conditions (230 rpm and 460 rpm) were used to understand the effects of mixing. The lower mixing condition was chosen to ensure uniform mixing inside the batch reactor. Kinetic samples were collected at 15 minute intervals during the first hour and at 30 minutes intervals for the remaining seven hours. Fraction of saponified solids was calculated based on the Equation 1 below in which all the characteristic saponification bands (the carboxylate ion symmetric stretching vibration, between 1300 and 1420 cm^{-1}; the carboxylate ion asymmetric stretching vibration, between 1550 and 1610 cm^{-1}; and the metal-oxygen bond vibration, around 670 cm^{-1}) were incorporated, as described in Iasmin et al. (2014). The computation of fraction of saponification was modified based on the modified band locations, as discussed in the results and discussions section.

$$Fraction\ of\ saponification = \frac{Absorbance\ in\ (near\ 670\ cm^{-1} + between\ 1300\ and\ 1420\ cm^{-1} + between\ 1550\ and\ 1610\ cm^{-1})}{Absorbance\ in\ (near\ 670\ cm^{-1} + between\ 1300\ and\ 1420\ cm^{-1} + between\ 1550\ and\ 1610\ cm^{-1} + 1745\ cm^{-1})} \quad (1)$$

2.3 Use of Fourier Transform Infrared (FTIR) in fat saponification

Attenuated total reflection (ATR) technique was adopted to measure spectral data of kinetic samples using a digilab FTS-6000 FTIR spectrometer. The spectral data was computed using a Bio-Rad Win-IR Pro software version 2.97 and analyzed with OriginPro 8.1 (Pro, O. 8, 2007). Details of the method can be found in Iasmin et al. (2014).

2.4 Fatty acid characterization

The saponified solids were analyzed for their fatty acid profiles following the official method, AOCS Ce 2-66 (AOCS, 2004). Samples were weighed into glass screw topped tubes and spiked with tridecanoin (C13:0) in ethanol to serve as an internal standard. Sodium hydroxide in methanol was then added and the tubes were heated for 10 min at 85 °C in a water bath. After cooling, boron trifluoride in methanol was added and the tubes were recapped, vortexed, and returned to the water bath for 10 min. After cooling, water was added followed by hexane to each tube. The tubes were vortexed at maximum speed for 30s and then allowed to stand to form layers. The top (organic) layer containing the fatty acid methyl esters (FAMEs) was removed and dried over sodium sulfate. The FAMEs were analyzed with a Perkin-Elmer Auto-system XL GC (Sheldon, CT) fitted with a capillary BPX-070 column (SGE Inc., Austin, TX) using Gas chromatography-flame ionization detector (GC-FID). The results were reported as percent of the total fatty acids based on peak areas according to the official method (AOCS Ce 1f-96), and the total fatty acids were calculated based on the ratio of internal standard to the fatty acid peaks present when compared to a standard mixture (Kel Fir Fame 5 Standard Mix, Matreya, Pleasant Gap, PA). The standard mixture of FAMEs was run with each sample set to determine retention times and recoveries.

3 Results and Discussions

3.1 Effects of presence of initial free fatty acids

The addition of FFA was hypothesized to form more saponified solids and faster kinetics with readily available free calcium ions in background water. Figures 1a and 1b display the effects of palmitic and linoleic acids on the kinetics of saponified solids, respectively. The results showed that a very small addition of palmitic or linoleic acid (0.5% by weight of source fat) increased the formation of saponified solids significantly. The effects were noticeable within two minutes of reactions. The results also show that the addition of palmitic acid produced a higher quantity of saponified solids than linoleic acid addition, i.e.

50% increase due to palmitic addition and 20% increase due to linoleic addition. Surprisingly, the addition of 10% FFA did not increase saponification beyond the results produced with the 0.5% addition. It is hypothesized that increasing addition of palmitic or linoleic acid may increase the negative charge cloud of fatty acids (i.e., palmitate or linoleate) around the positive calcium ions. As a result, electrostatic repulsion may take place that inhibits further saponification.

Figures 2a and 2b display the spectral analyses of saponified solids with palmitic and linoleic acid additions. Spectral analyses of pure linoleic acid, palmitic acid, and liquid canola fat are shown in Supplemental Figure 1. Supplemental Figure 2 displays the spectral analysis of saponified solids with no FFA addition under the same source conditions (i.e., canola and calcium chloride). The spectral data in Figures 2a and 2b displayed appearances of two new asymmetric carboxylate absorption bands (1540 cm^{-1} and 1576 cm^{-1}) in calcium based saponified solids with the presence of initial FFA when compared with no FFA addition. The symmetric carboxylate bands for palmitic added saponified solids were observed at 1419 cm^{-1} and 1435 cm^{-1} as shoulders to the stronger peak at 1464 cm^{-1}. For linoleic acid added solids, only 1419 and 1464 cm^{-1} bands were observed. The metal oxygen band was located at 670 cm^{-1} with the presence of palmitic, instead of 680 cm^{-1} in the saponified solids with linoleic acid and no FFA addition. Absorption bands at 1540 cm^{-1} and 1576 cm^{-1} were also found in FOG deposits collected from shopping centers, as presented by He et al. (2011). Pure palmitic acid also possesses absorption bands at 1411 cm^{-1}, 1430 cm^{-1}, 1463 cm^{-1}, and 1470 cm^{-1}, near the region of symmetric carboxylate bands (Supplemental Figure 1). In the same region, the pure linoleic acid contains absorption bands at 1412 cm^{-1} and dual peaks at 1457 cm^{-1} and 1465 cm^{-1}. All the saponified solids contained the bonded hydroxyl band in the region of 3400 cm^{-1} that was also present in FOG deposits presented in He et al. (2011) and Iasmin et al. (2014).

Table 1 displays the fatty acid profiles of the calcium based saponified solids with the FFA additions. As expected, the results showed that the increase in palmitic addition resulted in increased palmitic fractions in the saponified solids. The oleic and linoleic acid fraction

contents seem to decrease simultaneously. With the addition of linoleic acid, however, an interesting change was observed. The linoleic acid fraction increased with the 0.5% addition of linoleic acid, compared to no addition of FFA. However, as the quantity of the linoleic acid addition increased (i.e., 10% by wt of source fat), the palmitic fraction increased with a simultaneous decrease in the unsaturated fractions (i.e., oleic, linoleic, and linolenic). The oleic and linolenic acid fractions decreased significantly compared to the pure canola fat and the saponified solids prepared with no FFA addition. The decrease in the unsaturated fats and the simultaneous increase in saturated palmitic fraction suggests a possible effect of warm temperature in converting the unsaturated to saturated fractions. The conversion phenomenon is especially evident within the time-frame of reaction when readily available unsaturated FFA (i.e., linoleic) is present. Literature reviews also suggest that high temperature cooking (e.g., deep fat frying, baking, grilling, and pan-frying) can decrease the level of unsaturation and increase the FFA contents in oils due to thermal and oxidative decompositions of these unsaturated fatty acids (Duckett and Wagner, 1998; Warner, 1999). It has been reported that temperature profiles in GIs can range from 30 to 45 °C (Aziz et al., 2012). Therefore, literature reviews and the fatty acid results suggest that the operating conditions of FSEs may significantly influence in producing higher fractions of saturated FAs in the GI effluent stream and consequently in FOG deposits, based on the similarity to the source FA profiles observed in Iasmin et al. (2014).

Overall, the kinetics, FTIR spectral analysis, and metal analysis results observed in saponified solids prepared with palmitic and linoleic acid additions suggest that the presence of FFA in sewer system will enhance the formation of saponified solids, and therefore, FOG deposits. The predominance of palmitic in FOG deposits is largely related to the possible palmitic content in the GI effluent waste stream. The production of palmitic acid may occur in FSE premises due to the following: a) the hydrolysis of saturated fats having high palmitic content and b) the conversion of unsaturated fats (i.e., oleic, linoleic, and linolenic) to palmitic during the high temperature cooking and/or washing processes as well as prolonged exposure to these higher temperatures in the GI.

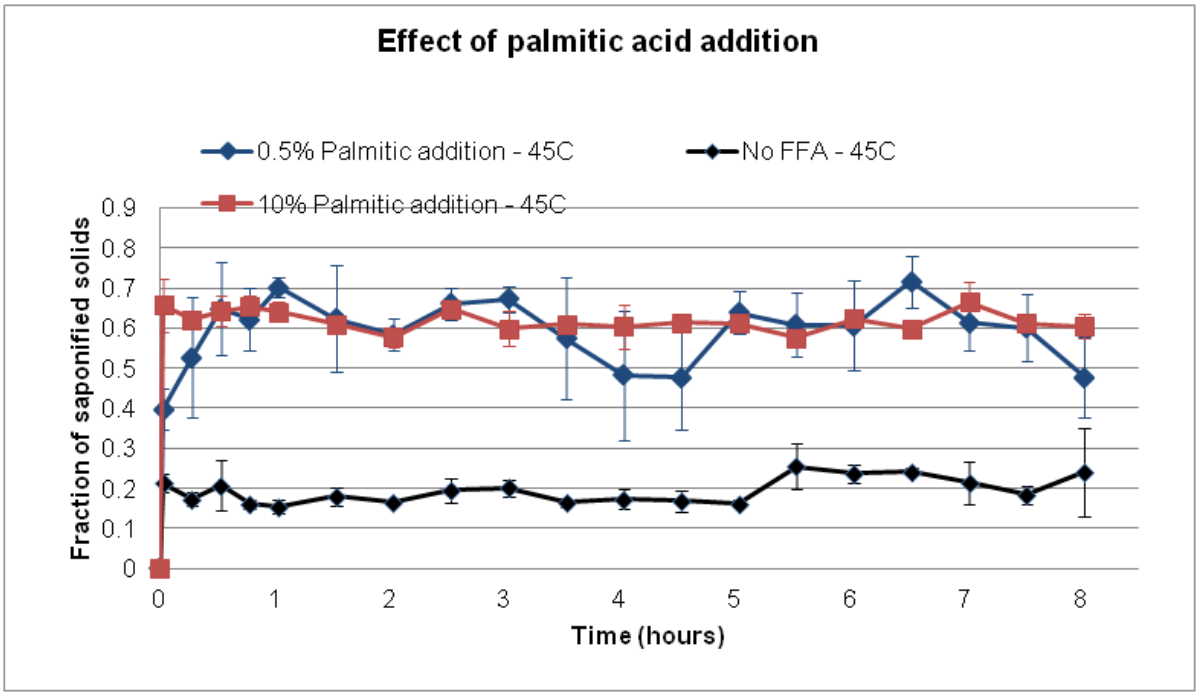

Figure 1a Effect of palmitic acid addition

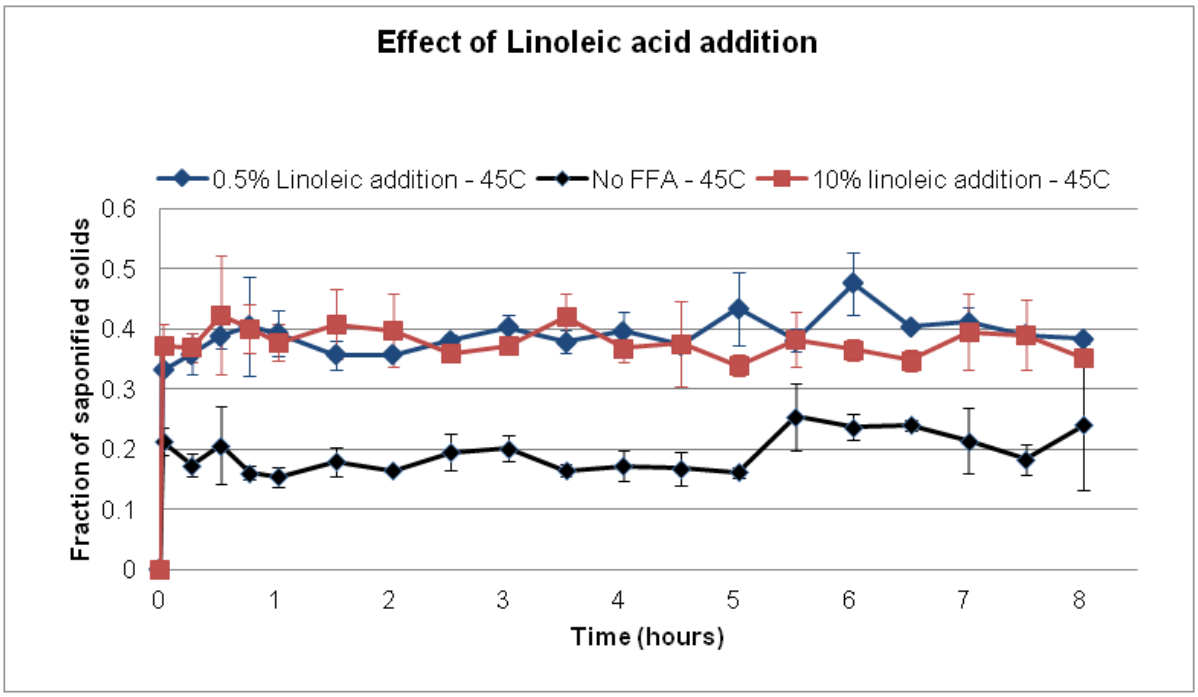

Figure 1b Effect of linoleic acid addition

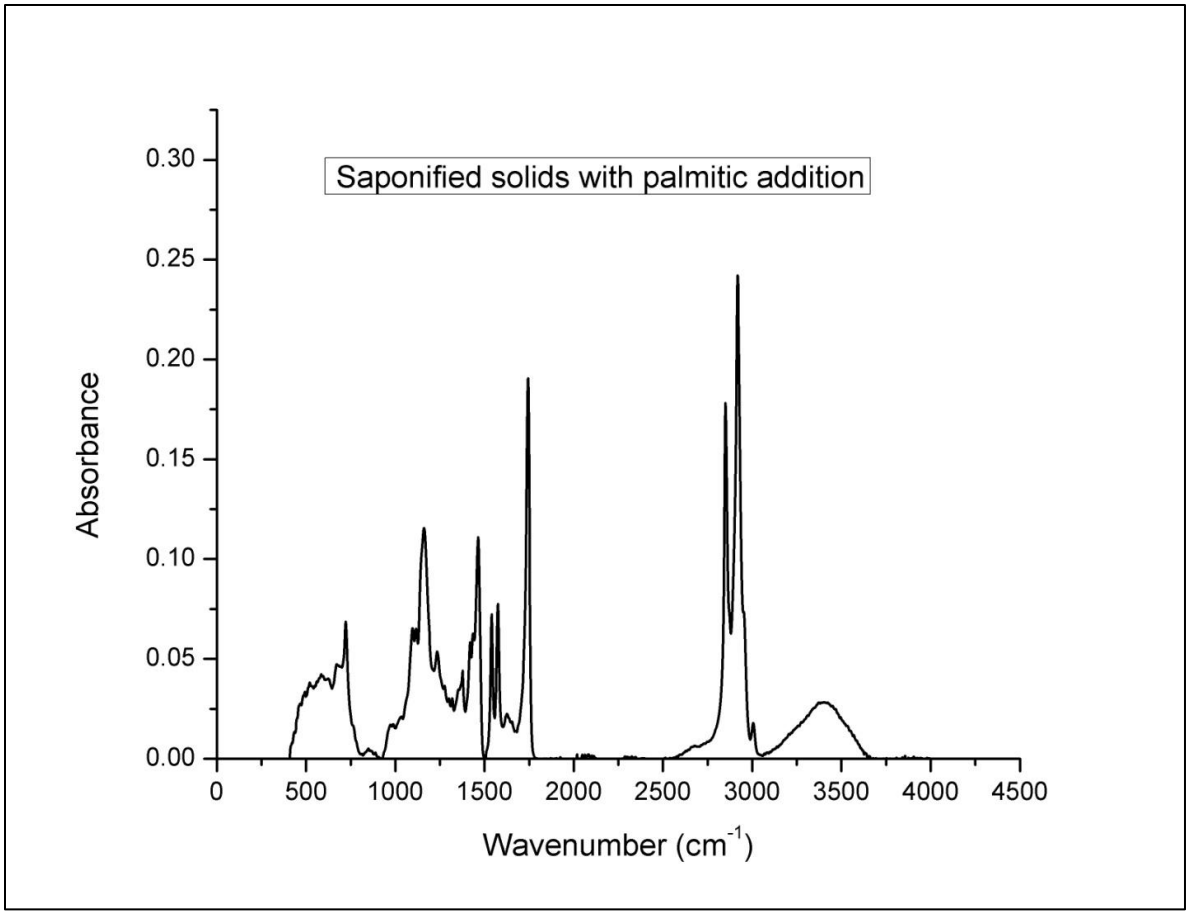

Figure 2 a Spectral analyses of saponified solids with 0.5% palmitic acid addition

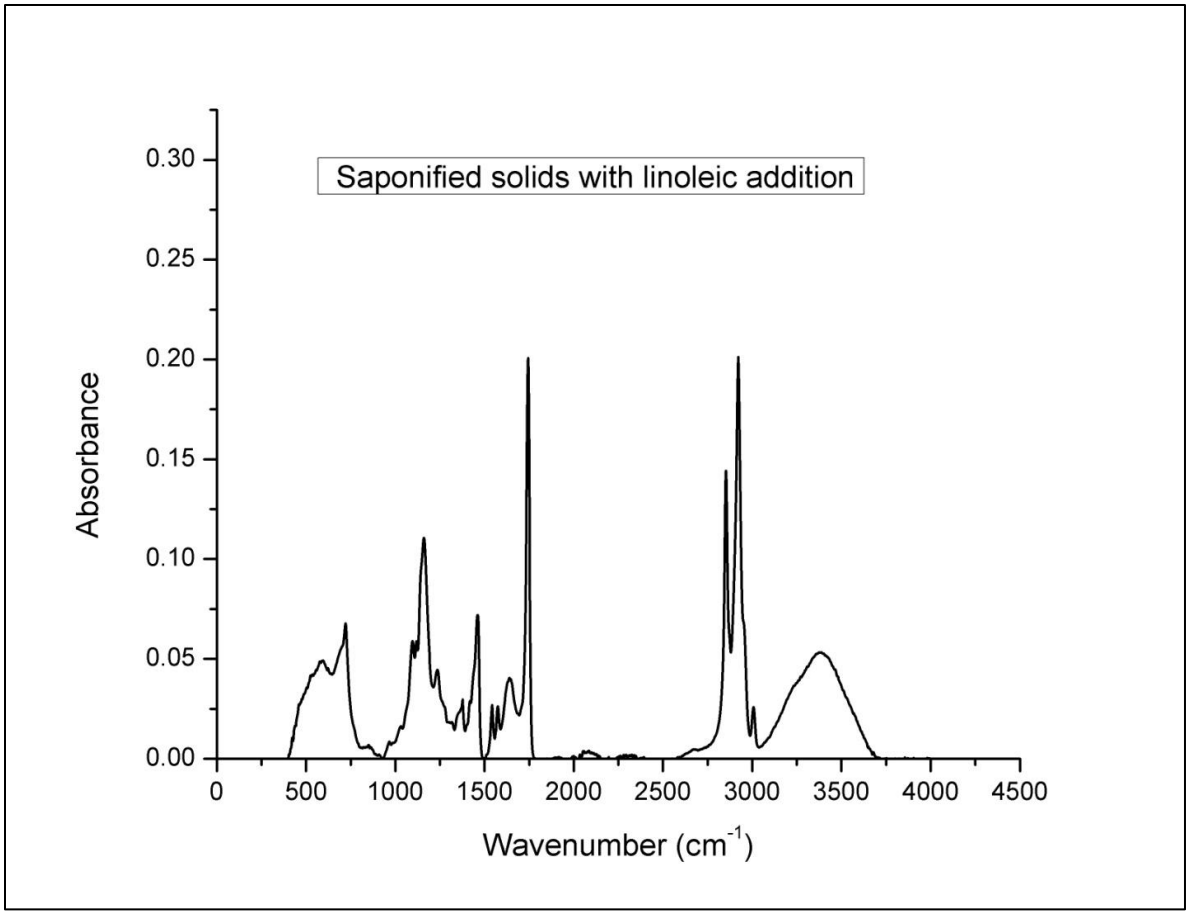

Figure 2 b Spectral analyses of saponified solids with linoleic acid addition

Table 1 Fatty acid profiles of the saponified solids

Type of FFA	Quantity of addition (% wt of source fat)	Palmitic (%)	Stearic (%)	Oleic (%)	Linoleic (%)	Linolenic (%)
Canola (source fat)	-	4.150±0.046	2.000±0.025	62.490±0.137	18.902±0.062	8.455±0.042
No FFA (Iasmin et al., 2014)	0	4.163±0.049	1.912±0.051	64.111±0.506	18.353±0.261	7.103±0.308
Palmitic	0.5	8.597±2.974	1.627±0.140	62.053±1.156	16.583±2.817	6.277±2.170
Palmitic	10	15.430±2.090	1.530±0.082	57.197±2.259	15.353±1.024	5.813±1.263
Linoleic	0.5	5.147±1.371	2.097±0.638	59.790±1.267	22.670±1.210	6.170±1.261
Linoleic	10	10.090±1.048	2.063±1.953	56.210±4.313	20.600±2.045	4.420±2.288

3.2 Effects of mixing intensity

Previous researchers have suggested that sewer configurations (such as T-connections, manhole regions, and pipe bends) may influence the mixing conditions inside sewer systems affecting FOG deposit formation (Ducoste et al., 2008, Dominic et al., 2013). Studies have shown that obstructions (i.e., roots intrusions) as well as pipe deformations (i.e., pipe sags) can lead to preferential accumulation of FOG deposits (Dominic et al., 2013). Figures 3 and 4

display the kinetics of saponified solids under two mixing conditions, i.e., 230 and 460 rpm, and under two pH conditions (7.0±0.5 and 10.0±0.5), respectively. The mixing conditions were chosen so that uniform mixing conditions prevailed inside the batch reactors for the benefits of kinetic sampling. The results showed that, under the well mixed environment, increased mixing intensity does not lead to increased formation of saponified solids during early periods of saponification. However, high intensity mixing (460 rpm) may form more saponified solids with continued mixing at neutral pH condition, as can be seen in Figure 3. This observation, however, is limited to fresh sources of fats and calcium (i.e., no addition of free fatty acid). Figures 5 and 6 display the effects of mixing intensity with the presence of some initial FFA, i.e., addition of 0.5% palmitic and 0.5% linoleic acid under two mixing conditions (230 rpm and 460 rpm), respectively. The Supplemental Figures 3 and 4 also display the effects of mixing intensity for higher percentage of initial FFA additions, i.e., 10% palmitic and 10% linoleic, respectively. The results are consistent with the saponified solids prepared with no FFA addition. Therefore, under well mixed environment, the mixing intensity does not play a significant role in changing the production of saponified solids.

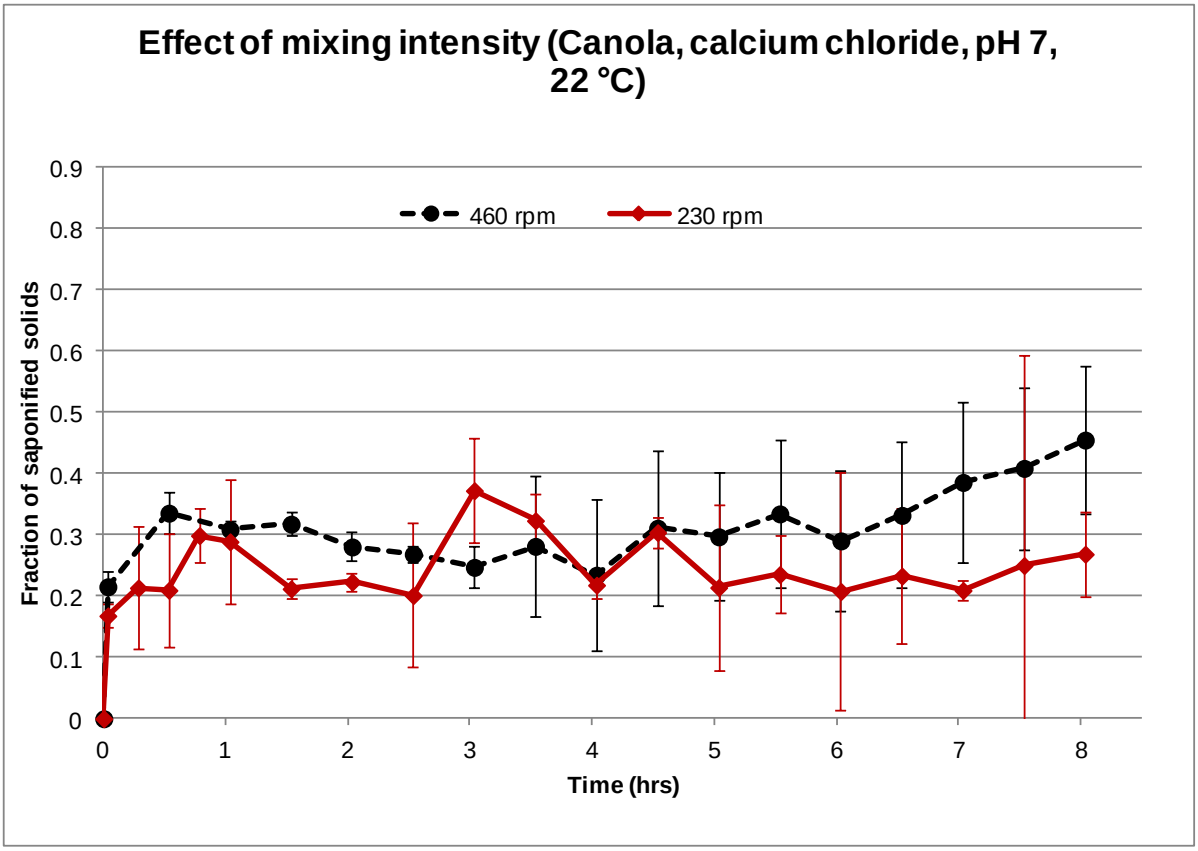

Figure 3 Effect of mixing (no addition of FFA, pH 7, 22 °C)

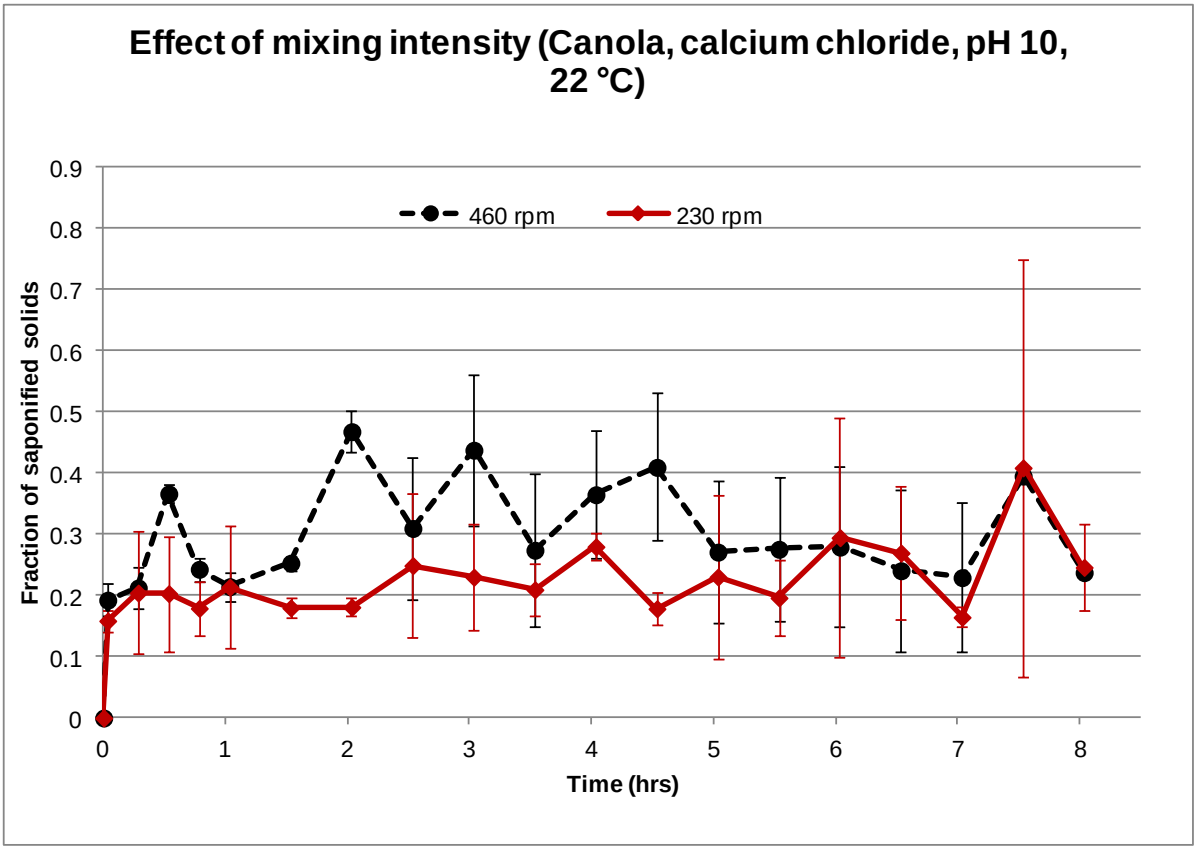

Figure 4 Effect of mixing intensity (no addition of FFA, pH 10, 22 °C)

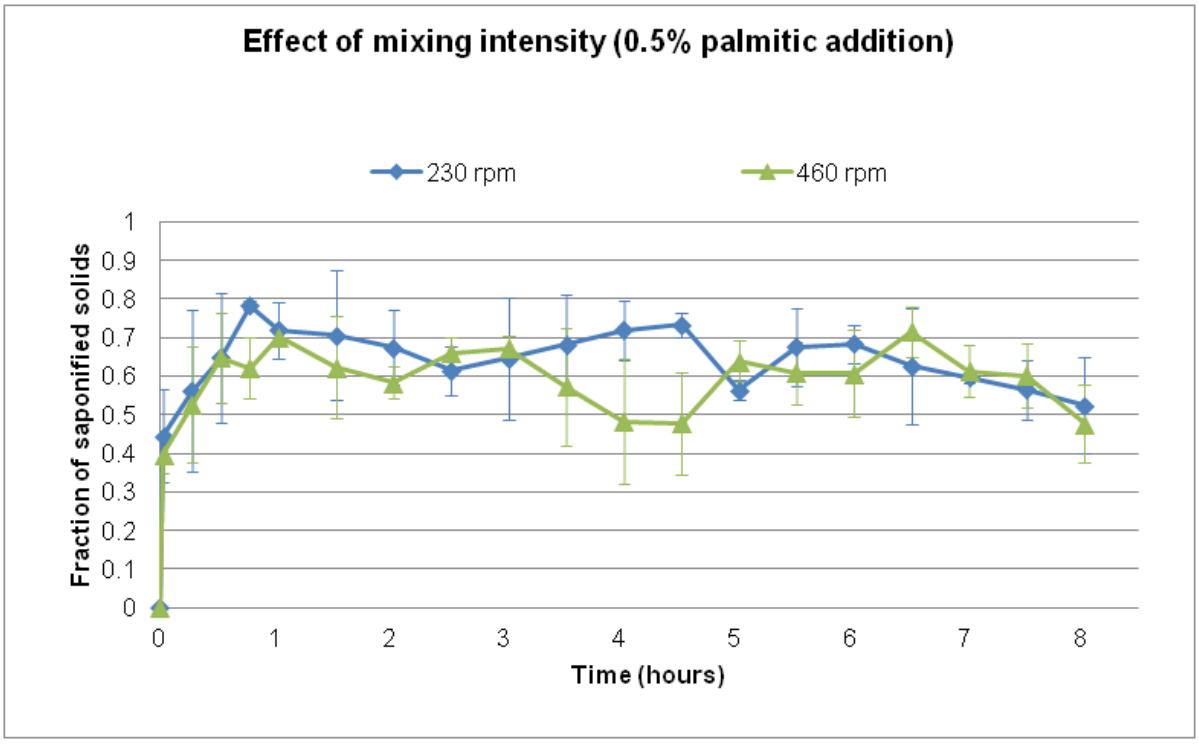

Figure 5 Effect of mixing (0.5% of palmitic addition, pH 10, 45 °C)

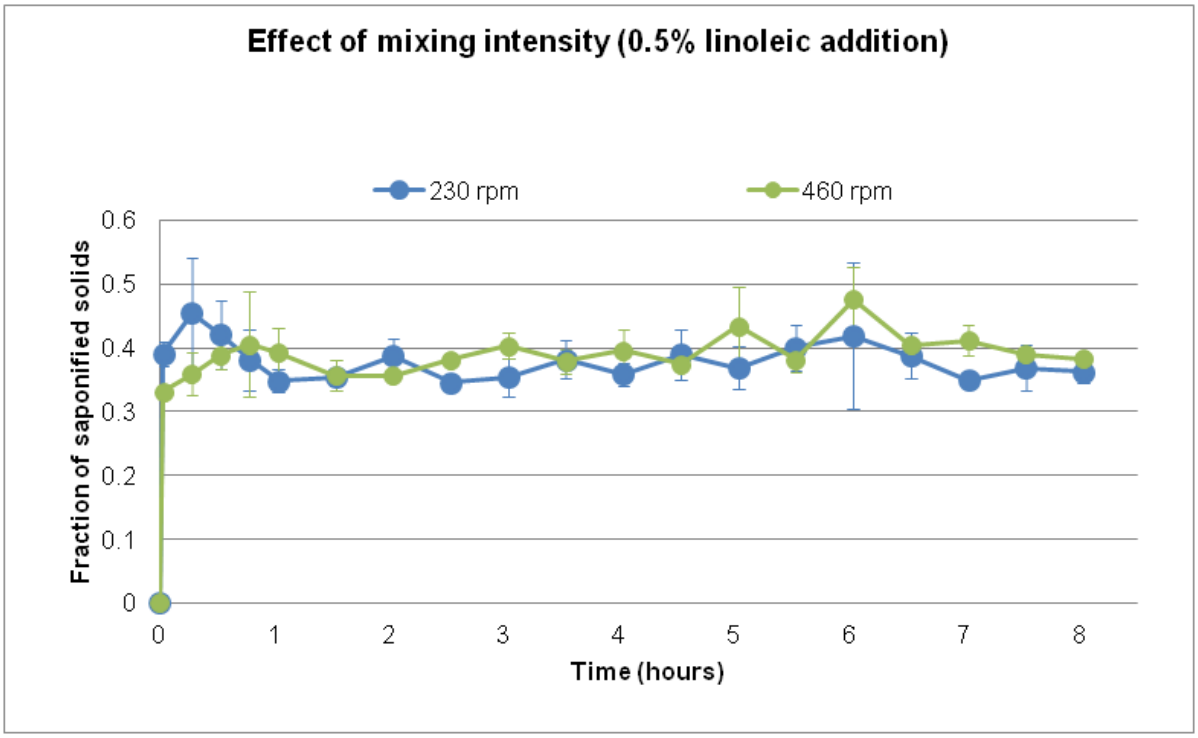

Figure 6 Effect of mixing intensity (0.5% of linoleic acid addition, pH 10, 45 °C)

3.3 Impacts of detergents on saponified solids formation and characteristics

Table 2 displays the effects of detergent additions on the formation of saponified solids and their fatty acid profiles. The results show that the presence of detergents in background water increases the production of saponified solids. Non-ionic detergent, having neutral pH in pure form, tends to create high pH conditions when in contact with the calcium solution. Although the exact reason of this observation is unknown, the higher pH conditions were assumed to contribute to fat hydrolysis, and therefore, increased formation of saponified solids. The presence of very small amounts of detergent (0.05% by wt.) seemed to influence the production of saponified solids at the initial periods (approximately 15% increase in saponification within two minutes of mixing till four hours) when compared with no addition of detergents. However, the saponified solid production was the same at later periods during

the saponification experimental test period. An increase in the detergent addition (5% by weight of source fat) also resulted in an increase in the mean fraction of the saponified solids.

The addition of the pure forms of the non-ionic and/or anionic detergents did not show a significant difference in the fatty acid profiles, compared to the fresh fat source and/or the saponified solids produced without the presence of detergents (Table 2). A minor change, however, was noted in the contents of the monounsaturated and poly-unsaturated fractions (i.e., oleic, linoleic, and linolenic). Alkali driven hydrolysis with no detergent additions resulted in a slight decrease in poly-unsaturated fractions (i.e., linoleic and linolenic) and a slight increase in mono-unsaturated fraction (i.e., oleic) compared to the fresh fat sources under the conditions tested (i.e., pH 7.0±0.5 and room temperature). The addition of the detergents seemed to inhibit any changes in the unsaturated fractions observed with no detergent additions and resulted in fatty acid profiles that were very similar to the fresh fat source (i.e., canola). This inhibition may be due to the addition of more unsaturated lipids in the pure forms of detergents, i.e., sorbitane trioleate, sodium alkyl ether sulfate, and formaldehyde. The mechanism for this proposed inhibition is unknown.

The commercial detergents that are potentially used in households, however, displayed a significant increase in the fraction of palmitic and linoleic acids with a simultaneous reduction in oleic acid fractions (Table 2). Significant quantities of saturated fats were measured in the commercial detergent, i.e., 0.31 mg/g of lauric and 0.40 mg/g of palmitic acid, compared to the pure forms of detergent that were mostly unsaturated fats. The linoleic acid produced from the addition of the commercial detergent may also result in significant conversion to palmitic under warm temperature conditions as noted earlier. The results of the fatty acid profiles suggest that the types of the added chemical agents, (i.e., for moisturizing, conditioning, and thickening) used in the production of commercial detergents may have significant influence in the chemical properties, and therefore, the production of FOG deposits, i.e., the predominance of palmitic (Grieveson et al., 1997; Keener et al., 2008). The results, therefore, suggest that careful consideration in the selection of the commercial dish-

washing detergents, while still maintaining the quality of public health, may be necessary as a management strategy to reduce FOG deposit formations in sewer systems.

Figures 7 and 8 display the infrared spectra of saponified solids produced with non-ionic and anionic detergent additions, respectively. In Figure 7, the results showed that saponified solids created with the addition of non-ionic detergent produced two new peaks in the region of asymmetric carboxylate bands at 1537 cm^{-1} and 1574 cm^{-1}. These peaks were also found in saponified solids created with FFA additions (i.e., palmitic and linoleic) and FOG deposits (He et al., 2011), as discussed earlier. In anionic detergent based saponified solids, a single strong absorption band in the region of asymmetric carboxylate band was observed at 1640 cm^{-1}, as was observed in saponified solids with fresh canola fat source (Supplemental Figure 2). The symmetric carboxylate bands were observed at 1417 cm^{-1} and 1460 or 1470 cm^{-1}. The saponified solids also displayed strong bonded hydroxyl band in the region of 3400 cm^{-1} and a growing metal oxygen band shoulder in the region of 690 cm^{-1}. The FTIR-ATR results suggest that saponified solids created with the pure forms of non-ionic and/or anionic detergents display the characteristic bands of FOG deposits (Poulenat et al., 2003; He et al., 2011; Iasmin et al., 2014). However, the use of high quantities of detergents may lead to faster and increased formations of FOG deposits. Therefore, optimum usage of detergents in FSEs may be necessary.

Table 2 Fatty acid profiles and saponified solid fractions with detergent additions

Type of Detergent	**Quantity of addition (%wt of source fat)**	**Palmitic (%)**	**Stearic (%)**	**Oleic (%)**	**Linoleic (%)**	**Linolenic (%)**	**Mean fraction of saponified solids (time = 2 mins)**	**Mean fraction of saponified solids (time = 8 hrs)**
Canola (source fat)		4.150±0.046	2.000±0.025	62.490±0.137	18.902±0.062	8.455±0.042	-	-
No detergent (Iasmin et al., 2014)	0	5.738±0.278	2.263±0.498	73.100±1.866	9.046±0.646	1.914±0.274	0.25	0.43
Non-ionic det.	0.05	4.487±0.338	1.780±0.252	65.650±1.439	17.587±3.299	6.7±2.366	0.36	0.49
Non-ionic det.	5	4.547±0.543	1.850±0.223	67.690±2.760	12.160±6.152	3.55±2.380	0.43	0.73
Anionic det.	0.05	4.443±0.242	2.017±0.140	67.280±1.374	15.713±2.016	5.28±0.962	0.37	0.48
Anionic det.	5	4.330±0.165	1.477±0.115	61.130±1.019	21.720±0.963	8.80±1.120	0.46	0.70
Commercial det.	1	11.763±0.609	4.527±0.335	24.433±2.224	52.390±2.334	6.63±0.335	-	0.60

The standard deviations of saponified solids vary from 0.01 to 0.25.

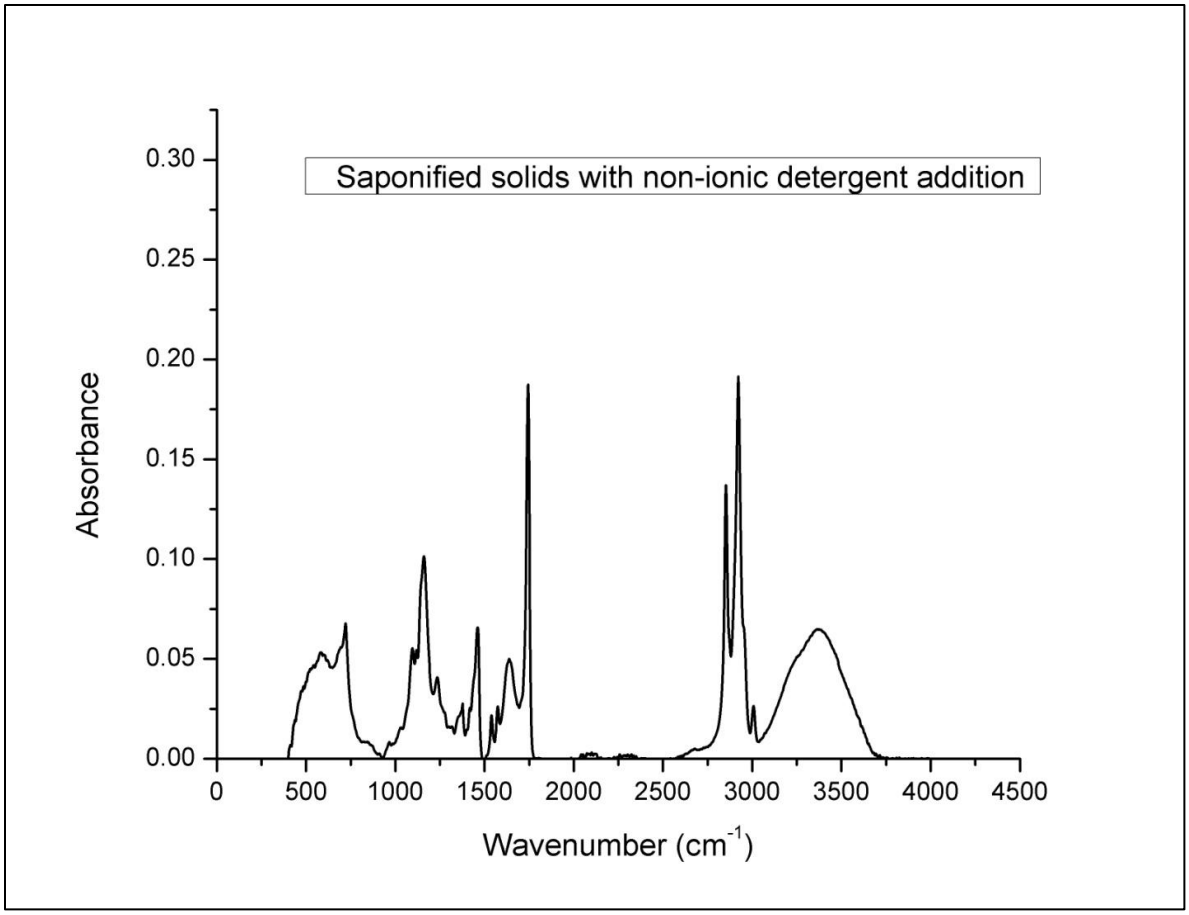

Figure 7 Saponified solids with non-ionic detergent addition

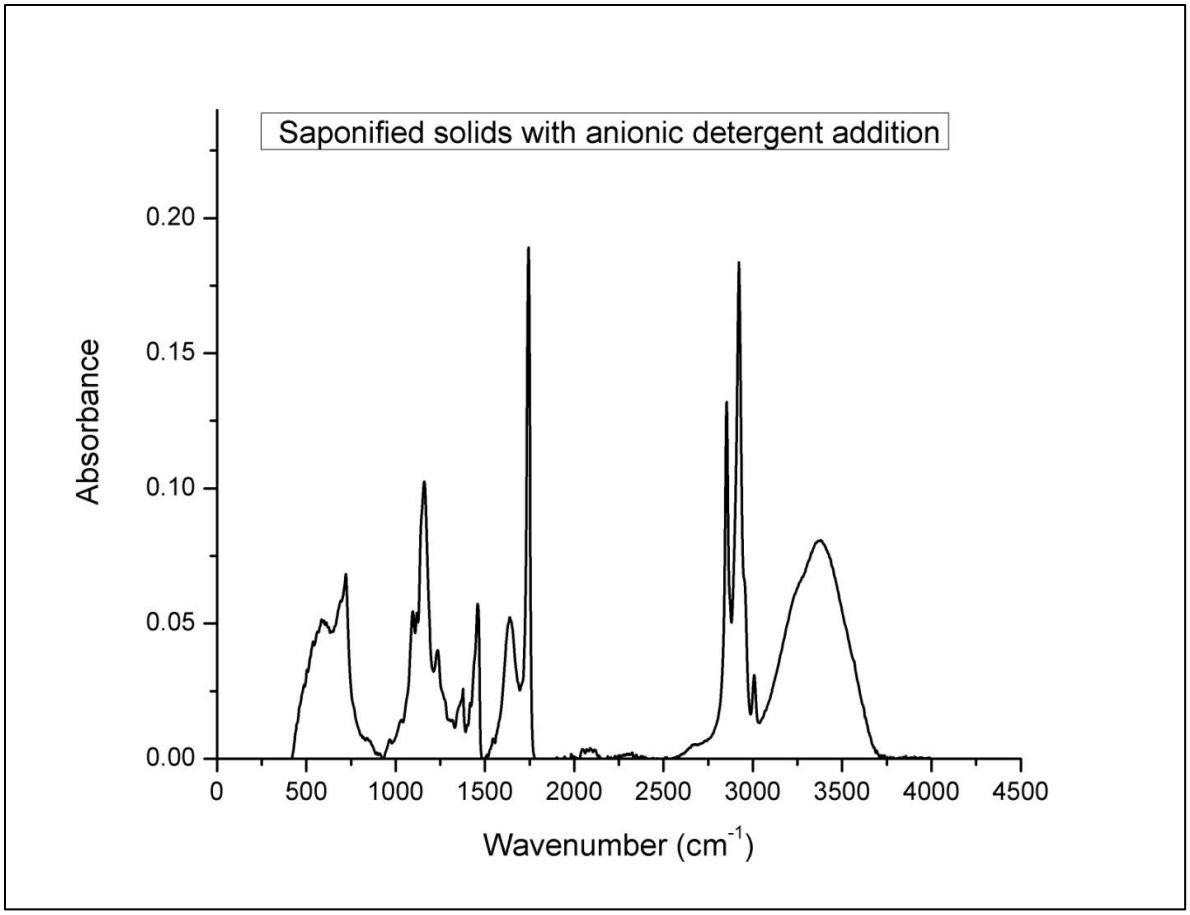

Figure 8 Saponified solids with anionic detergent addition (canola, calcium chloride, pH 10, 22 °C)

3.4 Effects of lipase driven hydrolysis

Significant amount of saponified solids were produced with lipase addition under room temperature and neutral pH conditions. Table 3 displays the fatty acid profiles of the saponified solids prepared under both the alkali and lipase driven hydrolysis conditions, respectively. In Table 3, an increase in lipase addition resulted in increased saponified solid fractions by 3 to 38% for 0.11gm and 1 gm additions, respectively. The use of *Candida rugosa* lipase did not display any significant change in the fatty acid (FA) profiles of the

saponified solids compared to the source fats and did not display a significant change in the palmitic fraction, as hypothesized. Moreover, when compared with the saponified solids produced with alkali driven hydrolysis, the addition of lipase resulted in a decrease in the saturated (i.e., palmitic and stearic) and monounsaturated fractions (i.e., oleic), and a general increase in the polyunsaturated fractions (i.e., linoleic and linolenic). Although it's unknown why this transformation occurred, the polyunsaturated fractions may later convert to saturated fractions (i.e., palmitic) due to warm temperature conversion processes, as discussed earlier with experiments that included the addition of linoleic acid.

Figure 9 displays the infrared spectra of saponified solids created with lipase additions (0.1 gm and 1 gm). The infrared spectrum of the pure lipase powder source is also shown in Figure 9. The results showed that these lipase-fortified saponified solids contained the characteristic bands of FOG deposits. With 0.1 gm lipase addition, strong bands at 1643 cm^{-1}, 1538 cm^{-1}, 1462 cm^{-1}, and a shoulder at 1419 cm^{-1} were observed in the region of carboxylate bands. A weak band was found at 650 cm^{-1}, in the region of metal oxygen band near 670 cm^{-1}. With 1 gm lipase addition, the ester carbonyl band at 1745 cm^{-1} that represents presence of un-reacted fat reduced in strength significantly compared to the strength in pure fat. The reduction in strength in carbonyl band is representative of increased hydrolysis, and therefore, increased formation of saponified solids, as can also be seen in Table 3. The asymmetric carboxylate band also shifted to the left, from 1643 to 1630 cm^{-1}, and its strength increased significantly compared to the saponified solids prepared with 0.1 gm lipase addition. A shoulder or hidden peak at 652 cm^{-1} was also observed in the region of the metal oxygen band. However, pure lipase powder contained similar absorption bands at 652 cm^{-1}, 1540 cm^{-1}, and at 1654 cm^{-1}, respectively.

Although pure lipase powder contained 652 cm^{-1} band, its strength increased significantly (approximately doubled) in the saponified solids prepared with 1 gm lipase addition. At the same time, the strength of the carboxylate absorption band at 1643 cm^{-1} increased significantly with an increase in saponified solid fractions (Table 3). Therefore, it is hypothesized that at least 50% of the 650 cm^{-1} band in the saponified solids created with 1

gm lipase addition was due to the metal oxygen band from the saponified solids. All the saponified solids prepared with lipase addition displayed the bonded hydroxyl band in the region of 3400 cm^{-1}, as can be seen in Figure 9. The results, overall, suggest that lipase driven hydrolysis is possible in GIs or sewer systems under neutral pH and room temperature conditions. The *Candida rugosa* lipase that is generally found in food sources and used as additives in detergents for cleaning purposes in FSEs may result in more saponified solids if present in high concentrations, compared to alkali driven hydrolysis (Benjamin and Pandey, 1998; Hasan et al., 2010). Although the exact quantities of the lipases used as additives in detergents are unknown, care must be taken in considering detergents with any addition of lipase.

As more lipase leads to more saponified solids (i.e., FOG deposits), the possible extracellular lipase produced due to the activity of *Selemonas lypolytica* in GIs could act in similar manner (He, 2011). Current FSE management practices include GI pumping frequency based on time (e.g., three months) or volume (e.g., > 25%) (Tupper, 2010). These management practices related to GI pumping frequency should be reviewed since prolonged accumulation of FOG in GIs could lead to conditions that promote FOG deposit formation based on lipase activities from microbial activity. The results also suggest that *Candida rugosa* lipase may increase the poly-unsaturated fractions that may later convert to the palmitic fractions under warm temperature conditions. The use of *Candida rugosa* lipase did not directly display an increase in palmitic fractions. Other types of microbial lipases may also contribute to the predominance of palmitic in FOG deposits due to their different types of substrate specificities (Hoshino et al., 1990; Ghosh et al., 1996). Further research in these other types of enzymes may be needed to better understand the roles of lipases in GIs.

Table 3 Fatty acid profiles and saponified solid fractions under lipase driven hydrolysis

Type of hydrolysis	Canola (source fat)	Alkali driven hydrolysis (Iasmin et al., 2014)	Lipase	Lipase
Quantity of addition (gm)	-	0	0.11	1
Palmitic (%)	4.150±0.046	5.009±0.097	4.597±0.191	4.193±0.140
Stearic (%)	2.000±0.025	1.769±0.498	1.610±0.170	1.463±0.214
Oleic (%)	62.490±0.137	68.930±1.037	61.220±1.766	60.343±2.673
Linoleic (%)	18.902±0.062	18.009±1.062	20.987±1.449	21.660±1.715
Linolenic (%)	8.455±0.042	5.897±0.671	9.063±1.673	8.847±1.857
Fraction of saponified solids	-	0.46	0.49	0.84

The standard deviations of fraction of saponified solids vary from 0.00 to 0.14.

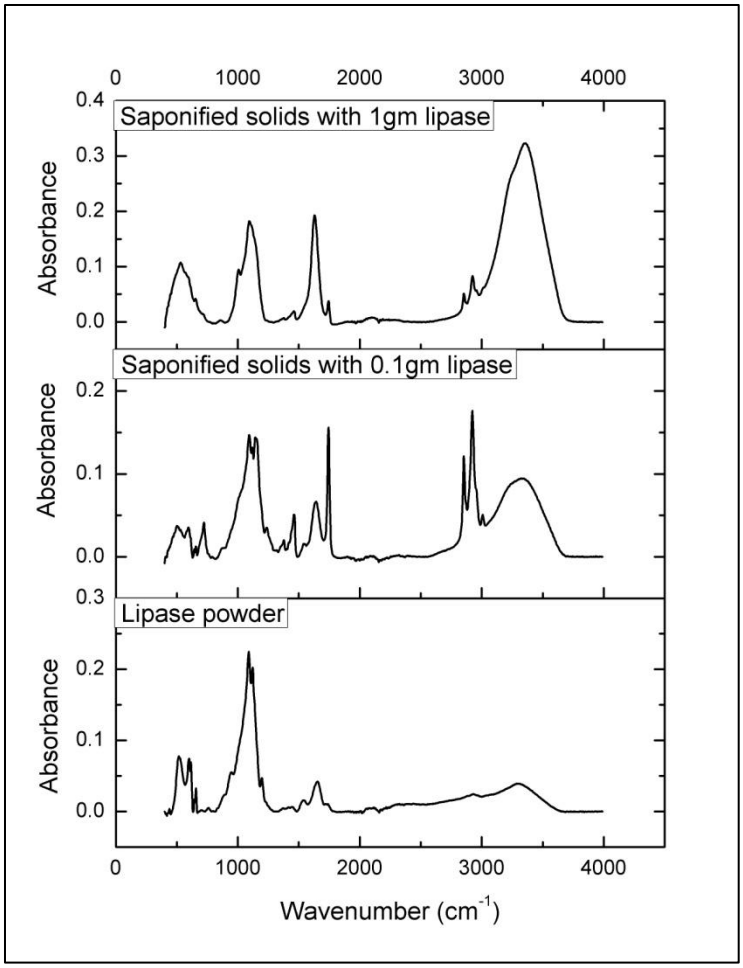

Figure 9 Saponified solids prepared with lipase additions (top- 1gm addition; middle- 0.1 gm addition) and pure lipase powder (bottom)

4 Conclusions

The results of this study suggest that the presence of initial FFAs and detergents in grease interceptors and/or sewer systems will likely result in more saponified solids, and therefore, an increased potential for FOG deposit formation. Lipase driven hydrolysis is also a likely mechanism that leads to FOG deposit formation. The results suggest that the high temperature operations in FSEs (i.e., cooking and/or washing) may have significant contribution in converting the unsaturated fats to palmitic, the saturated fraction. Moreover,

the additive agents used in commercial detergents compared to the pure anionic and/or non-ionic surfactants may have significant impact on increasing the palmitic fractions in FOG deposits. While selective removal of palmitic may not be an effective strategy to reduce the FOG deposit formation due to these complex transformation processes, FSEs can play a significant role in reducing these formations by focusing on some key issues without compromising food quality and public health safety: a) optimum usage of detergents in washing processes; and b) use of a heat-exchange chamber before GI to reduce the water temperature well below 45 °C to further avoid and/or reduce transformations due to warm temperature conditions. While the roles of FSE operations and GI maintenance may need to be assessed directly with a GI, the findings of this study provide indications of the maintenance of a full-scale system to help reduce FOG deposit formation, considering the difficulties of setting up the full-scale experimentation.

Acknowledgments

We would like to thank the United States Environmental Protection Agency (EPA STAR grant: 83426401) for funding this research. We are also grateful to the Department of Chemistry to use their laser spectroscopy facility.

References

Aziz, T.N., Holt, L.M., Keener, K.M., Groninger, J.W., and Ducoste, J.J. (2012). Field characterization of external grease abatement devices. *Water Environment Research, 84(3),* 237-246

Benjamin, S., and Pandey, A. (1998). Candida rugosa lipases: molecular biology and versatility in biotechnology. *Yeast, 14*(12), 1069-1087.

Dominic, C. C. S., Szakasits, M., Dean, L. O., and Ducoste, J. J. (2013). Understanding the spatial formation and accumulation of fats, oils and grease deposits in the sewer collection system. *Water Science & Technology, 68*(8), 1830-1836.

Duckett, S. K., and Wagner, D. G. (1998). Effect of cooking on the fatty acid composition of beef intramuscular lipid. *Journal of Food Composition and Analysis*, *11*(4), 357-362.

Ducoste, J. J., Keener, K. M., Groninger, J. W., and Holt, L. M. (2008). Fats, roots, oils, and grease (FROG) in centralized and decentralized systems. *Water Environment Research Foundation.IWA Publishing, London.*

Garcia, B., Mogollon, J., Lopez, L., Rojas, A., and Bifano, C. (1994). Humic and fulvic acid characterization in sediments from a contaminated tropical river. *Chemical Geology*, *118*(1-4), 271-287.

Ghosh, P.K., Saxena, R.K., Gupta, R., Yadav, R.P., and Davidson (1996). Microbial lipases: production and applications. *Science progress*, 79(2), 119-157.

Hoshino, T., T. Yamane, and S. Shimizu (1990). Bioreactor for Enzymatic Reaction of Fat and Fatty Acid Derivatives. Part XII Selective Hydrolysis of Fish Oil by Lipase to Concentrate n-3 Polyunsaturated Fatty Acids (n-3 Pufa*), Agric. Biol. Chem*. 54:1459–1467.

Grieveson, A. P. H., Jobling, M., Shen, S., and Tsaur, L. S. (1997). *U.S. Patent No. 5,661,189*. Washington, DC: U.S. Patent and Trademark Office.

Hasan, F., Shah, A. A., Javed, S., and Hameed, A. (2010). Enzymes used in detergents: lipases. *Afr J Biotechnol*, *9*(31), 4836-4844.

He, X., Iasmin, M., Dean, L. O., Lappi, S. E., Ducoste, J. J., and de los Reyes III, F.L. (2011). Evidence for fat, oil, and grease (FOG) deposit formation mechanisms in sewer lines. *Environmental Science and Technology*

He, X. (2011). Characterization of grease interceptors for removing fat, oil, and grease (FOG) and mechanisms of FOG deposit formations in sewer systems. PhD dissertation. North Carolina State University

He, X., de los Reyes III, F. L., Leming, M. L., Dean, L. O., Lappi, S. E., and Ducoste, J. J. (2013). Mechanisms of Fat, Oil and Grease (FOG) Deposit Formation in Sewer Lines. *Water Research*. 10.1016/j.watres.2013.11.012

Iasmin, M., Dean, L., Lappi, S., Ducoste, J. (2014). Factors that influence properties of FOG deposits and their formation in sewer collection systems. *Water Research Journal.* 10.1016/j.watres.2013.11.012

Keener, K. M., Ducoste, J. J., and Holt, L. M. (2008). Properties Influencing Fat, Oil, and Grease Deposit Formation. *Water Environment Research*, 80(12), 2241-2246.

Matsui, T., Miura, A., Iiyama, T., Shinzato, N., Matsuda, H., and Furuhashi, K. (2005). Effect of fatty oil dispersion on oil-containing wastewater treatment. *Journal of Hazardous Materials, 118*(1–3), 255-258. doi:10.1016/j.jhazmat.2004.10.023

Montefrio, M. J., Xinwen, T., and Obbard, J. P. (2010). Recovery and pre-treatment of fats, oil and grease from grease interceptors for biodiesel production. *Applied Energy, 87*(10), 3155-3161.

Pro, O. 8. About Origin Pro 8 SRO, V8.0724 Software, Copyright 1991-2007, *Origin Lab Corporation*: 2007

Smith, L. (1932). *The Kinetics of soap making*. Transactions and Communications. *Journal of the Society of Chemical Industry,* pp 337-348.

Warner, K. (1999). Impact of high-temperature food processing on fats and oils. In *Impact of Processing on Food Safety*, pp. 67-77. Springer US.

APPENDIX

Appendix S

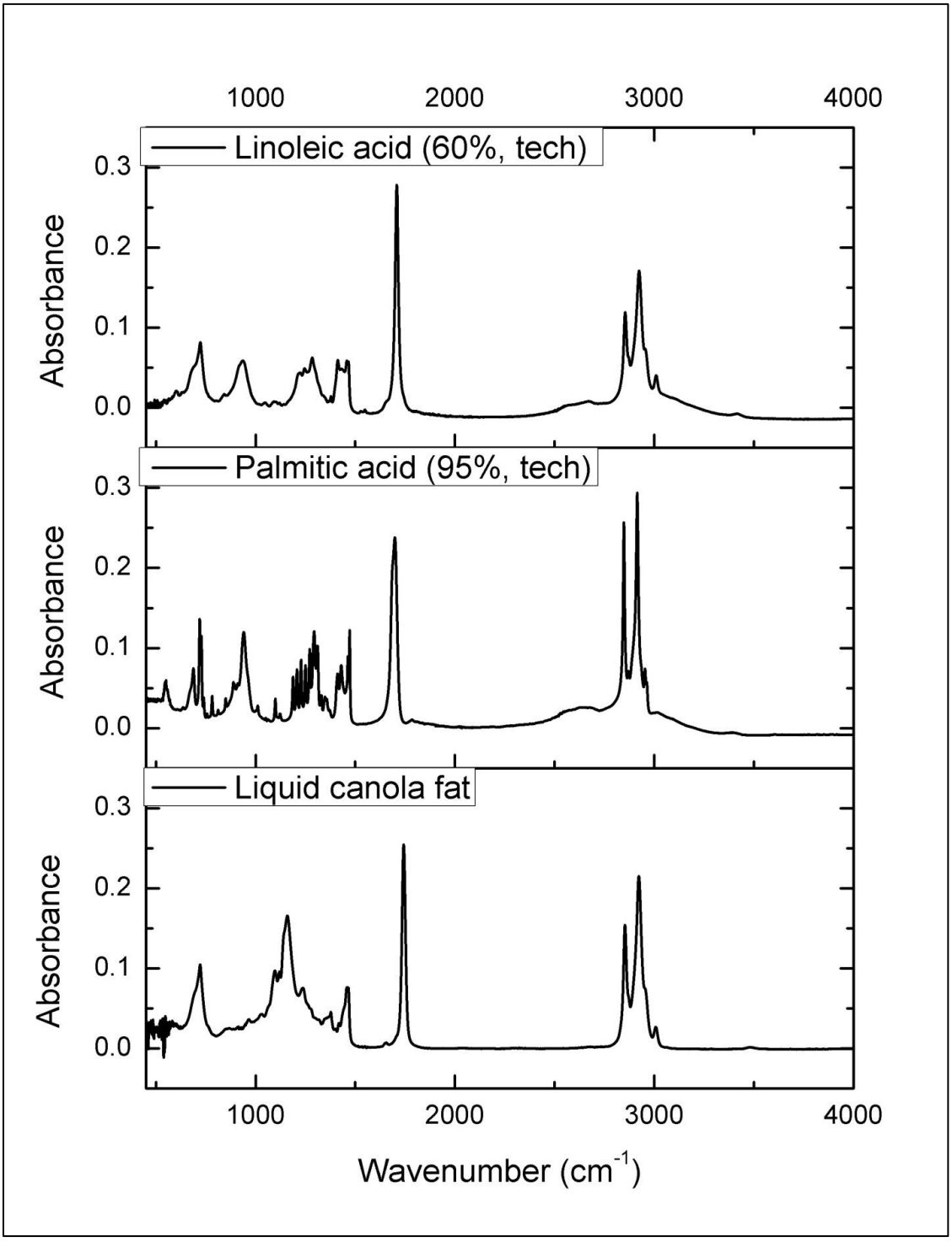

Supplemental Figure 1 Infrared spectra of pure components

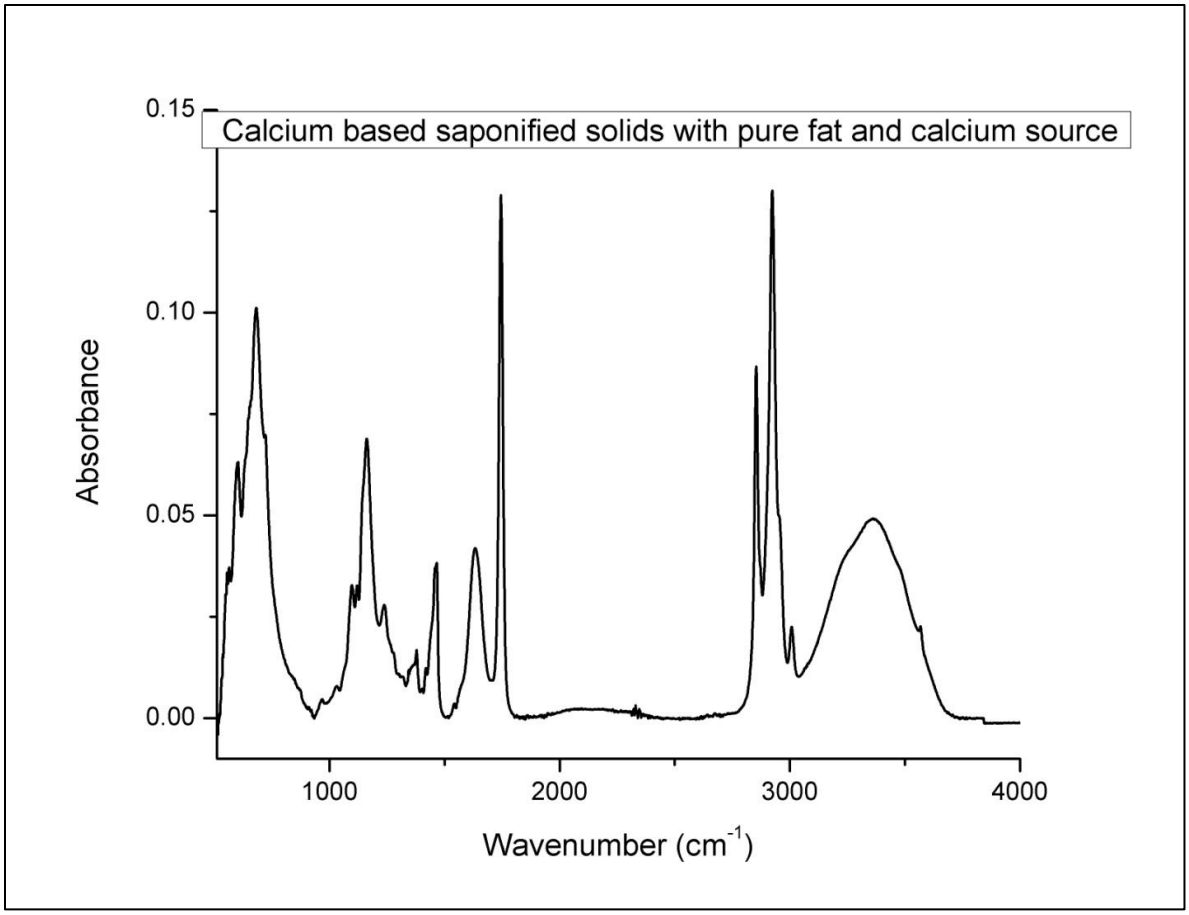

Supplemental Figure 2 Saponified solids with fresh fat and calcium sources (canola, calcium chloride, no addition of FFA or detergents)

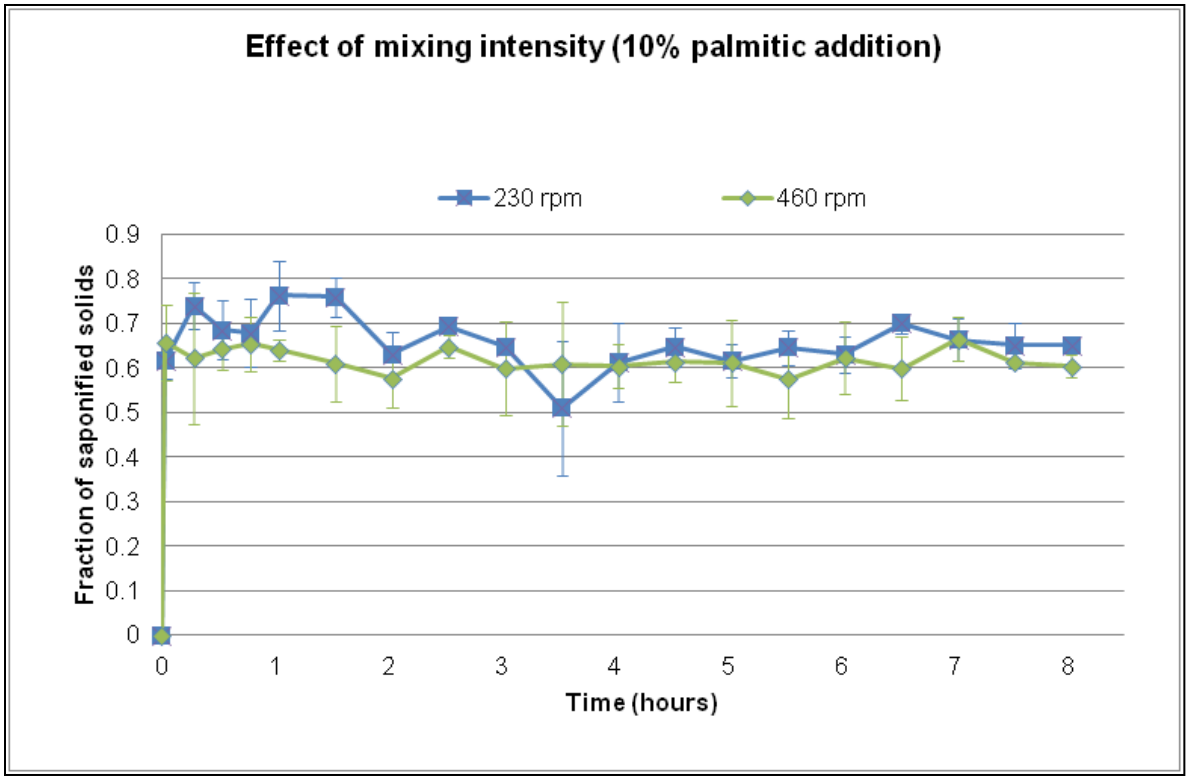

Supplemental Figure 3 Effect of mixing intensity (10% palmitic addition, pH 10, 45 °C)

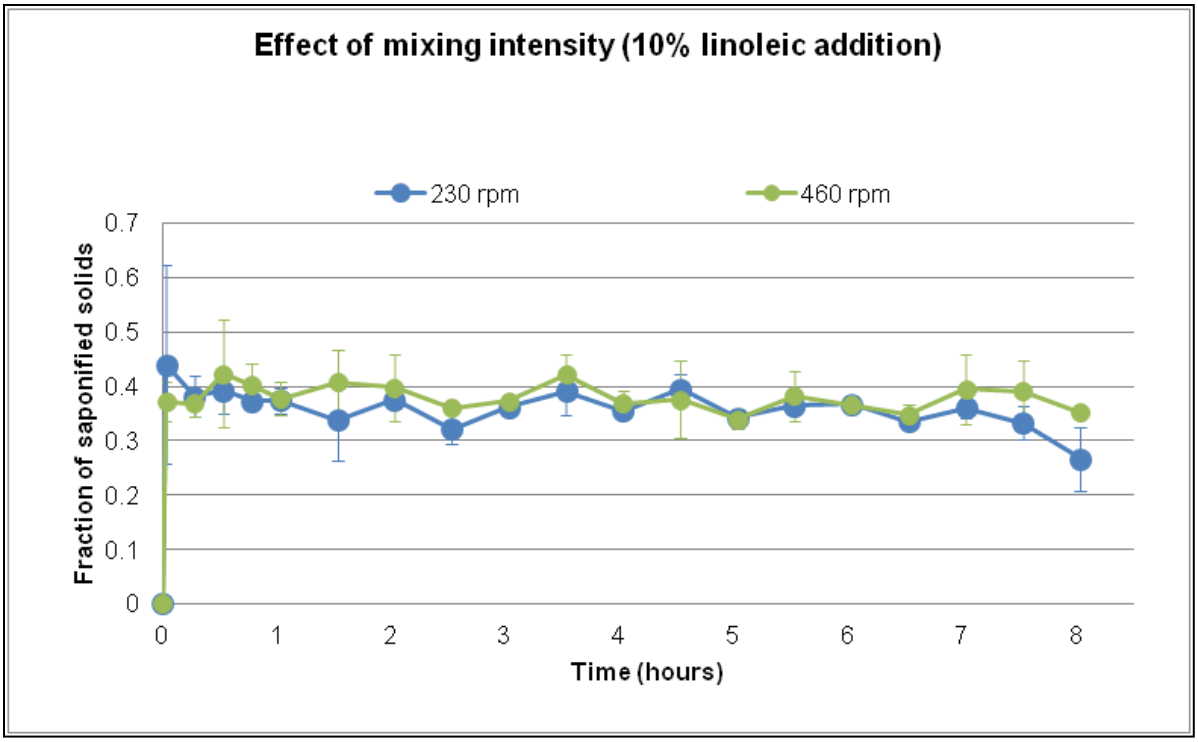

Supplemental Figure 4 Effect of mixing intensity (10% linoleic acid addition, pH 10, 45 °C)

CHAPTER 7 Conclusions and Recommendations

1. Conclusions

The objectives of the study were to understand the FOG deposit formation process, its properties, and its kinetics under alkali driven hydrolysis and influenced by source and environmental factors in food service establishments (FSE) effluents, grease interceptors, and in sewer systems. The source and environmental factors that were investigated in this research include the following: a) types of fats used in FSEs, b) types of calcium sources available in sewer systems, c) pH, d) temperature, e) presence of initial free fatty acids (FFAs), f) presence of detergents utilized in FSEs, and g) effects of mixing intensities on the kinetics of saponified solids. In addition to these factors, the effect of lipase was investigated to understand its influence on FOG deposit formation process.

The results of this study confirmed prior research that revealed similarities between FOG deposits and calcium-based saponified solids (He et al., 2011). When pure fat sources are used, these saponified solids prepared under alkali driven hydrolysis conditions displayed the same fatty acid profiles as the source fats introduced at the beginning of the saponification process. The environmental factors, i.e., pH and temperature conditions seemed to affect the solubility of the calcium sources. As a result, the quantities and the kinetics of the saponified solids may change, affecting the rate of accumulation of FOG deposits in sewer lines. The saponified solids produced under different calcium sources and environmental conditions may exhibit different color, texture, and rheological properties. However, all the saponified solids displayed limited flow properties which may help explain the rigid adherence of FOG deposits to sewer walls.

Two empirical models (i.e., Cotte saponification model and Foubert crystallization model) and one mass-action-based saponification model were investigated to capture the kinetics of the FOG deposit formation process. The model results suggest that high pH and high temperature conditions will lead to faster saponification, and therefore, the formation of FOG

deposits. However, the results further suggest that slower saponification is necessary for higher calcium content as seen in FOG deposits. The mass-action-based saponification model better elucidated the calcium based saponified solids formation chemistry due to its additional mass balance equations that track the saponified solids precursor chemical constituents (i.e., Ca, FOG, and FFA) and, therefore, is in a better position to predict the FOG deposit formation kinetics, compared to the empirical models evaluated in this study. Consequently, the use of the mass-action-based saponification model is recommended for potential incorporation in large scale FOG deposit prediction models to determine the most susceptible FOG accumulation zones or "hotspots" in sewer collection systems.

The roles of FSEs in the formation of FOG deposits were investigated based on their possible contributions in producing FFAs, and use of different types of cleaning detergents. In addition, the effect of *Candida rugosa* lipase that is found in food sources and used in detergents was studied to determine its role in the FOG deposit formation. The results suggest that the presence of initial FFAs (i.e., palmitic, oleic, and/or linoleic) in grease interceptor (GI) effluents will likely increase the production of calcium-based saponified solids, and therefore, production of FOG deposits. The high temperature operations in FSEs in cooking and/or sanitizing applications along with higher temperatures found in GIs may significantly influence in conversion of the unsaturated fats to saturated fats (predominantly palmitic) as the results of this study displayed approximately 6% increase in the production of these saturated fatty acids under the elevated temperatures performed in this research study. The pure detergent sources (i.e., non-anionic and anionic) increased the production of saponified solids, but did not display a significant change in the fatty acid profiles. However, the commercially available detergent used in household applications displayed significantly high fractions of palmitic in the saponified solids. Therefore, the external agents added to the surfactants that make-up commercial detergents in households and/or FSEs dishwashing applications may need to be carefully investigated as that information may impact the FSEs detergent selection process. Lipase driven hydrolysis was also shown to enhance the production of FOG deposits. While selective removal of long chain fatty acids may be a strategy to reduce the FOG deposit formation, FSEs can play a significant role in the

reduction in these formations by focusing on some key issues without compromising restaurant quality, public health, and sanitation. These strategies include the following: a) optimum usage of detergents; and b) use of a heat-exchange chamber prior to kitchen wastewater discharge into GI to reduce the water temperature well below 45 °C.

2. Recommendations for future study

The research performed in this study provided significant new information about the factors that increase the formation and kinetics of FOG deposits under a wide variety of conditions. Yet, there are a number of conditions that still need to be investigated to further increase our understanding of FOG deposits formation in sewer lines. The following are recommendations of experiments that should be performed in future research studies:

a) In this study, only room temperature conditions and above were investigated. While it is expected that colder temperatures would result in slower saponification reactions, it's unknown whether rheological properties will change due to these low temperatures. Therefore, lower temperature conditions should be explored (i.e., 5 - 20 °C) to reflect potential sewer pipe conditions.
b) The *Candida rugosa* lipase was only incorporated in the study of lipase driven hydrolysis. The other microbial lipases (e.g., *Candida cylindracea* and *Candida curvata*) can also be studied to test for their specificities, and therefore, their contributions in changing the FA profiles of saponified solids (Hoshino et al., 1990; Ghosh et al., 1996). Microbiological studies can also be performed with the lipolytic microbes found in grease interceptors, e.g., *Selemonas lipolytica* (He, 2011).
c) The current research discussed the effects of pure detergent sources and showed that the external agents added to pure detergents to produce commercial detergents could be a significant contributor to palmitic predominance in FOG deposits. Therefore, the commercial detergents that are currently used in FSEs can be studied in detail to understand their effects on FOG deposit formation.
d) The current research study proposed that warm temperature conditions found in GIs could promote the formation of saturated FFAs (i.e., palmitic). Full scale studies

could be performed that involve the use of a heat-exchanger prior to discharge into the GI and the long chain fatty acid profile could be monitored to evaluate the benefit of the influent heat exchanger.

e) The rheological properties of the saponified solids provided some explanation for the the rigid attachment of FOG deposits to sewer walls. Further research could be performed to reduce the attachment properties of saponified solids on different types of sewer walls (e.g., concrete, cast iron, ductile iron, clay, and PVC). This new research study would involve the investigation of alternative coating agents that are oleophobic and help reduce the attachment characteristics of the saponified solids.

f) In terms of chemical properties, Keener et al. (2008) measured a significant quantity of iron, sulfur, magnesium, and aluminum after the large calcium concentration in FOG deposits. Their observations seemed to suggest potential concrete corrosion processes involved in the formation of these FOG deposits (Hermansyah et al., 2007; Bielefeldt et al., 2010; Gutierrez-Padilla et al., 2010). He et al. (2013), while studying the effect of concrete corrosion on the FOG deposit formation, did not quantify the secondary metals and minerals coming from the corroding concrete block. Yet, He et al. results clearly showed significant release of calcium under concrete corrosive environments. Therefore, the formations of saponified solids under concrete corrosive conditions need to be studied to understand the contributions of the secondary metals and minerals to the rheological properties of FOG deposits. These concrete corrosive test would be performed with cementitious material produced with different starting mixtures (i.e. cement, sand, and gravel by volume or weight)

g) In terms of GI maintenance, the current study suggests critical problems associated with the production of FFA, and therefore, their contributions in FOG deposit formation. Further research can be performed that investigates the maintenance cycle of GIs to determine how they should be cleaned (i.e. frequency and limit of microbial activity) to reduce the potential release of long chain fatty acids.

h) The mass-action-based saponification model displayed certain limitations on capturing the experimental kinetic data for saturated fats (i.e., Beef tallow) compared

to unsaturated fats (i.e., Canola), under the same experimental conditions. The performance of the model may be improved by investigating the inclusion of separate rates of saponification for the three major FFAs (i.e., palmitic, oleic, and linoleic). Experimental tests to determine the saponification kinetics when using pure FFA sources can be performed and compared with the model predictions.

References

Bielefeldt, A., Gutierrez-Padilla, M. G. D., Ovtchinnikov, S., Silverstein, J., and Hernandez, M. (2010). Bacterial kinetics of sulfur oxidizing bacteria and their biodeterioration rates of concrete sewer pipe samples. *Journal of Environmental Engineering, 136*, 731

Ghosh, P.K., Saxena, R.K., Gupta, R., Yadav, R.P., and Davidson (1996). Microbial lipases: production and applications. *Science Progress*, 79(2), 119-157.

Gutiérrez-Padilla, M. G. D., Bielefeldt, A., Ovtchinnikov, S., Hernandez, M., and Silverstein, J. (2010). Biogenic sulfuric acid attack on different types of commercially produced concrete sewer pipes. *Cement and Concrete Research, 40*(2), 293-301

He, X., Iasmin, M., Dean, L. O., Lappi, S. E., Ducoste, J. J., & de los Reyes III, F. L. (2011). Evidence for fat, oil, and grease (FOG) deposit formation mechanisms in sewer lines. *Environmental Science & Technology, 45*(10), 4385-4391

He, X. (2011). Characterization of grease interceptors for removing fat, oil, and grease (FOG) and mechanisms of FOG deposit formations in sewer systems. PhD dissertation. North Carolina State University

He, X., de Los Reyes 3rd, F. L., Leming, M. L., Dean, L. O., Lappi, S. E., & Ducoste, J. J. (2013). Mechanisms of Fat, Oil and Grease (FOG) deposit formation in sewer lines. *Water Research, 47*(13), 4451-4459

Hermansyah, H., Kubo, M., Shibasaki-Kitakawa, N., and Yonemoto, T. (2006). Mathematical model for stepwise hydrolysis of triolein using Candida rugosa lipase in biphasic oil–water system. *Biochemical Engineering Journal*, *31*(2), 125-132

Hoshino, T., T. Yamane, and S. Shimizu (1990). Bioreactor for enzymatic reaction of fat and fatty acid derivatives. Part XII Selective Hydrolysis of Fish Oil by Lipase to Concentrate n-3 Polyunsaturated Fatty Acids (n-3 Pufa*), Agric. Biol. Chem*. 54:1459–1467

Keener, K.M., Ducoste, J.J., and Holt, L.M. (2008). Properties influencing fat, oil, and grease deposit formation. *Water Environment Research*, 80, 2241-2246